2014-02-05

ING3 Expression in Prostate Cancer and Its Association with ERG Gene Rearrangements and Patient Outcome

Almami, Amal

UNIVERSITY OF CALGARY

ING3 Expression in Prostate Cancer and Its Association with ERG Gene Rearrangements and Patient Outcome

by

Amal Ahmed Almami

A THESIS

SUBMITTED TO THE FACULTY OF GRADUATE STUDIES

IN PARTIAL FULFILMENT OF THE REQUIREMENTS FOR THE

DEGREE OF MASTER OF SCIENCE

MEDICAL SCIENCE DEPARTMENT

CALGARY, ALBERTA

JANUARY, 2014

Abstract

ETS Related Gene (*ERG*) rearrangement is one of the most common genetic changes seen in roughly about 50% of prostate cancer (PCA) cases. The inhibitor of growth family member 3 (ING3) is a member of the *ING* tumor suppressor family. The deregulation of *ING3* expression has been reported in various types of cancers. However, to date the role and function of ING3 in PCA as well as its relationship to *ERG* gene rearrangement has not been studied. Our initial observation from microarray expression profiling showed that *ING3* was down-regulated in *ERG* positive prostate cancer samples in comparison to *ERG* negative tumors. In this work, we examined the expression and localization of ING3 in prostate cancer cell lines and tissue samples and its association to clinical outcome. We documented a significant association between ERG and ING3 and showed a significant association to the patients' clinical outcome, thus highlighting a potential role for *ING3* in prostate cancer progression.

Acknowledgements

First of all, I would like to thank Almighty God for giving me the help and patience I need to proceed in this journey. Also, I would like to acknowledge the King of Saudi Arabia, King Abdullah bin Abdul-Aziz, who has given me the opportunity for education abroad. It is also a great pleasure to thank those who made this thesis possible:

I would like to express my sincere gratitude to my supervisor, Dr. Tarek Bismar, for allowing me to pursue my graduate studies in his laboratory and for his expertise, support and advice. I would like to express my special thanks to my co-supervisor Dr. Douglas Demetrick for his valuable thoughts, advice and feedback which helped to keep me on track and to work at a smooth pace.

I also extend my thanks to my thesis committee members, Dr. Karl Riabowol and Dr. Kiril Trpkov, for their valuable comments and insightful suggestions. They have been extremely helpful throughout the stages of my work. My thanks also go to Dr. Adnan Mansoor for donating his time to serve as my internal examiner.

I would like to express my deepest thanks to the Faculty of Medicine and the Department of Medical Science at the University of Calgary for their help and support during these past few years, especially Dr. Janice Braun, Dr. Tara Beattie, Dr. Shirin Bonni and Ms. Kiran Pandher, for their guidance and assistance throughout this program.

I would also like to thank all past and present members of Dr. Bismar's laboratory: all postdocs' fellows, Drs. Lars, Ting, Ashraf, Shuhong, Samar, Manal, Adrian, and Teng, for sharing their wealth of knowledge and training me in several techniques. Also, thank you to

Mike, Mohamed, Youjin, Ms. Maggie, Ms. Lori and Ms. Sze for the enjoyable group work and stimulating discussions. Special appreciation to Dr. Shoraf Dadakhujaev and Dr. Susie Rosales with whom I have enjoyed the many discussions we have had about science and life. I also extend my thanks to Claude Veillette from Dr. Demetrick's lab and to the members of Dr. Riabowol's lab: Arash, Subhash, Uma, Uyen, Yang and Ms. Donna for the ING3 (2A2) antibody. Additionally, my gratitude goes to all members of the Translation lab at Tom Backer Cancer Center, especially Mr. Brant Pohorelic for AQUA analysis and my best friend Alpana Saxena. Thank you everyone for the friendship and generous support you have given me throughout these years of my graduate study.

Moreover, I am deeply grateful and thankful to my family: my parents- Salma, and Ahmed; my uncles Mohamed Naji Al-Amin, Mohamed Mohamed Al-Amin and Hamid Alwaly; my brothers and sisters especially Mohamed Al-Husain and Zainab, for their unconditional love, continuous care and constant support in every aspect of my life. Many thanks go, in particular, to my husband, Abdullah, for his love and support, and also to my baby girl, Lama, for simply being there.

I also must mention my indebtedness to my family members, friends and teachers in Canada and back home in Saudi Arabia specifically Dr. Mohamed Basalamah from UQU and all laboratory members at the Armed Forces Hospital, particularly Dr. Yousef Saleem. Last but not least, I gratefully acknowledge financial support from the Ministry of Higher Education in the Kingdom of Saudi Arabia and from the Royal Embassy of Saudi Arabia Cultural Bureau in Canada.

To my family specially my mother Salma, brother Mohamed, husband Abdullah and my daughters

Thank you for your love and support

Table of Contents

List of Tables

List of Figures and Illustrations

List of Symbols, Abbreviations and Nomenclature

Symbol	Definition
AMACR	alpha methylacyl-CoA racemase
AQUA	automated quantitative analysis
AR	androgen receptor
BMI	body mass index
BPH	benign prostatic hyperplasia
cDNA	complementary DNA
ChIP	chromatin immunoprecipitation
CRPC	castration-resistant prostate cancer
CT	computed tomography
c-terminel	carboxy-terminal
DAPI	4’-6’-diamidino-2-phenylindole
DMEM	dulbecco's modified eagle medium
DMSO	dimethyl sulfoxide
DNA	deoxyribonucleic acid
DRE	digital rectal exams
EDTA	ethylenediaminetetraacetic acid
EMT	epithelial-mesenchymal transition
ERG	ETS-related gene
ETS	erythroblast transformation- specific
ETV	erythroblast transformation- variant
FFET	formalin-fixed tissue paraffin-embedded
g	gram
GAPDH	glyceraldehyde 3-phosphate dehydrogenase
GFP	green fluorescent protein
GUSB	glucuronidase beta
HAT	histone acetyltransferases
HCC	hepatocellular carcinoma
HEK293 cells	human embryonic kidney 293 cells
HGPIN	high-grade prostatic intraepithelial neoplasia
hNuA4	human nucleosomeacetyltransferase of Histone 4
ING	INhibitor of Growth
ING3	inhibitor of growth member 3
IP	immunoprecipitation
LID	lamin interacting domain
LZL	leucine zipper-like
mg	milligram
miRNA	microRNA

ml	milliliter
mM	millimolar
MRI	magnetic resonance imaging
mRNA	messenger RNA
ng	nanogram
NLS	nuclear localization signals
NP-40	nonyl phenoxylpolyethoxylethanol
NSCLS	non-small-cell lung carcinoma
^{o}C	degree Celsius
PAGE	polyacrylamide gel electrophoresis
PBS	phosphate buffered saline
PCA	prostate cancer
PCR	polymerase chain reaction
PHD	plant homeodomain
PI3K	phosphatidylinositol 3' -kinase
PIN	prostatic intraepithelial neoplasia
PSA	prostate-specific antigen
PTEN	phosphatase and tensin homolog
PVDF	polyvinylidene fluoride
RNA	ribonucleic acid
RT	room temperature
SDS	sodium dodecyl sulphate
siRNA	small interfering RNA
SVD	singular value decomposition
TMA	tissue microarrays
TMPRSS2	transmembrane protease, serine 2
TRUS	transrectal ultrasound
TURP	transurethral resection of prostate
UTI	urinary tract infection
UV	ultraviolet
µg	microgram
µl	microliter

Chapter One: Introduction

1.1 Prostate Gland

The prostate gland is the major secretory gland of the male reproductive system. It is a small, soft gland that is located underneath the urinary bladder and surrounds the upper part of the urethra and has the shape and size of a hazelnut [1]. The prostate gland consists of two groups of cells: stromal and epithelial, each of which is subdivided into different types [2]. The stromal cells consist of three types of cells: smooth muscle; fibroblast and endothelial cells, while the epithelial cells consist of five types of cells: luminal secretory; basal epithelia stem and neuroendocrine, each of which has specific morphology and functions [2]. The prostate gland is surrounded by a thin layer of connective tissue referred to as the "pseudo capsule". The gland itself is histologically divided into three zones: the peripheral, central and transition zones [3] . The majority of prostate cancers occur in the peripheral zone, which is the outer part and closest to the rectum. This area can be felt during a digital rectal examination (DRE). The transition zone, which is closer to the urethra, is the region where most of benign prostatic hyperplasia (BPH) occurs [4].

1.1.1 Physiology of Prostate

At birth, the prostate weighs a few grams, and then gradually the weight increases to approximately 20 g at 20 years of age. It typically remains at a stable weight until the age of 45 years [1]. The size and the function of the prostate is regulated by testosterone, which is an androgenic hormone secreted from the testes. The central function of the prostate is regulation

and development of spermatozoa through the production of alkaline fluid containing different products such as zinc, PSA and prostaglandin, to protect sperm from acidic environments [5].

1.1.2 Prostate Pathology

1.1.2.1 Non-neoplastic diseases of the prostate

Prostatitis is the inflammation of the prostate gland and is divided into acute and chronic prostatitis. Acute prostatitis is characterized by inflammation due to bacterial infection such as *E. coli* in the urinary bladder and urethra, which can spread to involve the prostate [6]. Chronic prostatitis refers mainly to the recurrence of acute prostatitis, which can lead to this chronic stage but can also occur without any history of acute prostatitis due to some non-bacterial factors such as *Chlamydia trachomatis* [6].

1.1.2.2 Neoplastic diseases of the prostate

1.1.2.2.1 Benign prostatic hyperplasia (BPH)

Benign prostatic hyperplasia is the enlargement of the prostate gland, which is a normal phenomenon in many men after the age of 40 years [7]. BPH is not considered a pre neoplastic condition but may cause some lower urinary tract symptoms [8].

1.1.2.2.2 High-grade prostatic intraepithelial neoplasia (HGPIN)

HGPIN is neoplastic transformation of prostatic epithelium and is considered the pre-carcinoma of prostate cancer. Unlike the normal prostate tissue, in HGPIN the prostate cells divide more rapidly than normal tissue; however, they have not yet become cancer [9]. HGPIN can be

detected in prostate biopsies performed due to elevated PSA levels and there are limitations to detecting it by ultra-sonography [9].

1.1.2.2.3 Prostate Cancer

Prostate cancer (PCA) is the malignant neoplastic proliferation that occurs in the prostate gland when cell growth is uncontrolled and the numbers of cells increase dramatically. The majority (about 95%) of PCA are derived from epithelial cells, which are called adenocarcinoma [10]. The main cause of mortality among prostate cancer patients is related to metastasis from the primary tumor in the prostate gland to distant organs or tissues such as the lymph nodes and bones [11-13].

1.1.3 Prostate Cancer Epidemiology

PCA is the most common malignancy in men and the second leading cause of cancer-related deaths in Western countries, with an estimated incidence of approximately 238,590 new cases and 29,700 deaths in USA in 2013 [14]. According to the American Cancer Society "one in six men will develop prostate cancer in his lifetime and one in 36 will die from it" [15]. In Canada, it is estimated that 23,600 new cases of prostate cancer and 3,900 related deaths will occur in 2013, according to the Canadian Cancer Society [16] .Ontario has the highest number of deaths, with a total of 1,500 cases, while the lowest mortality is in Prince Edward Island, with 20 cases. In Alberta, this number is 570 cases [16] .

1.1.4 Risk factors

Several risk factors have been reported for prostate cancer:

- Age is the highest risk factor. Men between 75-79 years old have approximately five time greater risk compared to men between ages 50-54 [17]. It is rare for men younger than 50 years old to develop prostate cancer [18].
- Family history: patients who have first degree relatives affected with PCA have an increased relative risk of developing prostate cancer, especially young age at onset [19].
- Ethnicity: the highest incidence is reported in African Americans, with 60% higher risk compared to other North Americans [20]. The lowest rate was shown among Asians, with about 25-fold less frequency compared with North Americans [21].
- Lifestyle, especially diet, has a significant effect on many types of cancer. In prostate cancer, it has been reported that diets rich in fat such red meat and dairy and low in vegetables, such as tomatoes and broccoli maybe linked to prostate cancer [22].
- Obesity: obese patients with prostate cancer have a worse prognosis compared with individuals with normal body max index (BMI) [23].

1.1.5 Prostate Cancer Detection

Usually, PCA is a silent disease and does not show symptoms until late in the disease stages. In early stages, symptoms may include increased urination, urgency, pain, burning and the presence of blood in urine. However, these symptoms are nonspecific and occur in other diseases such as urinary tract infection (UTI) [24]. Methods such as assessment of prostate specific antigen (PSA) in blood sample, digital rectal exams (DRE), transrectal ultrasound (TRUS) and bone scans for metastatic detection in bone have been widely used for PCA detection [22]. The normal

range of PSA is 0-4 ng/mL. However, this depends on the size of the prostate gland and the presence or absence of any inflammation. Depending on the situation, when PSA is elevated, it's recommended that patients undergo a prostate biopsy to examine the tissue microscopically [22]. DRE is additional tool used to assess the prostate gland where the physician assesses any lumps in the prostate gland that could be indicative of PCA. Computed tomography (CT) scans and magnetic resonance imaging (MRI) have been used in detection of many cancers including prostate cancer. Of note here, is that even within the "normal PSA range", there is a 10-15% chance of detecting PCA [24].

1.1.6 Prostate Cancer Prognosis

Currently, established prognostic factors are determined in biopsy tissues examined histologically to evaluate severity and aggressiveness of prostate cancer, and are known as Gleason score grading. Gleason score is a grading system which was first established by Donald Gleason in 1966 [25]. The grading system depends on the architecture of cells within the tumor. Grades are from 1 to 5, with 1 being the least and 5 being the most aggressive. The tumor grade is obtained by determining the sum of the most common two patterns. Therefore, the sum score can range from 2-10 with the most aggressive score being a grade of 10 [26, 27]. Figure 1.1 describes the pattern of different Gleason score. At initial pathologic assessment, the majority of prostate cancer patients will present with Gleason scores 6 and 7 [28]. In addition to pre-surgical pathological diagnostic methods, post-surgical methods used for prognostication include staging such as TNM system for staging the cancer the American Joint Committee on Cancer (AJCC), where T indicates tumor size, N indicates the presence of tumor in lymph nodes and M refers for distant metastasis involvement by cancer [29].

Figure 1.1 Gleason score.

Gleason score grading system used by a pathologist to evaluate the diagnosis of prostate cancer aggressiveness. It uses five grades based on the architecture of cells within the tumor, where grade 1 is more similar to normal cells and grade 5 is the worst pattern. The figure was taken from [30].

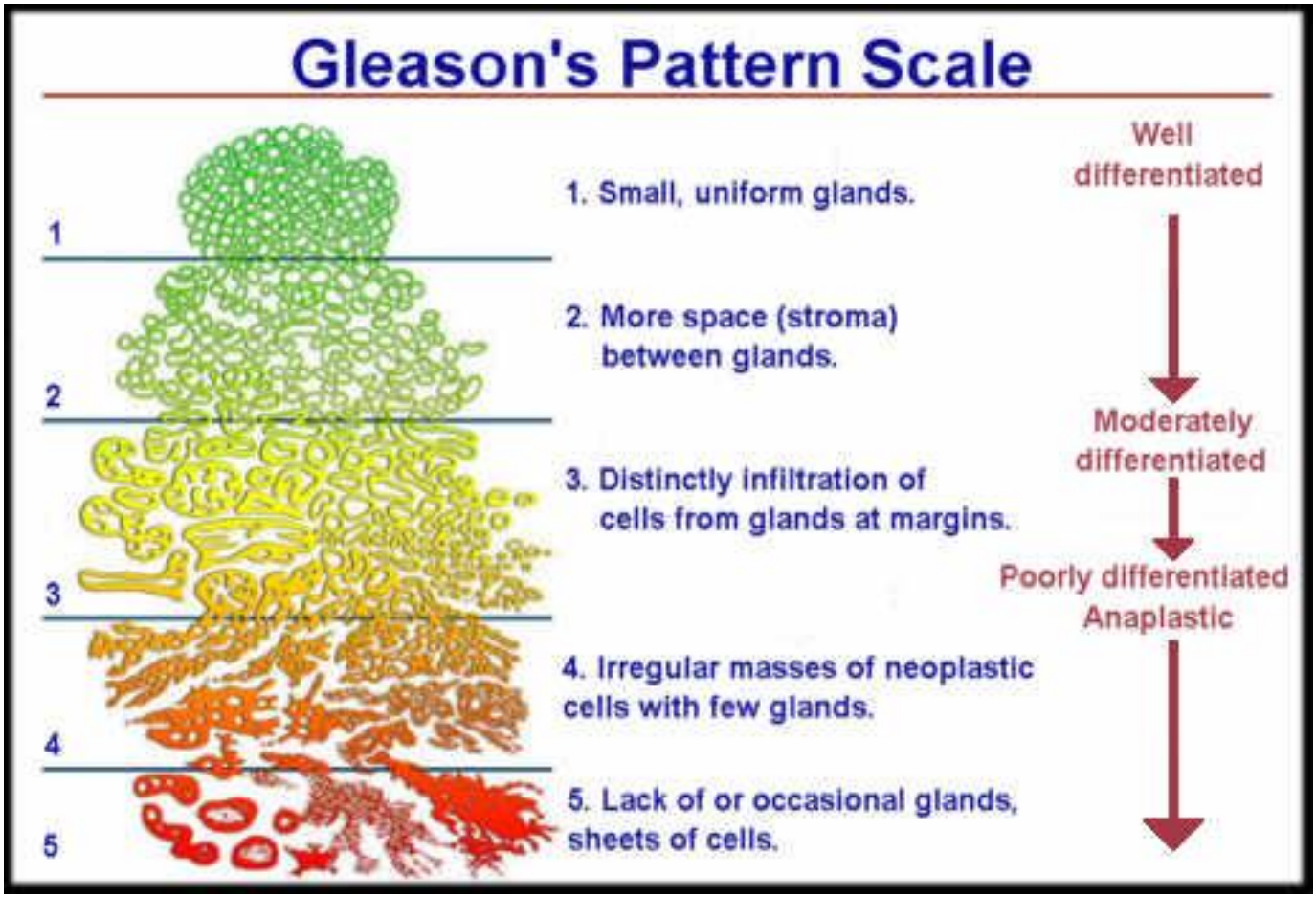
Gleason's Pattern Scale
1
2
3
4
5
1. Small, uniform glands.
2. More space (stroma) between glands.
3. Distinctly infiltration of cells from glands at margins.
4. Irregular masses of neoplastic cells with few glands.
5. Lack of or occasional glands, sheets of cells.
Well differentiated
Moderately differentiated
Poorly differentiated
Anaplastic

1.1.7 Prostate Cancer Treatment

The growth of tumor cells in prostate cancer is largely regulated by androgen receptor hormones, mainly the androgen receptor. Options of treatments include radiation, cryotherapy (freezing the cancer cells) and prostatectomy, which removes the prostate gland by surgery. Another option is Watchful waiting or active surveillance which is known as delaying the treatment especially in the older patients, small tumor volumes and lower stages disease [31]. Treatment with androgen deprivation (ADT) is widely used in metastatic prostate cancer. When this fails, chemotherapy is the last resource which is reserved for late castrate resistant state where the tumor is no longer responding to androgen blockade [32]. Castration of the prostate refers to the attempts to block the androgen receptor and thus decreasing or eliminating androgen levels in the hope of stopping or slowing down the progression of PCA [31]. This method is used in advanced and recurrent stages but eventually patients show recurrence of prostate cancer, which is complicated when prostate cancer resist hormonal blockade and re-populate regardless of the treatment [33].

1.2 Biomarkers in prostate cancer:

1.2.1 Potential Biomarkers

Micro RNAs (miRNAs) are small noncoding RNAs which are approximately 19-25 nucleotides long and have major role in protein synthesis and are not known to be translated. These miRNAs are conserved in both animals and plants [34]. They play an important biological role in apoptosis, proliferation and cell differentiation [34] and can be detected in body fluids such as plasma, urine, breast milk, serum, saliva and semen [35]. MiRNAs have been involved in several steps of cancer development and progression such as initiation, angiogenesis and metastasis [36]. The abnormality of miRNA expression was reported in different types of cancers such as breast,

ovarian and melanoma [37]. Differential expression of specific miRNAs has been reported in prostate cancer and proposed as biomarkers [38]. A review by Pang et al. [39] indicates that over 50 miRNAs have been linked to prostate cancer as either potential tumor suppressors or oncogenes. Mitchell et al. [40] showed that a specific mRNA, miRNA 141, was highly expressed in the serum of prostatic cancer patients compared with serum from normal men. Another study by Bryant et al. [41] indicated that miRNA 141 and miRNA 375 were detected in the serum of metastatic prostate cancer patient in addition to miR -574-3p and miR-107 which were detected in urine of prostatic cancer compared to normal controls.

A recent study by Walter et al. [38] on 37 patients of prostatic tumor tissue samples in comparison with normal samples shows an up-regulation of 14 miRNAs (miR-144,miR-335,miR-122,miR-193,miR-184,miR-138,miR-34,miR-198, miR-9,miR215, and miR373) where 8 miRNAs (miR-222, miR 96, miR-92, miR-148, miR-27, miR-125,miR-126, miR-) were down-regulated and there ware loss of other18 miRNA expressions.

1.2.2 Classical Biomarkers

1.2.2.1 PSA

Prostate Specific Antigen (PSA) blood screening remains the most common diagnostic test for the early detection of prostate cancer. However, PSA levels can be increased in benign disease, leading to the misdiagnosis of prostate cancer and its potential overtreatment [42].

A review by Adhyam and Gupta mentioned that even in the “normal” PSA range, there are numerous factors that affect a patient’s PSA level, such as age and race. It is normal to have a higher baseline PSA levels in older men and among African individuals, compared with middle aged Caucasians. Moreover, men with high BMI tend to have lower PSA level compared with

those who have a healthy BMI [43].

Therefore, there is a deep need to develop other, more accurate biomarkers for prostate cancer. For example, molecular biomarkers that identify genetic alteration in prostate cancer could provide useful tools to diagnose prostate cancer [44].

1.2.2.2 AMACR

Alpha methylacyl-CoA racemase (AMACR) is a mitochondrial enzyme which has a role in metabolism and is known as a growth promoter [45]. Normal endogenous *AMACR* expression is detected in liver, lung and kidney [46]. In prostate cancer; *AMACR* expression levels are increased about 7-8 fold compared to benign prostate tissue [47]. *AMACR* has been reported to be overexpressed not only in prostate but in other cancers such as bladder, colon, breast and renal cancers [48]. A study by Rubin et al. [49] showed that *AMACR* expression is associated with disease progression in prostate cancer clinical samples.

1.2.2.3 PTEN

Phosphatase and tensin homolog deleted on chromosome 10 (PTEN) is a tumor suppressor gene which has a role in cell growth, cell survival and genome stability [50]. Alterations of *PTEN* have been reported in rare genetic diseases such as Cowden Syndrome in addition to different types of cancer such as melanoma, breast cancer, thyroid and prostate cancer [51]. Loss of *PTEN* was shown to be associated with and lead to progression of prostate cancer through activation of PI3K/AKT pathway [52].

1.2.3 ERG-TMPRSS2 fusion rearrangements

The Ets Related Gene (*ERG*) belongs to the erythroblast transformation specific erythroblast transformation specific *(ETS*) family of transcription factors, which consists of 29 genes, subdivided into 13 groups [53]. The *ERG* gene consists of 17 exons and is subdivided into 5 *ERG* groups (*ERG1* - *ERG5*) [53]. The *ERG* gene has been reported to have a normal biological function in regulating cellular differentiation, cell growth and angiogenesis [54]. *ERG* fusion was first described in Ewing's sarcoma and acute myeloid leukemia [55].More recently, *ERG* gene rearrangements have been identified to be among the most common genomic aberrations in prostate cancer with the fusion between *TMPRSS2* and *ETS* family genes of transcription factors *ETV1*, *ETV4*, *ETV5* and the most common variant *ERG* [56].

The AR regulated transmembrane protease, serine 2 (*TMPRSS2*) gene has been identified as associated with *ERG* to form the most genomic alterations in prostate cancer [57]. Furthermore, it was indicated to be specific to detect and distinguish cancer from benign in prostate samples [58]. In prostate cancer, the most common types of *ERG* gene fusion with *TMPRSS2* occurs in exon 1 of *TMPRSS2* at the 5` end region and at the 3` end of exon 4 of *ERG* with deletion of 32 amino acids at *ERG's* N- terminus [59]. Figure 1.2 shows various types of *TMPRSS2-ERG* fusions that have been observed. Also, it has been reported that *PTEN* loss and *ERG* gene rearrangement may contribute to a worse outcome and poor survival in prostate cancer patients [60].

Figure 1.2 *TMPRSS2-ERG* Fusion variants.

Figure illustrates different type of *TMPRSS2-ERG* fusion. T1-E4 is the most common fusion type and it is the same variant we utilized in our cell line transfection .In addition 18 other types of *TMPRSS2-ERG* fusion has been documented. The number after "T" indicate s the exon number of *TMPRSS2* being fused with *ERG* exon. . The number after "E" indicates the exon number of *ERG* being fused with *ERG* exon The boxes with light green color illustrate last *TMPRSS2* exon and the yellow color boxes demonstrate the first exon of *ERG.* Light shading green in *TMPRSS2* represents untranslated regions, while dark shading green represents open reading frame. T represents *TMPRSS2* and E for *ERG.* figure was taken from [57] .

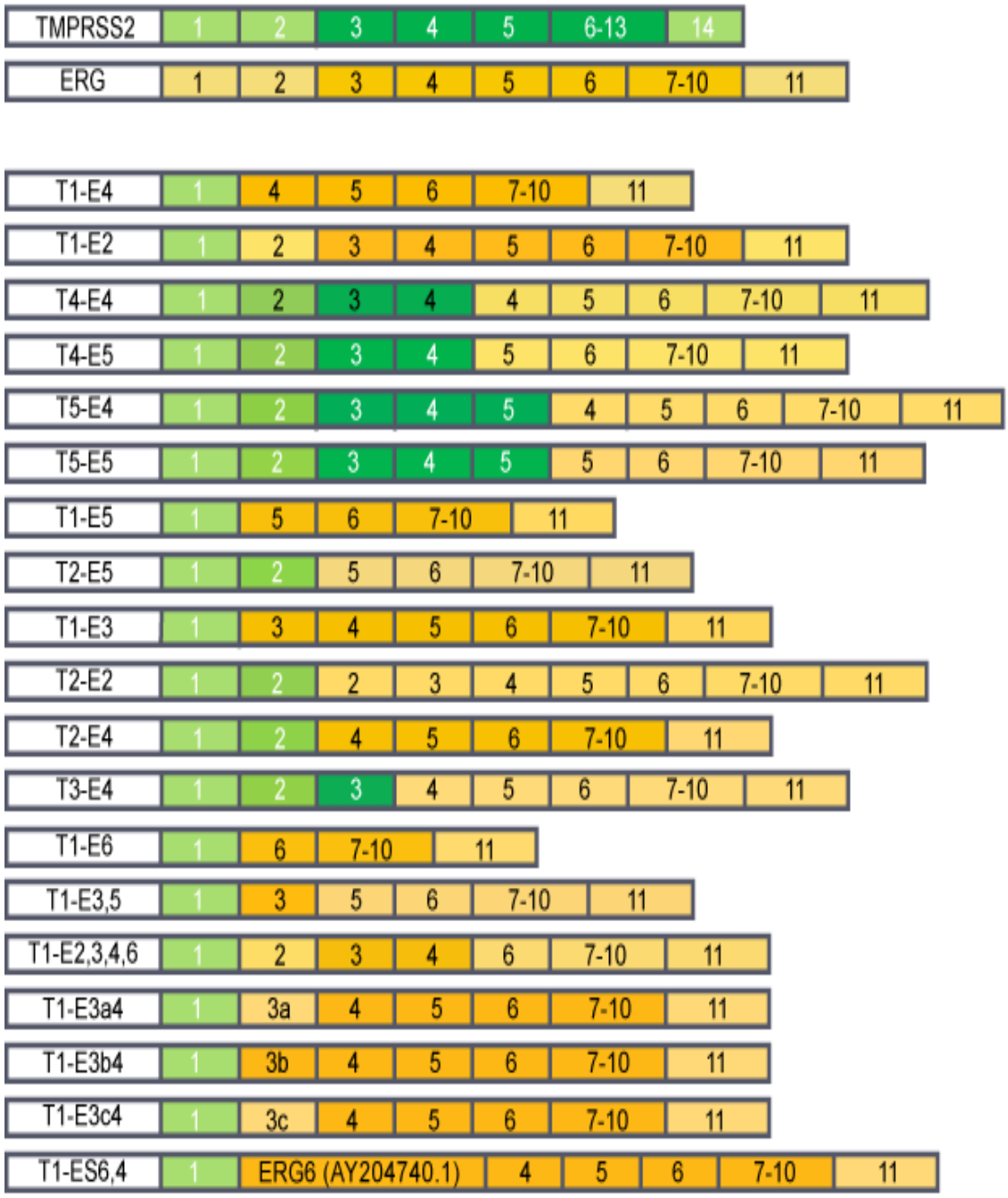
TMPRSS2 1 2 3 4 5 6-13 14
ERG 1 2 3 4 5 6 7-10 11
T1-E4 1 4 5 6 7-10 11
T1-E2 1 2 3 4 5 6 7-10 11
T4-E4 1 2 3 4 4 5 6 7-10 11
T4-E5 1 2 3 4 5 6 7-10 11
T5-E4 1 2 3 4 5 4 5 6 7-10 11
T5-E5 1 2 3 4 5 5 6 7-10 11
T1-E5 1 5 6 7-10 11
T2-E5 1 2 5 6 7-10 11
T1-E3 1 3 4 5 6 7-10 11
T2-E2 1 2 2 3 4 5 6 7-10 11
T2-E4 1 2 4 5 6 7-10 11
T3-E4 1 2 3 4 5 6 7-10 11
T1-E6 1 6 7-10 11
T1-E3,5 1 3 5 6 7-10 11
T1-E2,3,4,6 1 2 3 4 6 7-10 11
T1-E3a4 1 3a 4 5 6 7-10 11
T1-E3b4 1 3b 4 5 6 7-10 11
T1-E3c4 1 3c 4 5 6 7-10 11
T1-ES6,4 1 ERG6 (AY204740.1) 4 5 6 7-10 11

1.2.4 ERG and prostate Cancer

There are two types of *ERG-TMPRSS2* fusions. In the first type, the fusion takes place in *ERG1, ERG2* and *ERG3* with both the DNA binding domain of ETS and protein interaction domain of PNT being conserved. In the second type, the fusion occurs in *ERG8* and *TEPC* and lacks ETS domain. Both these domains play an important role in regulating target genes in different cellular processes such as proliferation, differentiation and apoptosis as reviewed in [61]. *ERG* structure, prostate cancer specific TMPSS2 –ERG transcripts type I and type II are summarized in Figure 1.3.

In clinical cohorts, *ERG* has been proposed to associated with aggressive disease; however, this is not uniformly noted in all publications, where some have documented no such prognosis or even better clinical outcome [62]. In localized PCA, Teng et al. [63] described the possible significance of ERG protein expression in localized prostate cancer reflecting higher pathological stage, however no association with biochemical relapse was noticed. A study by Demichelis et al. [64] has reported a significant association between *ERG* gene rearrangements and cancer related to death in prostate cancer patients in non-surgical cohorts.

Figure 1.3 Genomic structure of human ERG gene.

a) Shows the 17 E*RG* exons. b) Structure of known *ERG* transcripts. c) Prostate cancer specific *TMPRSS2-ERG* rearrangement transcripts: Type I containing ETS and PNT domains. d) Prostate cancer specific *TMPRSS2-ERG* rearrangement transcripts: Type II containing only PNT domain and lacking ETS domain [61]. (Image was taken from Sreenath et al. [61]).

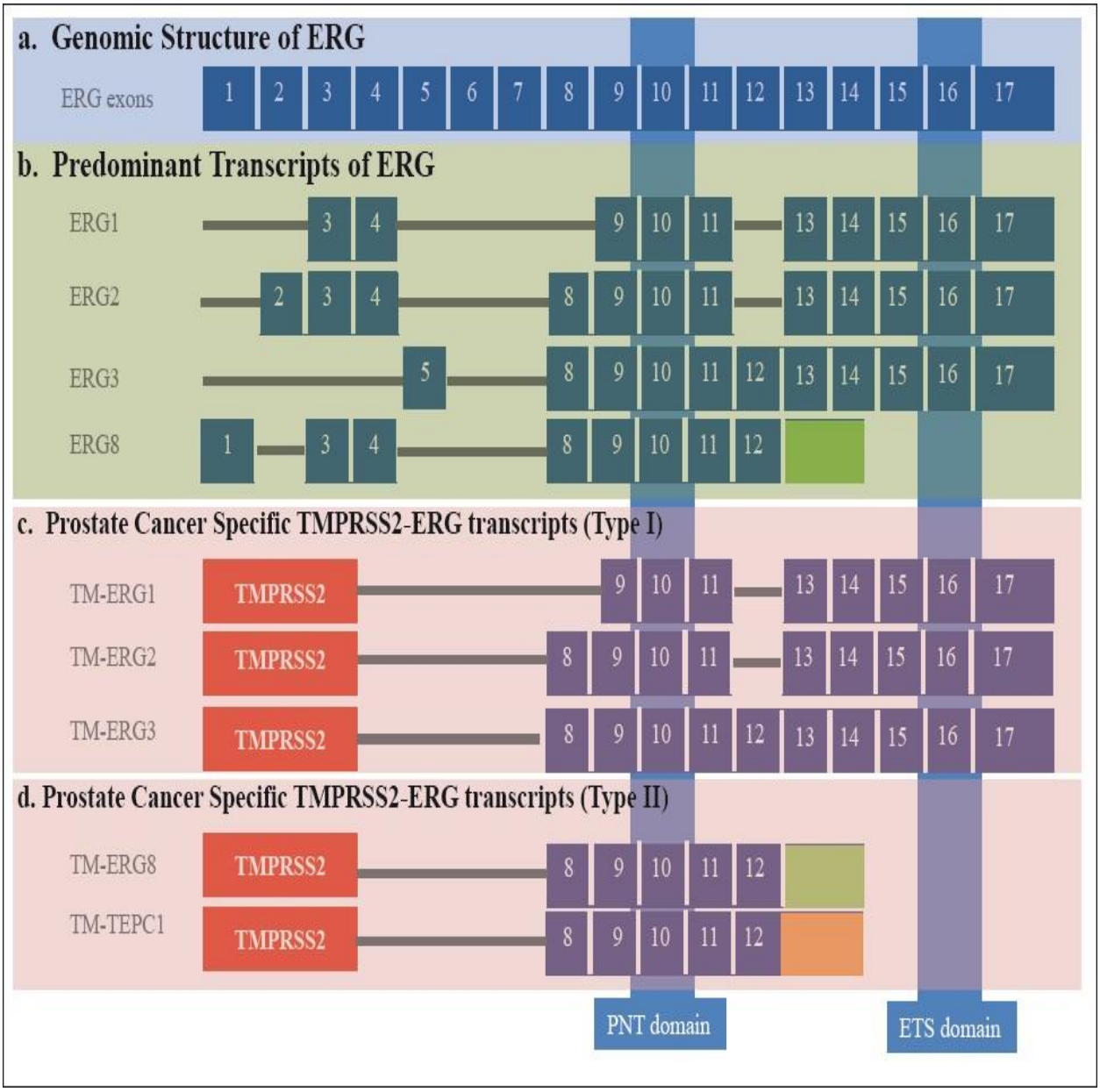
a. Genomic Structure of ERG
ERG exons
1 2 3 4 5 6 7 8 9 10 11 12 13 14 15 16 17
b. Predominant Transcripts of ERG
ERG1
3 4 9 10 11 13 14 15 16 17
ERG2
2 3 4 8 9 10 11 13 14 15 16 17
ERG3
5 8 9 10 11 12 13 14 15 16 17
ERG8
1 3 4 8 9 10 11 12
c. Prostate Cancer Specific TMPRSS2-ERG transcripts (Type I)
TM-ERG1
TMPRSS2
9 10 11 13 14 15 16 17
TM-ERG2
TMPRSS2
8 9 10 11 13 14 15 16 17
TM-ERG3
TMPRSS2
8 9 10 11 12 13 14 15 16 17
d. Prostate Cancer Specific TMPRSS2-ERG transcripts (Type II)
TM-ERG8
TMPRSS2
8 9 10 11 12
TM-TEPC1
TMPRSS2
8 9 10 11 12
PNT domain
ETS domain

1.3 ING3

1.3.1 ING family

The INhibitor of growth (*ING*) gene family encodes type II tumor suppressors, which represent the novel tumor suppressors family comprised of five conserved genes, *ING1-ING5* [65]. The *ING* family are evolutionarily conserved and related genes have been found in many different organisms such as mouse, frog, worms, yeast and human [65]. They have varied roles in different biological processes such as chromatin remodelling, DNA repair, cell senescence, apoptosis and cell cycle [66, 67].

1.3.2 ING structure

Each member of the *ING* family is located on a different chromosome [65]. ING1 is the first member of the INhibitor of Growth proteins that was identified in 1996 in the Riabowol's lab as a tumor suppressor. ING1 mapped to chromosome 13 and has 5 variants; three of which encode protein, while the other *ING* family members were identified based on the homology research [68].

ING2, the second member of the family, mapped to chromosome 4. *ING4* maps to chromosome 12 and has 8 variants, while *ING5* maps to chromosome 2 [65].

A review by Soliman at al. indicates that all ING family members have a number of conserved protein domains: a highly conserved plant homodomain (PHD), containing C4-H –C3 zinc finger domains, which recognizes the methylation of histone lysine residues at the C-terminal. The second most common domain is nuclear localization signals (NLS) domain which contains nuclear targeting signals and is responsible for targeting ING proteins to the nucleus under stress. The NLS domain also has a role in regulating cellular functions of nuclear proteins. A leucine

zipper-like (LZL) region in the N terminus functions as a protein-protein interaction mediator this domain conserved only in all 5 INGs except *ING1* and it has shown to have a role in DNA repair in *ING2*. Another domain, the lamin interacting domain (LID), has been identified, although little is known about its function. All these domains are shown in (Fig 1.4). In cancers, these proteins show altered cellular localization as it was reported for some INGs in cancers [68].

Figure 1.4 Structure of ING Family

Five types of ING proteins are demonstrated in blue rectangles boxes; all share different common domains. PHD (plant homeodomain), in green color, contains a C4HC3 zinc finger motif which has a role in interacting with the methylated form of histone H3. NLS (nuclear localization signal), in red color, regulates cellular functions of nuclear proteins. A LID (lamin interacting domain), blue color, and LZL domain (Leucine zipper-like), light green, functions as protein-protein interaction mediator. The poly basic region (PBR) orange color, is only present in *ING1* and *ING2* next to PHD and has a role in activating PHD in these proteins [68]. (Image adapted from Soliman et al.[68]).

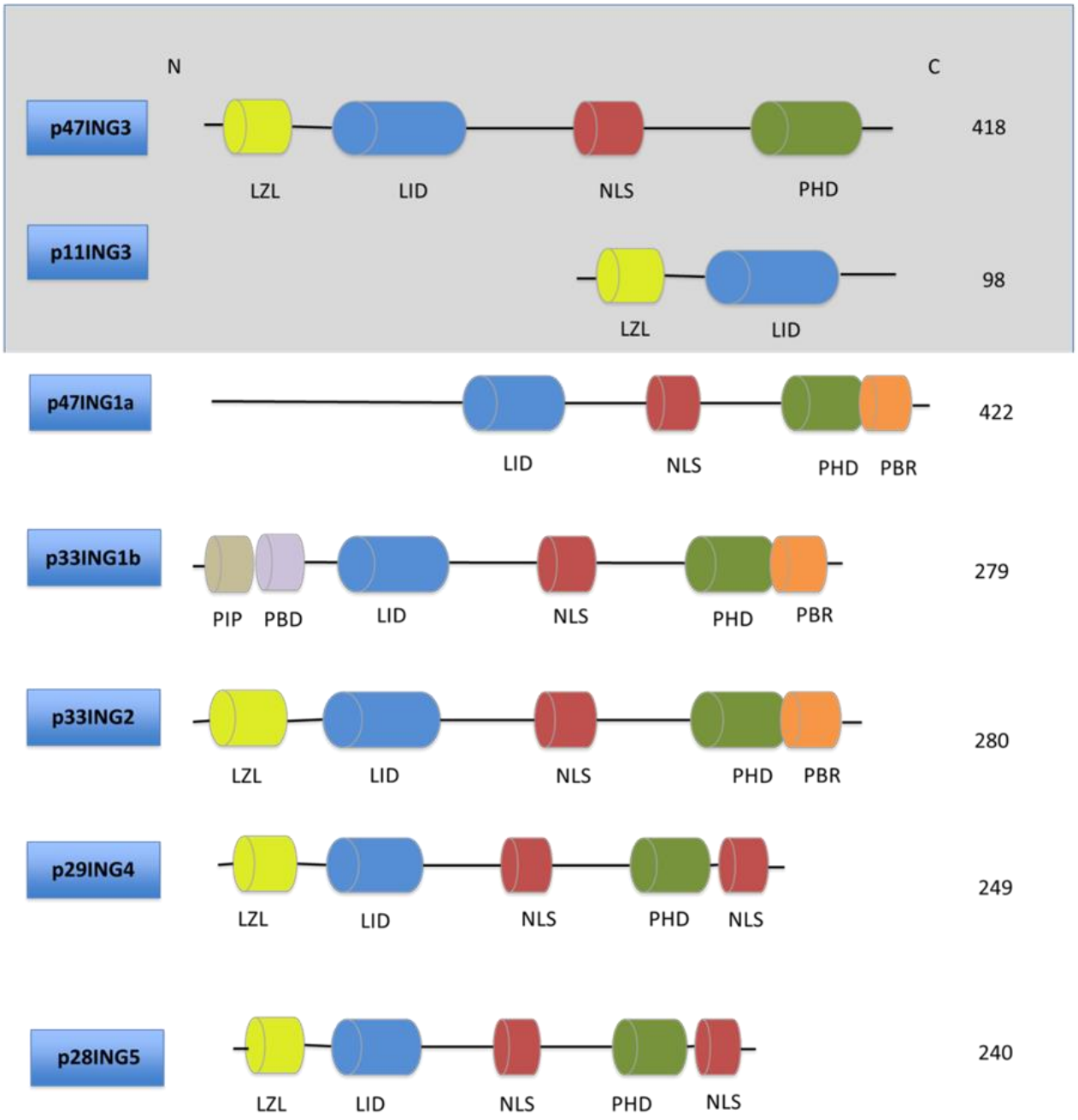
N
C
p47ING3
418
LZL
LID
NLS
PHD
p11ING3
98
LZL
LID
p47ING1a
422
LID
NLS
PHD
PBR
p33ING1b
279
PIP
PBD
LID
NLS
PHD
PBR
p33ING2
280
LZL
LID
NLS
PHD
PBR
p29ING4
249
LZL
LID
NLS
PHD
NLS
p28ING5
240
LZL
LID
NLS
PHD
NLS

1.3.3 ING family and Cancer

Alterations of INGs family members have been reported in different types of cancer. First, *ING1* inhibits growth in normal cells and its expression was found to be reduced in breast cancer [69]. ING1 was also shown to be down-regulated in other various types of cancers such as head and neck squamous cell carcinoma (HNSCC), non-small cell lung cancer (NSCLC) [70, 71] and was found to promote cellular invasion and tumor lymphatic metastasis in gastric cancer [72].The expression of ING2 was reduced in hepatocellular carcinoma, head and neck squamous cell carcinoma (HNSCC), and melanoma [73-75]. Lower *ING4* expression was detected in breast cancer samples and was associated with larger tumor sizes and higher grade [76]. Also, lower expression of ING5 was detected by IHC in colorectal carcinoma correlated with shifting in localization from nuclear to cytoplasm [77].

1.3.4 ING3 and Cancer

ING3 consists of 12 exons and encodes a 47 kDa protein with 418 amino acids and maps to chromosome 7q31 region [78]. *ING3* sequencing varies among species. For example, it shows about 90% similarity between the human and mouse ING3 protein. This percentage decreases in lesser species to 82%, 30% and 23% identified between human and frogs, worms and yeast ING3, respectively [79]. It is expressed in normal human tissues such as heart, kidney, testis, spleen, skeletal muscles, thymus, liver, peripheral blood leukocytes and placenta, while lower expression was detected in normal brain and lung tissues [80].

Deregulation of ING3 expression has been found in human head and neck squamous cell carcinomas HNSCC, hepatocellular carcinoma (HCC) and melanomas [80-82].

A study by M. Gunduz et al. [83] showed that lower level of *ING3* mRNA expression is correlated with worse prognosis in head and neck cancer patients. Moreover, they indicated that there are no significant correlations between ING3 and smoking, age or sex of patients. ING3 was also reported to be deregulated in 18 liver tumor derived cell lines and in three randomly selected pairs of HCC tissue samples compared with normal liver cell lines and normal hepatic tissue, respectively [84]. M. Nagashima et al. [78] used *ING3* overexpressed in poorly differentiated colon carcinoma derived cell line RKO that contain wild type P53 and RKO-E6 with inactivated p53 *ING3* to study its biological function. They indicated that *ING3* could inhibit cell growth by controlling cell cycle control and inducing apoptosis in a p53 dependent manner.

ING3 has been studied in some cancers as shown in (Table 1.1). However, neither the role of *ING3* in prostate cancer, nor its correlation with *ERG* gene rearrangements has been elucidated.

Table 1.1 Expression of ING3 in different cancers

Type	Expression	Experiments	Reference
Liver	**down**	**IHC/ mRNA**	Lu et al (2008) Yang HY et al (2012)
Head and neck cancer	**down**	**mRNA/survival**	Gunduz M et al (2008)
Melanoma	**down**	**IHC/5-year survival**	Wang Y et al (2007)

Acetylation of histone mechanism has important roles in cell cycle, DNA repair and gene transcription regulation by remodelling the chromatin structure [85]. Alteration in the human NuA4/Tip60 histone acetyltransferase (HAT) complex is a common feature contributing to different types of cancers including prostate cancer [86]. ING3 is a stable subunit of the HAT complex and is required for acetylation of chromatin substrates [87]. A study done by Fortson et al. [88] indicated that *ERG* binds to HAT and inhibits its function in VCaP prostate cell lines, which suggested the role of *ERG* in deregulation in protein acetylation.

1.3.5 Previous work related to our proposal

Our initial observation from microarray expression profiling of 38 prostate cancer patients comparing tumors with positive *ERG* rearrangement (ERG1) versus *ERG* rearrangement negative tumors *(ERG0*) is shown in (Fig 1.5). 10 potential genes candidates were identified to be differentially deregulated between the two groups. One of the genes, *ING3*, was down-regulated in about 50% of *ERG* positive prostate cancer samples in comparison to *ERG* negative ones. However, to date, the role and function of *ING3* in prostate cancer as well as its relationship to *ERG* gene rearrangements has not been studied.

Figure 1.5 Heat map of 10 top deregulated genes predicting ERG rearrangement status.

A) Heat map gene expression based on analysis performed on groups of prostate cancer samples with known *ERG* status; where (*ERG*=0) refers to no *ERG* rearrangements and (*ERG*=1) indicate positive *ERG* rearrangements. Microarray analysis identified potential 10 genes to be deregulated between the two groups.

B) Magnified portion of the map highlighting *ING3* mRNA expression, which is the main gene investigated in this study. Samples are reorganized based on *ERG* status (the image proved by Mr. Mohamed Alshalalfa).

A

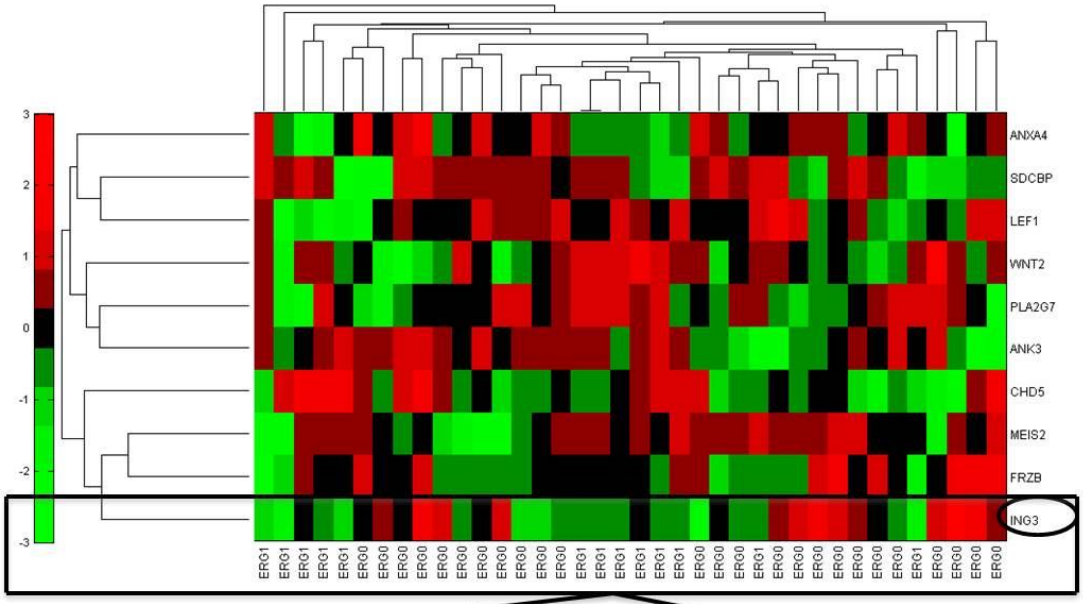
3
2
1
0
-1
-2
-3
ANXA4
SDCBP
LEF1
WNT2
PLA2G7
ANK3
CHD5
MEIS2
FRZB
ING3
ERG1
ERG0

B

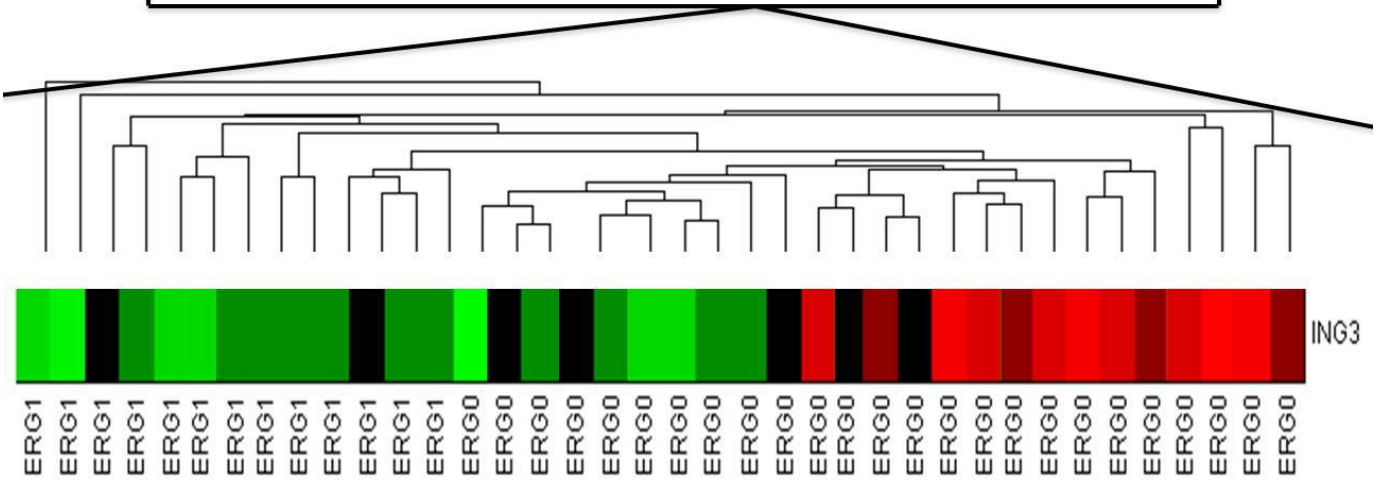
ING3
ERG1
ERG0

1.3.6 Hypothesis and objectives

Based on the microarray gene expression profiling of *ING3* on specimens with known *ERG* status, we hypothesized that down-regulation of *ING3* mRNA levels is potentially associated with *ERG* gene rearrangement and that it could have a potential prognostic value in prostate cancer.

Objectives:

1. Determine expression levels of ING3 protein and mRNA and its localization in normal and prostate cancer cell lines.
2. Investigate the potential relationship between *ERG* gene rearrangements and *ING3* levels and localization in clinical samples and prostate cell lines
3. Investigate ING3 expression and its subcellular localization in prostate tissue samples in relation to disease progression and clinical outcome.

Chapter Two: Materials and Methods

2.1 Cell lines

Human PCA cell lines DU145 and PC-3 and HEK-293 cells were provided by Dr. Don Morris (Translational Labs, University of Calgary, Alberta, Canada). RWPE-1 and VCaP cell lines were purchased from American Type Culture Collection (ATCC; Manassas, CA, USA). Prostate cancer cells (PC-3, DU145 and LNCaP) were grown in RPMI 1640 medium (GIBCO life technology, Grand Island, NY, USA) supplemented with 10% FBS (GIBCO) at 37°C in 5% CO_2 atmosphere. The VCaP cell line (ATCC) was maintained in DMEM (GIBCO) with 10% FBS. RWPE-1 cells were grown in Keratinocyte-Serum Free Medium (K-SFM, GIBCO Catalogue Number 17005-042). RWPE-1 GFP (control), RWPE-1 ERG, PC-3-Luciferase and PC-3-ERG (in which ERG is stably transfected) were kindly provided by Dr. Felix Feng, University of Michigan. Human embryonic kidney HEK293 cells were transfected with *ING3* pc DNA, and used as positive control in both the Western blot and immunofluorescence experiments. List of used prostate cell lines and expression of AR, PTEN and ERG on these cells is shown in Table 2.1.

2.2 Mycoplasma test

Mycoplasma is a type of bacteria that lacks a cell wall and can induce pathogenicity in mammalian cells. Contamination with Mycoplasma affects many types of cell lines including prostate cell lines, where it was reported that this bacteria has the ability to transform benign prostate cells into malignant ones, both *in*-vivo and *in*-vitro [89]. Therefore, prior to using the cell lines for any experiments, cells underwent a mycoplasma detection test using the LookOut®

Mycoplasma PCR Detection Kit (Catalogue number MP0035, SIGMA-ALDRICH, St. Louis, MO, USA). According to the manufacturer's instructions, the supernatant from the cell culture of each cell line was tested directly by preparing PCR samples. First, a mix of DNA polymerase and rehydration buffer, 0.5 µl and 22.5 µl respectively, were prepared for each reaction. Negative and positive control transparent reaction tubes were included in the kit where the tubes contained primers, nucleotides, and internal control DNA. In the provided tubes, we added 23 µl of DNA polymerase/ rehydration buffer and 2 µl of RNA-free water as a negative control or 2 µl of sample. For positive controls, which are in the pink provided tubes, we added 25 µl of the mix. Then, all samples, including the positive and negative controls, were preceded to the PCR reaction and run in agarose gels. For negative samples, the band shows at 481 bp in the electrophoresis gel, and the mycoplasma positive samples will show bands in the range of 270 ± 8 bp. All cell lines used in this study were mycoplasma negative, while any positive samples were terminated to avoid any contamination.

Table 2.1 Expression of *AR*, *PTEN* and *TMPRSS2-ERG* in prostate cell lines used in this study

Cell Line	Type of Prostate Cell line	AR	PTEN	TMPRSS2-ERG
RWPE-1	HPV-18 immortalized prostate cell line	+	+/+	-
LNCaP	Lymph node metastasis	+	-/-	-
VCaP	Vertebral metastasis	+	+/+	+
PC3	Bone metastasis	-	-/-	-
DU145	Brain metastasis	-	+/-	-

2.3 Cell culture

Cell lines were stored in a 10 % Dimethyle Sulphoxide DMSO (D2640) solution (Sigma, St. Louis, MO, USA) at -80^{o} C for a few months or in liquid nitrogen for extended periods of time. Cell culturing commenced with the sterilization of the Biosafety cabinet and all related working areas. All working steps for cell culturing were performed inside the hood and all materials used including gloves, were sterilized with alcohol to avoid contamination. The vials of frozen cells were thawed quickly in a 37^{o}C water bath and transferred to 15 or 50 ml tubes (BD Falcon, Franklin lakes, NJ, USA) containing 8-10 ml of the proper medium and centrifuged at 1000 rpm for 8 minutes. The supernatant was discarded to remove DMSO and only the cell pellets were re-suspended in 3-5 ml of media. The cells were then transferred to a flask that contained extra media, 10-15 mls depend on the flask size, and placed in the incubator for 1-2 days. After

reaching 70-80 % confluence, cells were passaged to second plates after trypsinizing them with 0.25% Trypsin –EDTA (GIBCO by Lifetechnology, Grand Island, NY, USA) for 3-5 minutes in 37 C^o incubator. To deactivate trypsin action, FBS containing medium (or Trypsin inhibitor (Glycin Max T6414) (Sigma, St. Louis, MO, USA) for RWPE-1 cells) was added to the cells. Subsequently, the cell suspension was transferred to a Falcon tube and centrifuged for 8 minutes at 1000 rpm. After centrifuging, the supernatants were discarded and 3-5 ml of required media was added to re-suspend the pellets. Cells were then diluted 1:4-1:5 in 10 cm cell culture dishes (CELLSTAR® Greiner Bio-One GmbH, Frickenhausen, Germany). When cells reached ideal confluence, they were ready for both protein and RNA extraction.

2.4 Antibodies

Different mouse monoclonal antibodies were used in this study. ING3 2A2 is a house made antibody made in the University of Calgary Antibody facility. Androgen receptor AR (sc-7305) and α tubulin (sc-53646) were purchased from Santa Cruz Biotechnology (Santa Cruz, CA, USA). GAPDH (14C10) were purchased from Cell Signalling Technology (Beverly, MA, USA). Rabbit polyclonal antibodies were also utilized. ING3 (10905-1AP) was purchased from Proteintech (Proteintech Group, Inc. Chicago, IL, USA). ERG (sc-353) and Lamin A (sc-20680) from Santa Cruz Biotechnology (Santa Cruz, CA, USA). In addition, the following Rabbit monoclonal antibodies were used: PTEN (138G6) and β actin (13E5) from Cell Signalling Technology (Beverly, MA, USA).

2.4.1 ING3 Antibody (2A2)

ING3 (2A2) is a mouse monoclonal antibody and was generated as following: 5 mice were injected intraperitoneally (IP) with 10 µg of human ING3 protein twice, two weeks apart. Ten days after the injection, a blood test was performed using ELISA to analyze the serum. The best mice are sacrificed and spleens are fused to Sp2/mIL6 myelomas using PEG 1500. Cells were then plated into 96 well plates and left for 12 to 14 days for colonies to grow. The positive wells are sub-cloned to give single cells. Once the single cell colonies grow to a testable size, they are re-screened by ELISA. Positive colonies are grown to a larger volume; cells are frozen and supernatant is saved for further use [90].

2.4.2 HEK-293 cell line control

In this study, human embryonic kidney HEK-293 cell lines transfected with ING3 plasmid were used as positive control in both the Western blot and immunofluorescence experiments. In addition, HEK293 with suppressed ING3 were used as a negative control to confirm the correct molecular weight band of ING3 in Western blot.

2.4.2.1 Overexpression of ING3 in HEK-293 cell lines

HEK-293 cell lines were maintained in DMEM medium (GIBCO) supplemented with 10% FBS. Cells were cultured and were infected the following day with 10µl ING3 plasmid and 5µl GFP in diluted Lipofectamine 2000 lipofectamine® RNAiMAX Reagent (Invitrogen, Life technology, Carlsbad, CA, USA) with Optimum Opti-MEM (GIBCO, Life technology, GrandIsland, NY, USA). After 48 hours, cells were harvested and the protein was collected for Western blot analysis, for both total cell protein and fractionation methods.

2.4.2.2 Knocking down ING3 in Cell lines

HEK-293 and Du 145 cell lines were cultured in 6 well plates and grown to 70% confluence. Cells were transfected with 15µl lipofectamine 2000 diluted in 235µl of opti-MEM and incubated at room temperature for 5 minutes. In three separate sterile tubes, ING3 siRNA with different concentrations and GFP were diluted with opti-MEM and added to the cells. A siRNA-control with GFP was also added in one of the wells.

2.4.3 Overexpression of ERG

RWPE-1 and LNCaP Cells were seeded at $6x10^5$cells/well in 6-well plates. On the next day, cells were transfected with 2.5µg of *GFP* or *TMPRSS2-ERG* DNA using 6µg of lipofectamine LTX (Invitrogen) and 250 ml of Opti-MEM (GIBCO) per well. Cells were harvested for 48 hours after transfection and Western blot was performed using 20µg of each protein sample.

2.4.4 Knocking down ERG in VCaP cell lines

VCaP cells were seeded in 6 well plates and transfected on the second day. 500mg of opti-MEM containing 30mg of lipofectamine was mixed with either 500mg of opti-MEM containing 5ml of non-targeting siRNA (Non-targeting pool Thermo Scientific Dharmacon ® On-target plus® Control pool) or 5 µl of ERG siRNA (Hu-ERG form Sigma, St. Louis, MO, USA) and incubated for 5 minutes at room temperature. This mix was added drop wise into the cells after changing the media and incubated for 24, 48 and 72 hours to see results.

2.4.5 Protein Extraction

2.4.5.1 Protein Extraction from cell lines

Cells were cultured in 37^{o}C in 5 % CO_2 atmosphere until 70-80 % confluence is reached. After 3 washes with ice-cold phosphate buffered saline (PBS), cells were scraped from the plate on ice and collected in 10 ml PBS and centrifuged for 10 minutes at 4^{o}C. 500µl RIPA lysis buffer (R0278) (Sigma, St. Louis, MO, USA), supplemented with protease inhibitor cocktail tablets EDTA-Free complete mini (Roch, Mannheim, Germany) was added to the cells. Pellets were mixed by pipetting in an up and down motion. Protein lysates were then sonicated and subsequently centrifuged at 15,000 rcf for 15 min at 4^{o}C. The supernatant was transferred to fresh pre-chilled tubes. Protein concentration was determined using the Quick Start Bradford Protein Assay Kit (Bio-Rad Laboratories Inc. Hercules, CA, USA).

2.4.5.2 Protein Extraction from tissue samples

To extract protein from tissue, samples were subjected to Illustra Triple Prep Kit (GE Healthcare UK limited, Buckinghamshire, UK) according to the manufacturer's protocol. We used the protein isolation which was the last step of the protocol. After samples were homogenized and lysed, they underwent different steps of DNA binding, RNA binding, protein precipitation, protein wash, protein re-suspension and finally protein isolation. Later, the protein samples were used in Western blot analysis.

2.4.6 Nuclear and cytoplasmic fractionation

To investigate the localization of ING3 in cell lines and tissue samples, the fractionation method was applied in all cell lines and tissue samples.

2.4.6.1 Nuclear and cytoplasmic fractionation for cell lines

Nuclear and cytoplasmic protein fractionations were isolated using a Rapid, Efficient And Practical (REAP) method for subcellular fractionation of primary and transformed human cells in culture [91]. The confluent cells were placed on ice and the media was aspirated and discarded. Cells were then washed twice with cold PBS. One ml of PBS was added to the plate and cells were harvested and collected in 1.5ml microtubes (MCT-150) (AXYGEN Inc. Union City, CA, USA). Following centrifugation and discarding the supernatant, 1ml of 0.1% NP40 was added to the cells and pipetted for 5 times, and 300µl was collected in a tube and labelled as whole cell lysate (W). The remaining supernatant was centrifuged for 10 seconds at 10000 rpm and another 300µl were transferred in a clean tube and labelled as cytoplasmic (C). The remaining 600µl supernatant was discarded and 1 ml of NP40 solution mix was added to the pellet and re-suspended and centrifuged again for 10 seconds at 1000 rpm. The entire supernatant was discarded and 200µl of 1X of Laemmli sample buffer was added to the pellet; the tube being labelled as nuclear portion (N). 100µl of 4X Laemmli buffer was added to the cytoplasmic and whole cell lysate. The whole cell lysate and the nuclear fraction were sonicated using microprobes (Misonix, NY, USA) at level 2, twice for 5 seconds each. Subsequently, all three tubes were boiled for 1-2 minutes. For the Western blot loading, 10µl, 10µl and 5µl of whole cell lysate, cytoplasmic and nuclear fractionations were used, respectively.

2.4.6.2 Nuclear and cytoplasmic fractionation for tissue

For tissue fractionation, frozen tissue samples were cut in 3X5 mm and put in a 1.5ml tube submerged in liquid nitrogen. The samples were smashed using a 2 ml tissue grinder from WHEATON (Millville, NJ USA) and then the REAP method for subcellular fractionation was

performed using the manufacturer's protocol for cell lines with only minor modifications in the amount of solution that was used. Anti- α –tubulin and anti- lamin A antibodies (Santa Cruz Biotechnology Inc. Santa Cruz, CA, USA) were used as cytoplasmic and nuclear protein markers, respectively, in cell lines and tissue samples.

2.4.7 Western blots

The protein concentration of the samples was determined using Quick Start Bradford Protein Assay Kit (Bio-Rad). The samples were diluted to the same protein concentration and an equal volume of 4X loading buffer was added. Equivalent quantities of protein (30 mg) were separated by 10% SDS-polyacrylamide gel. Following transfer to Polyvinylidene Fluoride Immuno-blot ^{TM}PVDF (Bio-Rad) membrane in the transfer buffer for two hours at 100V on ice, the membrane was incubated with a blocking buffer (2.5g of powdered skim milk or Bovine Serum Albumin (BSA) (AMRESCO, Ohio, USA)) diluted in 50 mL PBS/0.1% Tween 20 (Sigma)) for overnight in 4° C or 1 hour at room temperature with constant shaking. After that, the membrane was incubated with the primary antibody for 30 minutes with anti ING3 antiserum 2A2 at room temperature or overnight at 4° C for other proteins of interest. The following primary antibodies were used for this study: anti-ING3 2A2 Ab house made (Raibowol's lab, Antibody facility University of Calgary) , ERG 1/2/3 sc-353(Santa Cruz Biotechnology) (1:500), Lamin A sc-20680 (Santa Cruz Biotechnology) 1:1000 , α-tubulin sc-53646 (Santa Cruz Biotechnology) (1:2000), GAPDH-14C10 (Cell Signaling,) and β-actin13E5 (Cell Signaling) (1:5000). The membranes were washed 3 times for 10 minutes each with Tris Buffered Saline with Tween 20 (T-BST buffer). The membranes were then incubated with either Anti-mouse IgG- HRP- linked antibody or Anti-rabbit IgG-HRP- linked antibody (Cell Signaling) (1:10,000) in the blocking

buffer for 1-2 hours at room temperature. After 3 washes with TBST (5 minutes each), the membrane was covered with ECL (GE Healthcare, Buckinghamshire, UK) for 2-3 minutes, exposed to X-ray film (Amersham Hyperfilm ^{TM} ECL, Buckinghamshire, UK) or FUJI Medical x-ray film FUJIFILM Corporation, Tokyo, Japan) in the dark room and developed by a Kodak X-OMAT 2000A Processor (Carestream Health, Inc, Rochester, NY, USA) for appropriate time. List of used antibodies is summarized in Table 2.2.

Table 2.2 Antibodies used in Western Blot experiments

List of antibodies used in this study for Western blots analysis with details of suppliers and dilutions used and the proper secondary antibodies

Primary antibody	Supplier	Catalogue Number	Dilution	Secondary antibody
ING3	Proteintech	10905-1-AP	1:500	Anti-rabbit Cell Signaling
ERG 1/2/3	Santa Cruz Biotechnology	sc-353	1:500	Anti-mouse Cell Signaling
Lamin A	Santa Cruz Biotechnology	sc-20680	1:1000	Anti-rabbit Cell Signaling
α-tubulin	Santa Cruz Biotechnology	sc-53646	1:2000	Anti-mouse Cell Signaling
AR	Santa Cruz Biotechnology	sc-7305	1:1000	Anti-mouse Cell Signaling
PTEN	Cell Signaling	138G6	1:500	Anti-rabbit Cell Signaling
GFP	Santa Cruz Biotechnology	Sc-9996	1:500	Anti-mouse Cell Signaling
GAPDH	Cell Signaling	14C10	1:5000	Anti-rabbit Cell Signaling
β-actin	Cell Signaling	13E5	1:5000	Anti-rabbit Cell Signaling

2.4.8 RNA Extraction

After cells reached confluence in 10 cm cell culture dishes (CELLSTAR®), they were placed on ice. The media was aspirated and discarded. Cells were washed twice with cold PBS. Subsequently, 700µl of Trizol® Reagant (cat No. 15596062, Life-technology, Carlsbad, CA, USA) was dropped on the plate and cells were scraped with clean cell lifter (Costar Corning Incorporated, NY Mexico). They were then collected in 1.5 ml microtubes (AXYGEN Inc) and vortexed for 1-2 minutes. Tubes were left at room temperature for 5 minutes then 140 µl of chloroform was added. After shaking the tubes for ten to fifteen seconds, they were placed on a rack at room temperature for 3 minutes and then centrifuged for 15 minutes at 12,000 g at 4^{o} C. After centrifugation, the samples were separated into three layers. The upper colorless layer, which contains RNA, was transferred into a new collection tube where 525 µl of 100% of ethanol was added, mixed and centrifuged for 15 seconds at room temperature, followed by steps of washing and separating. After the series of washing and separating, the final tube would contain total RNA of interested cell lines.

2.4.9 cDNA

RNA was extracted from all cell lines with miRNeasy ®mini Kit (Qiagen sciences, Maryland, USA mat Number 1038703). After extracting RNA from the cell lines, the samples were quantified using a NanoDrop spectrophotometer (Nano drop 2000 by Thermo Scientific) to determine RNA concentration. The cDNA was synthesized from 1 µg of total RNA using qScript™ cDNA SuperMix (Quanta BioSciences TM, Gaithersburg, MD, USA) by Authorized Thermal Cycle eppendorf.

2.4.10 Real-time reverse transcription (RT)–PCR

mRNA analysis of ING3 and ERG in cell lines and tissue samples was performed according to standard qRT-PCR procedures using the PerfeCta ®SYBR® Green FastMix® ROX according to the manufacturer protocol (Quanta BioSciences TM) using StepOne Real time PCR system (Applied BioSystems, CA, USA). In 96 well plates, each sample was triplicated. Each well contained 2.5µl cDNA, 1µl each of forward and reverse primer, 10µl SYBER green and 5.5µl of DNAase and RNAase free water. The expression of GUSB was used for normalization. Mean Ct was always determined from triplicate PCRs and statistical significance was determined from three independent experiments. Primer sequences of the genes tested by real time PCR are shown in Table 2.3.

Table 2.3 Primer sequences of genes tested by qRT-PCR

Gene	Forward sequence	Reverse sequence
GUSB	CGTCCCACCTAGAATCTGCT	TTGCTCACAAAGGTCACAGG
ING3	CGACAGCGAGTGACACAAAT	ATCCATTGCATTCTGCACCT
AR	CTCCCCAAGCCCATCGTAGA	GAGGATGTCTTTAAGGTCAGCG
TMPRSS2-ERG	TAGGCGGAGCTAAGCAGGAG	GTAGGCACACTCAAACAACGACTGG

2.4.11 Invasion assay

The CytoSelect ^{TM} 24-well cell invasion assay Basement membrane, Flourometric Format kit (Catalogue number CBA-111, Cell Biolabs, Inc San Diego, CA. USA) was used to determine the invasion ability of DU145 cells. The invasion Chamber plate was brought to room temperature for 10 minutes. 0.3 mL of serum free DMEM media (37 °C) was applied to the interior of the inserts and allowed to rehydrate for 1 hr at room temperature. Then, this was discarded carefully and 0.5 ml of DMEM containing 10% FBS was added to the lower wells and 0.3 mL of DU145 cell suspension in free serum media (5 x104 cells/mL) was added to the interior of the insert. The chambers were incubated for 24 hrs. in a humidified tissue culture incubator (37^{o}C, 5% CO2) to allow cells for invasion. Then, each insert was placed into a new well containing 225µl of Cell Detachment Solution and was incubated for 30 minutes at 37°C.

Later, 75µl of a 4X Lysis Buffer/ CyQuant GR dye solution was added and the plate was incubated at room temperature for 20 minutes. 200µl of the mixture was transferred into a 96 well plate and was read for fluorescence at 480/520 nm. Therefore, only cells that have efficiently passed through the membrane were detected.

2.4.12 Wound-healing Assay

A wound was created on a monolayer of confluent cells cultured in six-well plates by the scratch of a p200 pipette tip. The wounded monolayer was then washed twice with fresh PBS to remove debris, and then cell culture media were added. At that point, cell-free space was compared by images taken by Moticam Pro camera (Hong Kong, China) at different times 0, 6, 24 hours.

2.4.13 Immunofluorescence staining

2.4.13.1 Immunofluorescence staining for cell lines

Cells were seeded on sterile glass coverslips to 50% confluence. After 24 hours of attachment, they were fixed at room temperature in 4% paraformaldehyde in PBS for 15 minutes and then washed three times in PBS. Cells were permeabilized for 10 minutes in a 0.2 – 0.5 % solution of Triton X-100 and blocked in 1% Bovine Serum Album BSA (AMRESCO Biotechnology). After a series of washes with PBS, the coverslips were incubated with primary antibody ING3 (Antibody facility University of Calgary) for 15 minutes and then washed in PBS three times for 5 minutes each. This was followed by one hour incubation with Alexa Fluor 568 goat anti-mouse secondary antibody Molecular Probes (Invetrogen). The coverslips were mounted on glass slides using a ProLong® Gold Antifade Reagent with DAPI (Invetrogen) to label the nuclei.

2.4.14 Tissue Samples

In this study, the expression of ING3 in prostate tissue samples was determined. Normal human kidney tissue was used as a positive control for localization of ING3 in the tissue by immunohistochemistry and Western blot.

2.4.14.1 Patients Samples and Study population

Two tissue microarray (TMA) cohorts of male patients comprised of benign cores (n=83), incidental PCA cores (n=233), Advanced prostate cancer AdvPCR cores (n=173) and castration resistant prostate cancer (CRPC) cores (n=126) between 2005 and 2008 were used in this study. Each cohort consisted of an average of two cores per patient ranging from 2 to 4 cores, the total cores being 615. All blocks were assembled without prior knowledge of any clinical or

pathological staging information. Clinical and pathologic data were obtained with approval from the institutional review board at the University of Calgary, Faculty of Medicine, Calgary, Alberta. These TMA were placed on a slide and the core diameter was 0.6 mm and the distance between each one is 0.5 mm. After construction, 4μm sections were cut then stained with H&E for histological diagnosis. Later protein ING3 expression was analyzed.

2.4.14.2 Manual scoring of ING3 expression

To assess expression of ING3 in clinical samples, all tissue microarray cores were examined under the microscope and a diagnosis was determined (i.e., benign, high-grade intraepithelial neoplasia, or prostate cancer) by the pathologist (Dr. Bismar). Protein expression of ING3 was determined using AQUA system based on percent area of the nuclear mask that was also positive for ING3 based on the ING3 mask, while, protein expression of ERG and AR was evaluated using a four-tiered system (0, negative; 1, weak; 2, moderate; and 3, strong) expression.

2.4.15 H&E staining for paraffin-embedded tissues

The paraffin-embedded tissues were cut in five-micrometer sections and placed in a warm water bath. Then the sections were transferred onto slides and labelled with the same block numbers. After the slides dried, they were incubated in a hot air oven at 37^{o}C overnight followed by emersion in two Xylene baths and incubated for 5 minutes each for de-parafinization. The slides were rehydrated in descending concentration of alcohol starting with absolute ethanol for 2 minutes then 95% ethanol for 1 minute and 70% for one minute. After rinsing in running tap water for one minute, slides were placed in Haematoxylin for 3 minutes and washed in running tap water, again. Slides were then stained with Eosin for 30 seconds and washed in running tap

water for a short time. The slides were then passed through a series of ascending concentrations of alcohol for dehydration starting with 70% through 95% and then absolute; the same concentrations that had been used in the rehydration process. Slides were kept in two different Xylene baths. Excess Xylene was removed with paper tissue and the slides were placed in a tray. A drop or two of mounting medium or liquid cover slip from Lener Laboratory (Cat # 137703, Pittsburgh, PA, USA) was added for mounting and slides were covered with a cover slip and left to dry before microscopy examination.

2.4.16 Frozen tissue sectioning:

Prostatic tissue biopsies were embedded in cascades blocks with Optimal Cutting Temperature OC clear frozen section compound catalogue number 95057-838 VWR® Frozen Section Compound (VWR International, West Chester, PA. USA). Blokes kept on dry ice for 20-30 minutes, and then samples were sectioned 4-5 µm using cryotome cryostat -20C. Sections were placed on slides and labelled with matched blocks then went for staining or kept on -80C until time of using.

2.4.16.1 H&E staining for frozen tissues:

After placing the sections on slides, they were kept in -80^{o}C or directly went for staining. First, they were dipped in Alcoholic formalin for one minute and rinsed with tap water. Slides were placed in Haematoxylin for 4 minutes and rinsed with tap water followed with 6-10 seconds in Eosin then 10 seconds of 100% ethanol twice. Slides were mounted and covered with cover slips and kept in the fume hood for drying overnight.

2.4.17 Immunohistochemistry

Five micrometer paraffin embedded sections were placed on slides and incubated with sodium citrate antigen buffer (10 mM pH 6.0) for 40 minutes. Then slides were kept in room temperature to cool down for about 20-30 minutes. The immunohistochemical experiments were performed using automated Ventana autostainer. Slides were incubated with ERG rabbit monoclonal antibody (Epitomics, clone EPR 3864) at 1:50 dilution. Before the staining, heat-induced antigen retrieval was carried out by a vegetable steamer in sodium citrate antigen retrieval buffer (10 mM pH 6.0) for 40 minutes, followed by cooling down to room temperature for about 20 minutes. Slides were incubated for 60 minutes at 37C with the ERG antibody and a Ventana iView DAB detection kit (Ventana, Tucson, AZ) was used for horseradish peroxidase detection and counterstain. Negative control was performed by omitting the primary antibody and substituting it with normal mouse 1/200 pre-diluted serum (Ventana). This experiment was provided by Ms. Shohung Liu.

2.4.18 Quantitative fluorescent immunohistochemistry

Quantitative fluorescent immunohistochemistry was provided by Mr. Brant Pohorelic using the following method. TMA blocks were cut 4 μm thick sections and deparaffinised in xylene, rinsed in ethanol, and rehydrated. Heat-induced epitope retrieval was performed by heating slides to 121°C in a citrate-based buffer (pH6) Target Retrieval Solution (Dako, Mississauga, ON, Canada) for 3 minutes in a decloaking chamber (Biocare Medical, Concord, CA, USA). Slides were stained using a Dako Autostainer. Endogenous peroxidase activity was quenched with a 10 minute incubation of peroxidase block (Dako) followed by a 15 minute protein block (Signal

Stain, Cell Signaling, Danvers, MA, USA) to eliminate non-specific antibody binding. Slides were washed with TBST wash buffer (Dako) and then incubated at room temperature for 60 minutes with Signal Stain protein block (Cell Signaling) containing a 1:1500 dilution of ING3 Mouse mAb (Riabowal lab) (2A2) and a 1:100 dilution of anti-pan-cytokeratin rabbit polyclonal antibody (Dako). Slides were then incubated at room temperature for 60 minutes with secondary antibody Alexa-555 conjugated goat anti-rabbit antibody (Invitrogen, Burlington, ON, Canada) at 1:200 dilutions. After three washes in TBST wash buffer, the TMA slides were mounted with ProLong® Gold anti-fade mounting medium containing DAPI (Invitrogen) and stored at 4^{o}C overnight before scanning.

2.4.18.1 Automated image acquisition and analysis

Automated image acquisition was performed using an Aperio Scanscope FL (Aperio Inc., Vista, CA, USA). Seamless high-resolution slide images were acquired using the Scanscope FL 8/10-bit monochrome TDI line-image capture camera using filters specific for DAPI to define the nuclear compartment, Cy3 (Alexa555) to define the tumor cytosolic compartment based on cytokeratin, and Cy5 to define the target antibody for ING3. Images were then analysed using the AQUAnalysis® program, version 2.3.4.1 as previously described (PMID: 12389040). Briefly, a nuclear mask was generated by thresholding the DAPI images. Thresholding created a binary mask that identified the presence or absence of nuclei by the presence of a pixel that was ‘on’ or ‘off’, respectively. Thresholding levels were verified and adjusted, if necessary, by spot-checking a small sample of images to determine an optimal threshold value. An ING3 positive mask was also generated by thresholding the ING3 images in the Cy5 channel to show only positive staining nuclei based on visualization of normal prostate sporadic positive nuclei. All

images were then processed using these optimal threshold values and all subsequent image manipulations involved only image information from the masked areas. Images were validated to determine unusable areas within each image based on image quality. Areas determined to be out of focus, folded tissue, necrotic or auto-fluorescing due to blood cells were manually cropped to exclude those areas from the final analysis. Scores were based on the percent area of the nuclear mask that was also positive for ING3 based on the ING3 mask.

2.4.19 Microarray Expression Profiling and Bioinformatics

Singular Value Decomposition (SVD) was used as an effective method for analysing gene expression data based on their ERG status. This experiment was done by M. Alshalalfa, (Computer Science Department, University of Calgary, Calgary, Alberta. Canada).

2.4.20 Statistical Analysis

Data are expressed as mean ± SD. A student's *t*-test and chi-square test were used to compare the association of both ING3 to ERG, AR, tumor volume and Gleason score. The Kaplan–Meier approach was used for the survival analyses to test the association between ING3 expression and prostate cancer related death. Cox regression analysis where used to test multivariate analysis of ING3 and GS to outcome. Values of $p \leq 0.05$ were considered to be statistically significant. Part of statistical analysis assistance was provided by Mike Dolph.

Chapter Three: Results

3.1 Characterization of parental prostate cancer cell lines

Before determining *ING3* expression in prostate cancer cell lines included in this study, we sought to determine the protein expression for ERG, AR and PTEN, as well known surrogate markers for PCA. We used RWPE-1, a cell line derived from immortalized normal prostate epithelium, as well as four prostate cancer cell lines (LNCaP, VCaP, PC3 and DU145). Figure 3.1 demonstrates the protein expression levels for ERG, AR and PTEN as determined by Western blot. Among all of the cell lines, only VCaP cells showed ERG expression which is the only cell line that known to harbour the *ERG* gene fusion. AR was expressed by both LNCaP and VCaP and there was a slight expression in RWPE-1. PTEN was not detected in both PC3 and LNCaP cell lines, which are known to have PTEN deletion. β actin and GAPDH were used as loading controls. All these genes expressed in these cell lines were previously reported in other studies supporting our results [92, 93].

3.2 Generation of ING3 positive control in HEK293 cell line

HEK293 cell line was transiently transfected with *pcDNA-ING3* and labeled as (PCL) and used as a positive control for ING3 expression in Western blot and immunofluorescence experiments. (Figure 3.2), (A) RT-qPCR results shows that *ING3* mRNA level was increased about 18 fold in PCL cells compared to the negative control HEK 293 cells. The same was observed at the protein levels assessed by Western blot (B).

Figure 3.1 ERG, AR and PTEN expression in prostate cell lines.

The total cell lysate of prostate cancer cell lines (LNCaP, VCaP, PC3 and DU145) were loaded onto 10% acrylamide SDS-PAGE gels and transferred to a PDVF membrane. Membranes were blotted to detect protein levels of ERG, AR and PTEN by the Western blot analysis. RWPE-1, immortalized normal prostate epithelium, was used as a control. β-actin and GAPDH were used as loading controls.

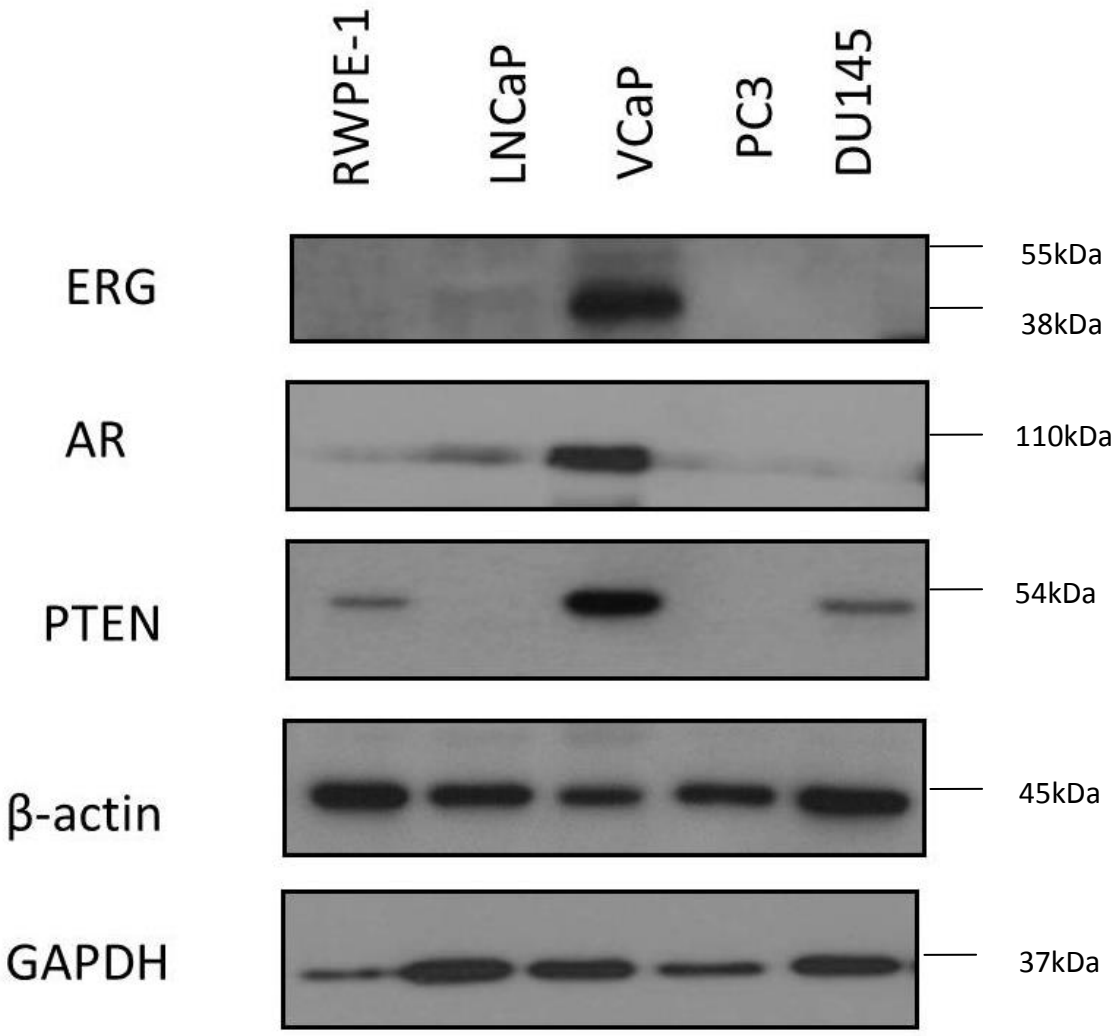
RWPE-1
LNCaP
VCaP
PC3
DU145
ERG
55kDa
38kDa
AR
110kDa
PTEN
54kDa
β-actin
45kDa
GAPDH
37kDa

Figure 3.2 ING3 expression in normal HEK-293 cells and in (PCL) ING3 transfected HEK-293 cells.

Untreated HEK-293 cells and PCL (HEK293 transiently transfected with *ING3* used as a positive control). A) qRT-PCR for *ING3* mRNA in normal HEK-293 and PCL cell lines. Student t-test was performed to calculate the p value with $p< 0.05$ considered significant. The experiments represented were repeated three times (n=3).

B) Western blot of 30 µg of total cell lysates from both HEK=-291 and PCL to detect ING3 levels using 2A2 ING3 antibody. GUSB was used as an internal control in qRT-PCR while GAPDH was the loading control in Western blot.

A

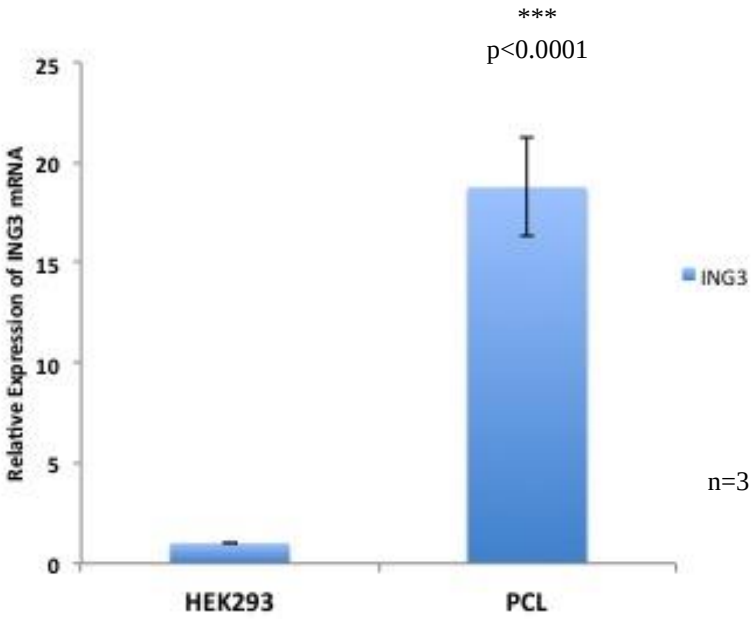
***
p<0.0001
Relative Expression of ING3 mRNA
25
20
15
10
5
0
ING3
n=3
HEK293
PCL

B

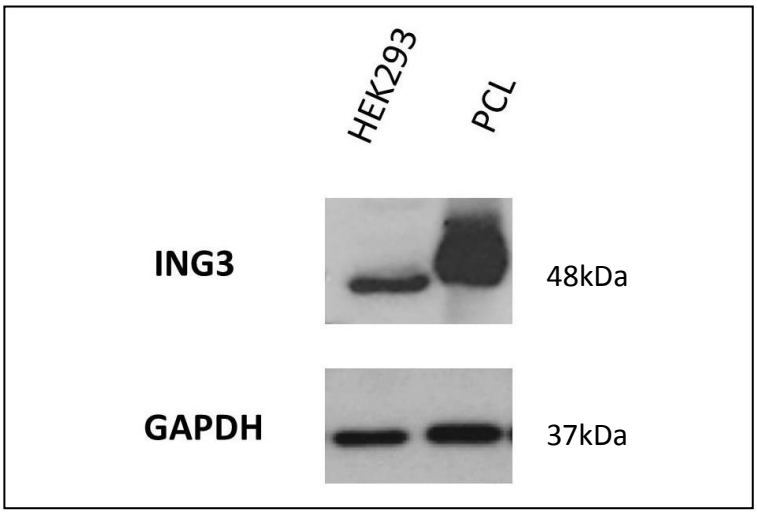
HEK293
PCL
ING3
48kDa
GAPDH
37kDa

3.3 Specificity of ING3 Antibody

Initial experiments were performed with Rabbit polyclonal anti ING3 from Protein-Tech until a potentially superior reagent for ING3 (2A2) was obtained from Dr. Riabowol's lab. The specificity of the two reagents was compared using ING3 deficient cell lines created by siRNA knockdown of ING3. Moreover, the cross reaction between ING3 and ING1a was tested since both have similar molecular weights. The results showed that the ING3 (2A2) antibody was more specific than the commercial one acquired from Protein-Tech when using the cells with knocked-down ING3 (Figure 3.3 A and B). In addition, the cross-reactivity of ING1 antibody with ING3 antibody was tested by blotting proteins from HEK293 over expressing ING1 and HEK293 over expressing ING3 with both ING3 antibodies, 2A2 (C) and the commercial antibody (D). There was no cross reaction between ING1 and ING3 when using 2A2 as shown in (C), whereas some cross-reactivity was observed between both proteins ING1 and ING3 when using the commercial antibody (Proteintech) as shown in (Figure 3.3 D).

3.3.1 ING3 expression in the prostate cancer cell lines

To demonstrate ING3 expression in prostate cancer cell lines, five different cell lines were used in this study. Four prostate cancer cell lines (VCaP, LNCaP, PC3 and DU145) and one HPV-18 immortalized normal prostate epithelial cell line were utilized (RWPE-1). Examining ING3 mRNAs levels using quantitative Real Time PCR experiments showed up-regulation of *ING3* expression in both VCaP and LNCaP compared to RWPE-1 ($P<0.007$ and $P<0.0003$) respectively). In PC3 and DU145 cells, *ING3* mRNA expression was significantly down-regulated compared to RWPE-1, ($P<0.0007$ and $P<0.0003$, respectively). GUSB was used as an internal control (Figure 3.4A).

Western blot analysis for ING3 protein levels was performed in the immortalized normal prostate cell line (RWPE-1) and prostate cancer cell lines (LNCaP, VCaP, PC3 and DU145) using the ING3 (2A2) antibody. ING3 protein levels were markedly high in LNCaP, VCaP and DU145 cell lines as well as in the immortalized prostate cell line RWPE-1 (Figure 3.4B).

Figure 3.3 Specificity of ING3 antibody.

HEK293 cells overexpressing ING3 labelled with GFP were used. Lane 2, the previously mentained cells were transfected with si-RNA control. Lanes 3, 4 and 5 cells were transfected with different concentration of si-RNA against ING3 (A and B).

A) The membrane was blotted with ING3 (2A2) antibody in addition to GFP and β-actin as loading control.

B) The membrane was blotted with ING3 Protein-Tech (commercial antibody) using the same order of cell lines as in (A). Also, GFP and β-actin were used as loading controls.

C) Total protein from HEK293 cells overexpressing ING1 (lane 1) and ING3 (lane 2) were blotted with ING (2A2) antibody. β-actin was used as a loading control.

D) Total protein from HEK293 cells overexpressing ING1 (lane 1) and ING3 (lane 2) were blotted with ING Protein-Tech (commercial antibody). β-actin was used as a loading control.

A

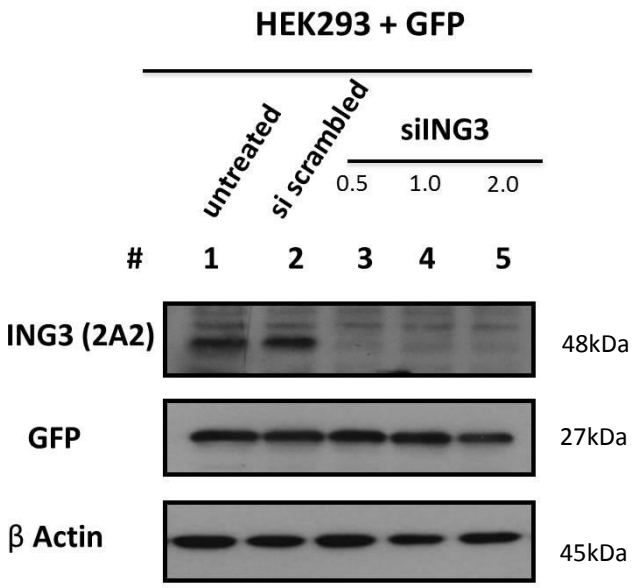
HEK293 + GFP
untreated
si scrambled
siING3
0.5
1.0
2.0
#
1
2
3
4
5
ING3 (2A2)
48kDa
GFP
27kDa
β Actin
45kDa

B

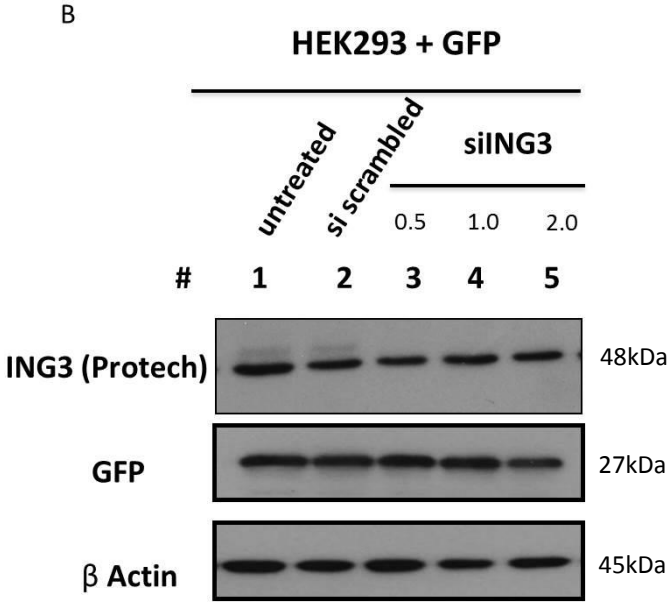
HEK293 + GFP
untreated
si scrambled
siING3
0.5
1.0
2.0
#
1
2
3
4
5
ING3 (Protech)
48kDa
GFP
27kDa
β Actin
45kDa

C

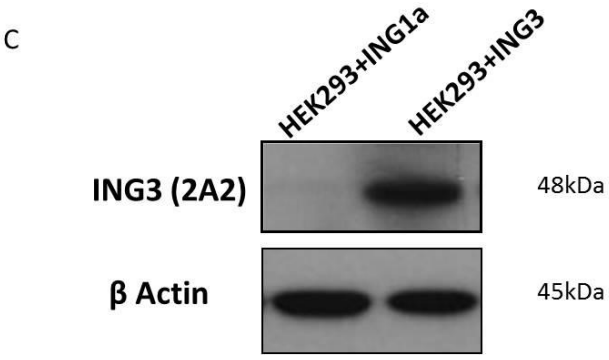
HEK293+ING1a
HEK293+ING3
ING3 (2A2)
48kDa
β Actin
45kDa

D

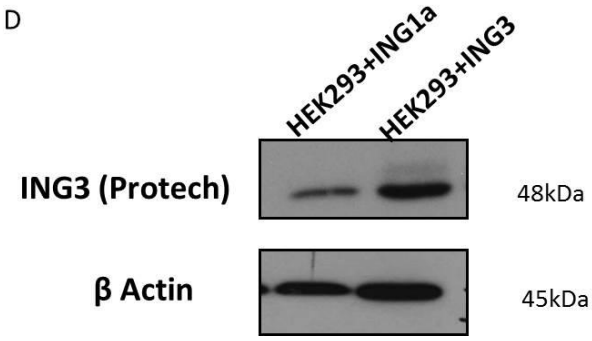
HEK293+ING1a
HEK293+ING3
ING3 (Protech)
48kDa
β Actin
45kDa

Figure 3.4 ING3 expression in prostate cell lines.

A) Quantitative Real time PCR experiments of *ING3* mRNA expression in four prostate cancer cell lines (LNCaP, VCaP, PC3 and DU145) relative to the expression of ING3 in RWPE-1 cells. GUSB was used as an internal control. The ING3 and GUSB primers that were used are shown in table 2.3. Student-test $p < 0.05$ was considered significant and the figure represents experiments repeated three times (n=3).

B) 30 µg of total protein cell lysates from all prostate cell lines was used to determine the protein level of ING3. Western blot performed on all prostate cancer cell lines was compared to the immortalized prostate cell line RWPE-1. ING3 (2A2) antibody was utilized in Western blot experiments. HEK293 cell lines were used as positive control for ING3 expression and β-actin was used as an internal control.

A

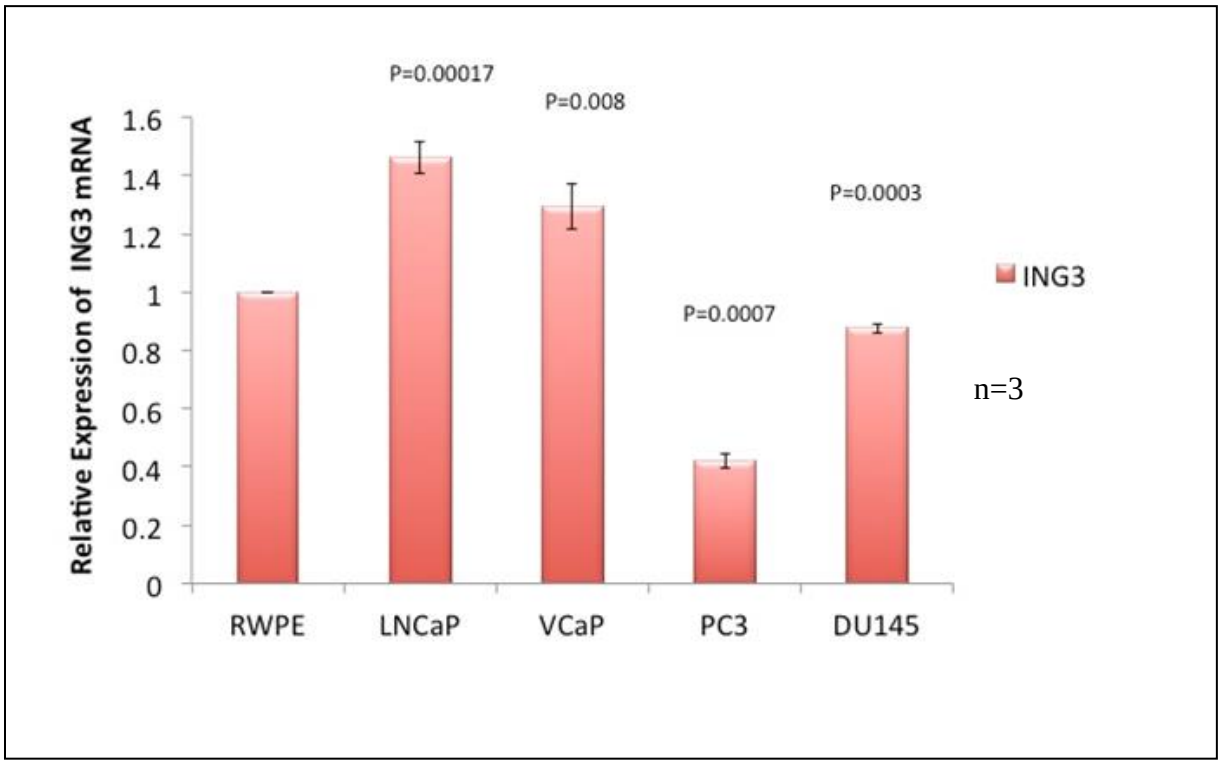
P=0.00017
P=0.008
P=0.0003
P=0.0007
Relative Expression of ING3 mRNA
1.6
1.4
1.2
1
0.8
0.6
0.4
0.2
0
RWPE
LNCaP
VCaP
PC3
DU145
ING3
n=3

B

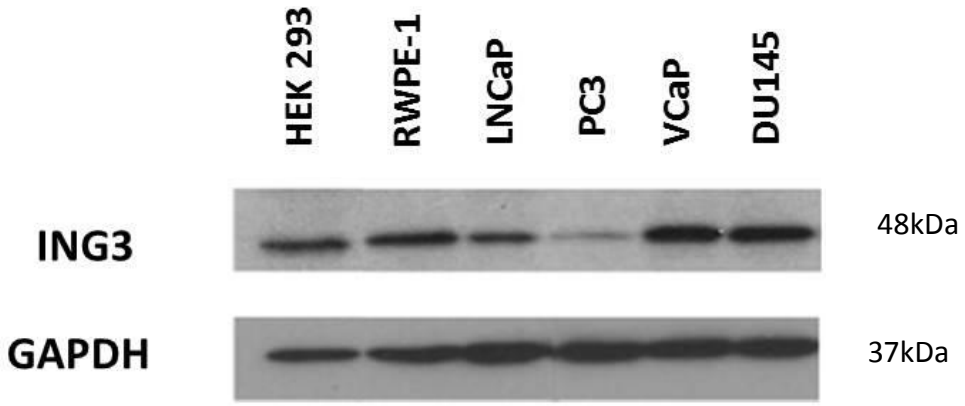
HEK 293
RWPE-1
LNCaP
PC3
VCaP
DU145
ING3
48kDa
GAPDH
37kDa

3.3.2 Overexpressing ERG in RWPE-1, LNCaP and PC3cell lines

To investigate the correlation between *ERG* and *ING3*, we overexpressed *ERG* in RWPE-1, PC3 and LNCaP prostate cell lines. The VCaP cell line is the only prostate cancer cell line that contains the ERG fusion. PC3-ERG and its control, PC3-Luc, were kind gifts from Felix Feng's lab, while RWPE1-ERG and the LNCaP-ERG were stably transfected with ERG in our lab. VCaP cells, which harbour *TMPRSS2-ERG* gene fusion, were used as a positive control for *ERG* expression. (Figure 3.5 A, B and C) shows mRNA levels of overexpressed ERG in RWPE-1, LNCaP and PC3 cell lines by RT-qPCR, while (D, E and F) demonstrates the ERG protein levels in those cell lines by Western blot. The gray bars indicate the quantification of protein levels as detected by densitometry. Both experiments confirmed the successful transfection of *ERG* in these cells.

3.3.3 ING3 in prostate cancer cell lines stably overexpressing ERG

To study the influence of *ERG* on *ING3* expression, we used RWPE-1, LNCaP and PC3 cell lines stably expressing *ERG*. VCaP cells, which harbour *TMPRSS2-ERG* gene fusion, were used as a positive control for *ERG* expressions. In *ERG* stable cell lines, q RT-PCR indicated that *ING3* mRNA expression was down-regulated in all transfected cells RWPE-1, LNCaP and PC3-ERG compared to their controls ($P< 0.001$, $P< 0.0001$, $P <0.0003$; respectively) (Figure 3.6 A). However, at the protein level, ING3 did not show significant changes in RWPE1-ERG cells. Although not significant, ING3 was slightly increased in LNCaP-ERG. On the other hand, there was a significant reduction in PC3-ERG in comparison to the control PC3-Luc (Figure 3.6 B).

Figure 3.5 Overexpression of ERG in prostate cell lines.

ERG was cloned from VCaP cell lines and then stably transfected in RWPE-1, LNCaP and PC3 cell lines. Transfection was confirmed with qRT-PCR and Western blot, by comparing the transfected cells to its control. A,B,C) Relative expression of *ERG* mRNA levels in ERG overexpressed (RWPE1-ERG, LNCaP-ERG and PC-ERG) cell lines to it controls (RWPE1-GFP, LNCaP-GFP and PC3-Luc) .GUSB was used as internal control. The *ERG* and *GUSB* primers that were used are shown in (table 2.3). Student t-test $p < 0.05$ was considered significant and the figure represents experiments run in triplicates (n=3).

(D, E, F) represents protein levels of ERG in RWPE-1, LNCaP and PC3, respectively, depicting overexpression of ERG compared to their controls. GAPDH were used as loading controls for Western blot. Gray bars indicate quantification of three separate Western blots experiments. P values ($p<0.05$) were considered significant.

A

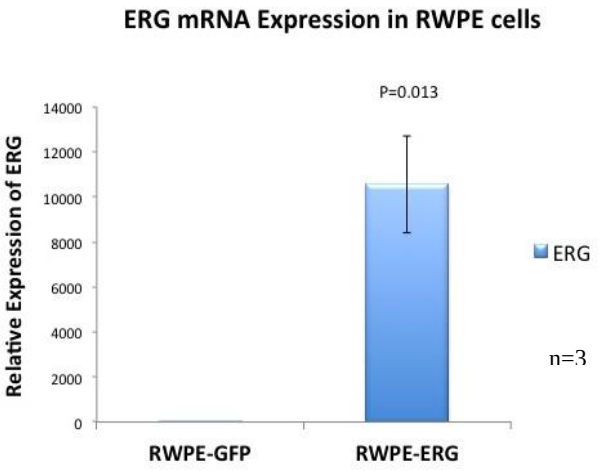
ERG mRNA Expression in RWPE cells
P=0.013
Relative Expression of ERG
14000
12000
10000
8000
6000
4000
2000
0
RWPE-GFP
RWPE-ERG
ERG
n=3

B

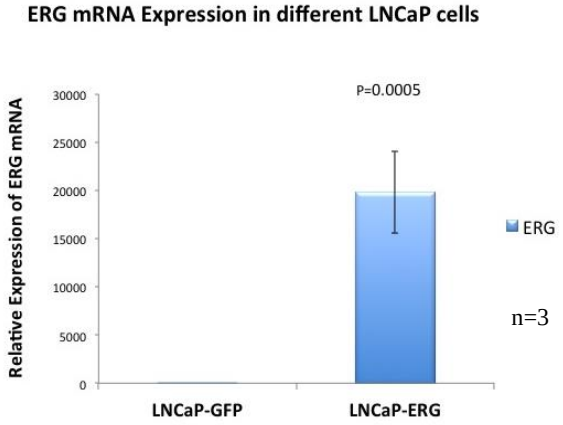
ERG mRNA Expression in different LNCaP cells
P=0.0005
Relative Expression of ERG mRNA
30000
25000
20000
15000
10000
5000
0
LNCaP-GFP
LNCaP-ERG
ERG
n=3

C

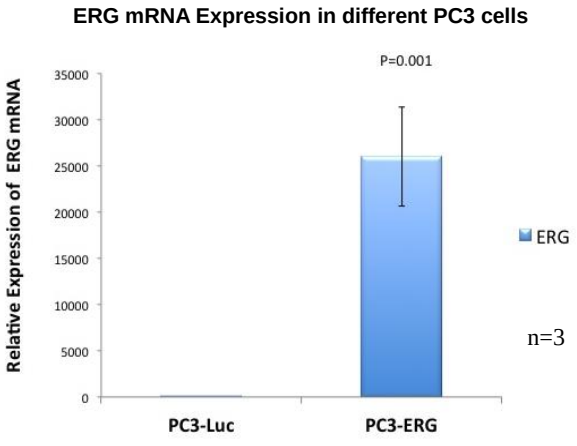
ERG mRNA Expression in different PC3 cells
P=0.001
Relative Expression of ERG mRNA
35000
30000
25000
20000
15000
10000
5000
0
PC3-Luc
PC3-ERG
ERG
n=3

D

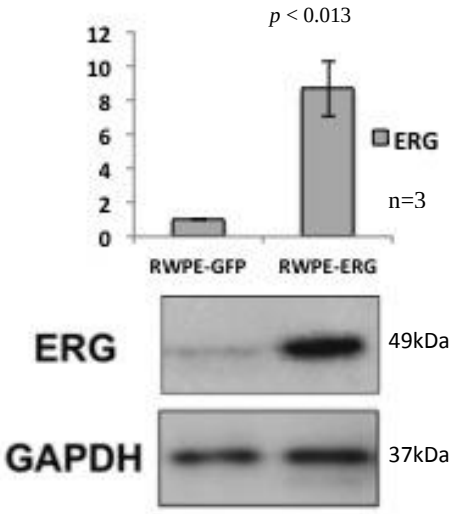
p < 0.013
12
10
8
6
4
2
0
RWPE-GFP
RWPE-ERG
ERG
n=3
ERG
49kDa
GAPDH
37kDa

E

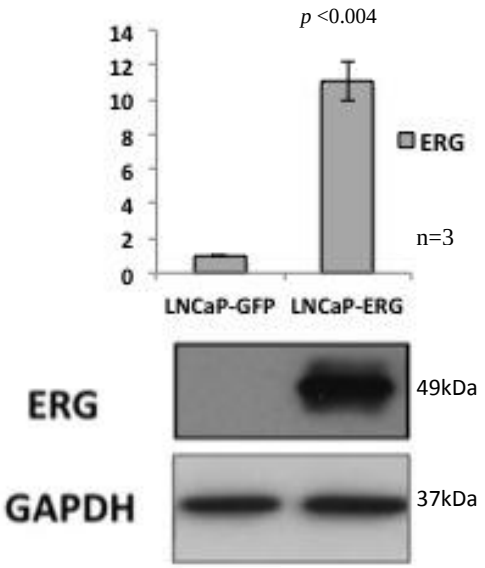
p <0.004
14
12
10
8
6
4
2
0
LNCaP-GFP
LNCaP-ERG
ERG
n=3
ERG
49kDa
GAPDH
37kDa

F

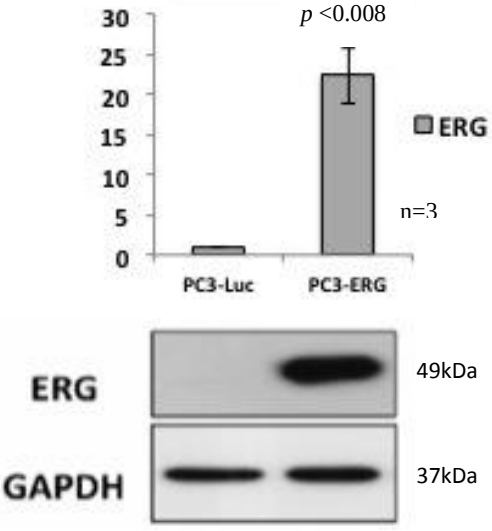
p <0.008
30
25
20
15
10
5
0
PC3-Luc
PC3-ERG
ERG
n=3
ERG
49kDa
GAPDH
37kDa

Figure 3.6 ING3 expression in prostate cancer cell lines stably overexpressing ERG.

A) Relative expression of *ING3* mRNA in RWPE-1, LNCaP and PC3 where *ERG* is overexpressed in those cell lines compared to their controls (RWEP-GFP, LNCaP-GFP and PC3-Luc). *GUSB* was used as an internal control. Student t-test was used to calculate the p value where $p<0.05$ was considered significant. The figure represents experiments repeated three times (n=3). The *ING3* and *GUSB* primers that were used are described in (table 2.3)

B) Total cell protein lysates from cells stably overexpressing ERG by Western blot. Upper panel: ING3 protein Middle panel: ERG exogenous expression in RWPE1-ERG, LNCaP-ERG and PC3-ERG. Lower panel: GAPDH was used as loading control. ING3 2A2 antibody was used in the Western blot.

A

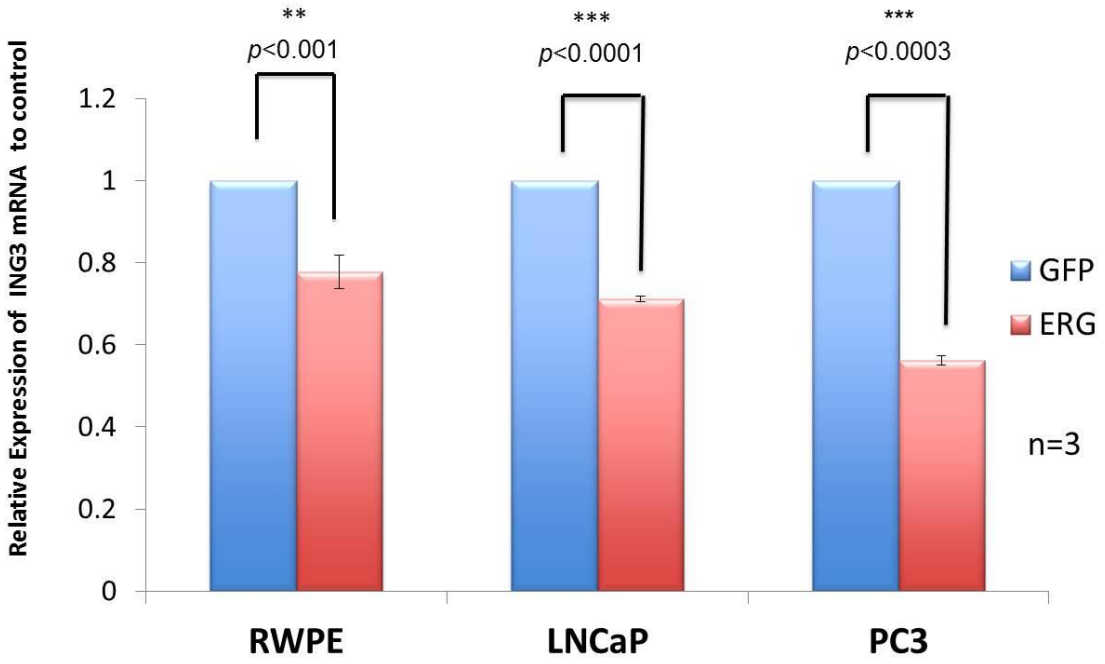
**
p<0.001
***
p<0.0001
***
p<0.0003
Relative Expression of ING3 mRNA to control
1.2
1
0.8
0.6
0.4
0.2
0
GFP
ERG
n=3
RWPE
LNCaP
PC3

B

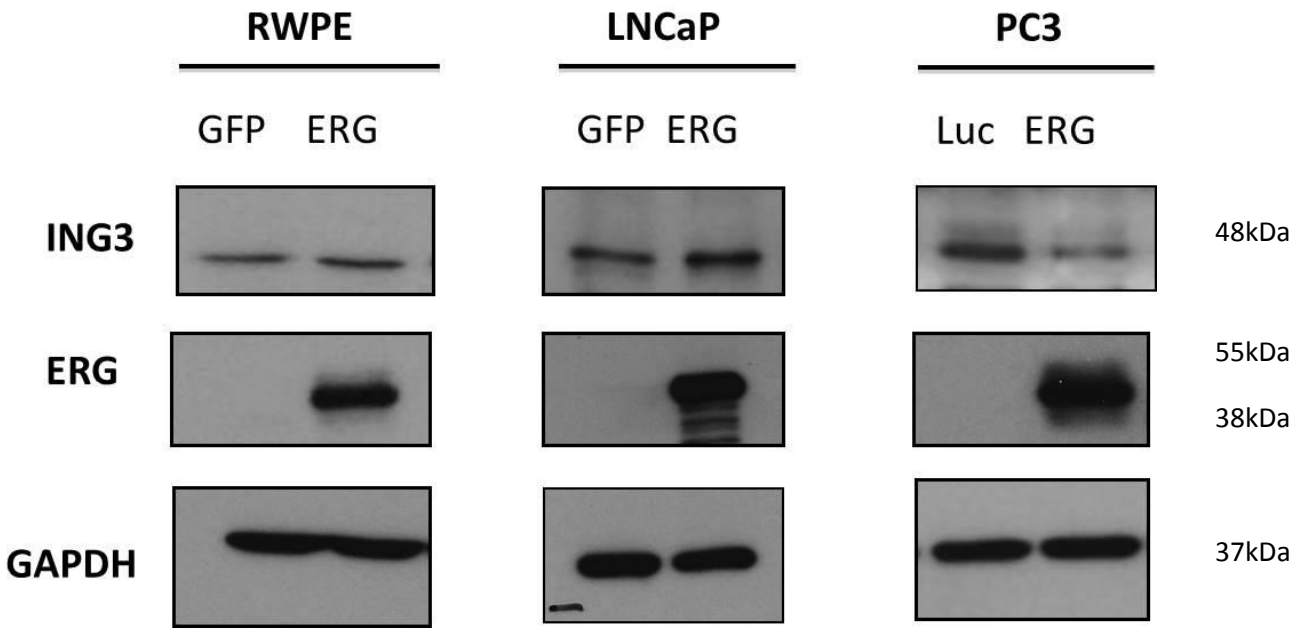
RWPE
LNCaP
PC3
GFP ERG
GFP ERG
Luc ERG
ING3
ERG
GAPDH
48kDa
55kDa
38kDa
37kDa

3.3.4 Expression of ING3 in VCaP cell line with knocked-down ERG

Since VCaP cells express *ERG* normally, we were interested in testing ING3 expression influenced by ERG. Therefore, we knocked down *ERG* transiently in VCaP cells and measured *ING3* expression via qRT-PCR. At the mRNA expression level, qRT-PCR showed a non-significant but increasing trend of *ING3* mRNA levels in VCaP *siERG* ($p=0.06$) as shown in (Figure 3.7 A). At the protein level, there was a slight increase in ING3 expression in VcaP *siERG*. Interestingly, when AR was determined in that cell line, it showed an increase of AR protein level when ERG was suppressed as seen in (Figure 3.7B).

Figure 3.7 ERG associated with the expression of ING3 in VCaP cell lines.

A) Quantitative RT-PCR of ING3 mRNA in VCaP when ERG was knocked-down by siRNA. qRT-PCR represents relative expression in si-RNA ERG VCaP cells compared to si-RNA -control VCaP for both ING3 and ERG mRNA levels. GUSB was used as internal control. The statistical student t-test was utilized to calculate the p value, where $p < 0.05$ was considered significant. The experiments were repeated three times (n=3).

B) Western blot analysis of whole cell lysates extracted from VCaP with knocked down ERG. Upper panel: ERG expression in siControl and *siERG* VCaP cells. Middle panel: ING3 and AR expressions in VCaP cells, siControl and *siERG*. Last panel: β-actin was used as a loading control.

A

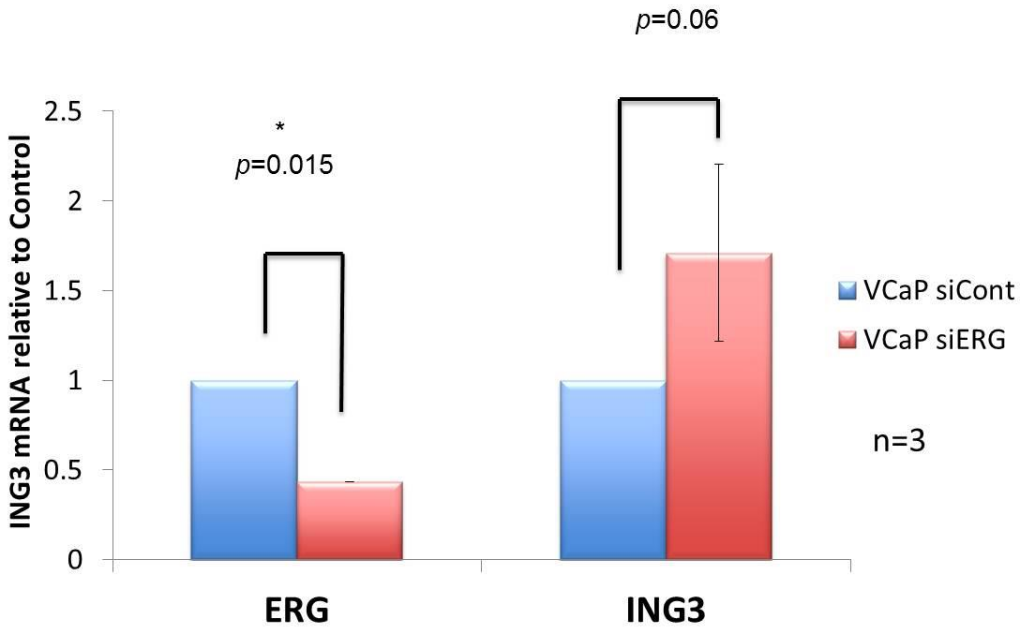
p=0.06
*
p=0.015
ING3 mRNA relative to Control
2.5
2
1.5
1
0.5
0
VCaP siCont
VCaP siERG
n=3
ERG
ING3

B

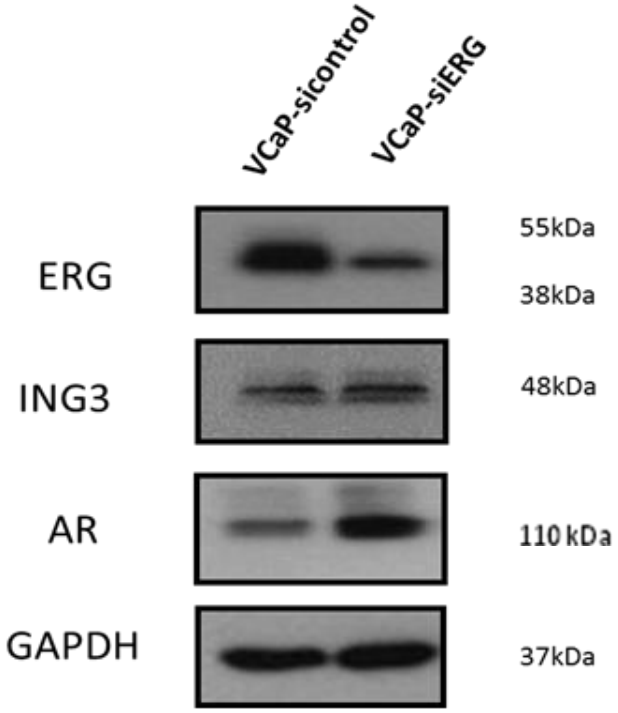
VCaP-sicontrol
VCaP-siERG
ERG
55kDa
38kDa
ING3
48kDa
AR
110 kDa
GAPDH
37kDa

3.4 Localization of ING3

3.4.1 ING3 localisation in control cell lines

We used Western blot analysis to examine the subcellular localization of ING3 and then we confirmed those findings by immunofluorescence. HEK-293 cells transfected with *ING3* plasmid served as a positive control in all experiments. To confirm the transfection of ING3 in HEK-293, we tested both mRNA and protein levels of ING3 in PCL in comparison to the untreated HEK-293 (Figure 3.2). Cellular fractionation studies showed that ING3 was predominantly located in the nucleus of HEK-293 cells with a higher expression in PCL transfected cells in both cytoplasmic and nuclear compartments (Figure 3.8 A and B).

3.4.2 ING3 localization in prostate cancer parental cell lines

Immunofluorescence results showed that ING3 is localized to the nuclei (N) of all PCA cell lines with the exception of PC3 that showed some cytoplasmic (C) expression. RWPE-1 showed ING3 in both cytoplasmic and nuclear compartments (Figure 3.9).

3.4.3 ING3 localization in ERG cell lines

In *ERG* stably transfected cell lines, ING3 exhibited translocation from the cytoplasm to the nuclear compartment in RWPE1-ERG, shown in both Western blot and immunofluorescence (Figure 3.10 A and D). The localization of ING3 in LNCaP –ERG did not change compared with its control, but the expression was increased in LNCaP-ERG compared with LNCaP-GFP (Figure 3.10 B and E). In PC3-ERG cells, there was a slight, non-statistically significant, reduction of ING3 in cytoplasmic fractions as compared to their controls, whereas the nuclear fraction was unchanged (Figure 3.10 C and F).

3.4.4 ING3 localization in control tissue

To investigate the localization of ING3 in tissue samples, we utilized human kidney specimens as a positive control since ING3 was reported to be highly expressed in normal kidney tissue [80]. Western blot analysis performed to determine the localization of ING3in frozen kidney sample using ING3 2A2 antibody in addition to immunofluorescence to confirm the results. 4-6 μm thick sections were cut from the frozen kidney sample blocks using cold microtome and following the protocol of handling frozen sections. REAP method was performed on the section then Western blot was performed [91]. Same IF protocol experiment was performed on tissue slides with slight modifications .Both experiments showed that ING3 is expressed in the cytoplasmic compartment using antibodies 2A2. Western blot results of ING3 in (Figure 3.11A) and immunoflorecence in (Figure 3.11B). Upper panel; kidney tissue incubated and stained without primary antibody PBS. Lower panel; kidney tissue incubated and stained with ING3 2A2 antibody to test the sensitivity of the primary reagent in IF experiments.

Figure 3.8 ING3 localisation in positive control cell lines.

A) Western blot was performed to detect ING3 localization in HEK293 and in PCL by using the ING3 (2A2) antibody. For cytoplasmic control α tubulin was used. (W) represents whole cell lysate, cytoplasmic fractionation (C) and nuclear fractionation (N).

B) Immunofluorescence was used to detect ING3 endogenous expression in HEK293 cells (upper panel) and in PCL cells (lower panel). ING3 (2A2) antibody was used as the primary antibody and Alexa 568 anti-mouse was used as the secondary antibody.

Nuclei were stained using DAPI (cyan blue), ING3 (hot red) and merge (pink).

A

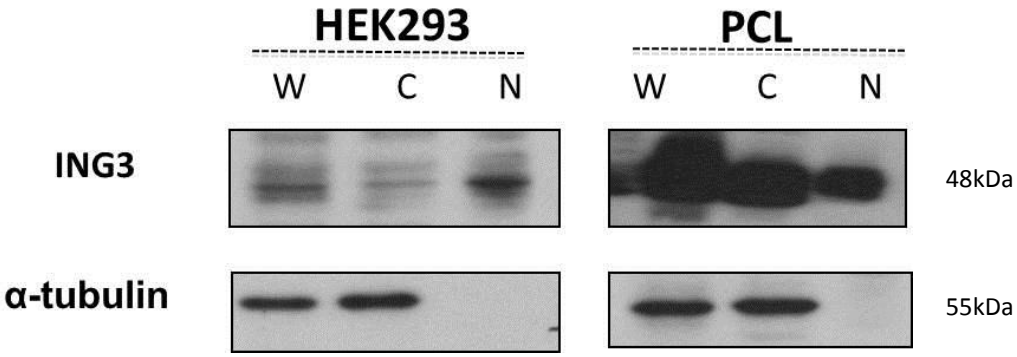
HEK293
PCL
W
C
N
W
C
N
ING3
48kDa
α-tubulin
55kDa

B

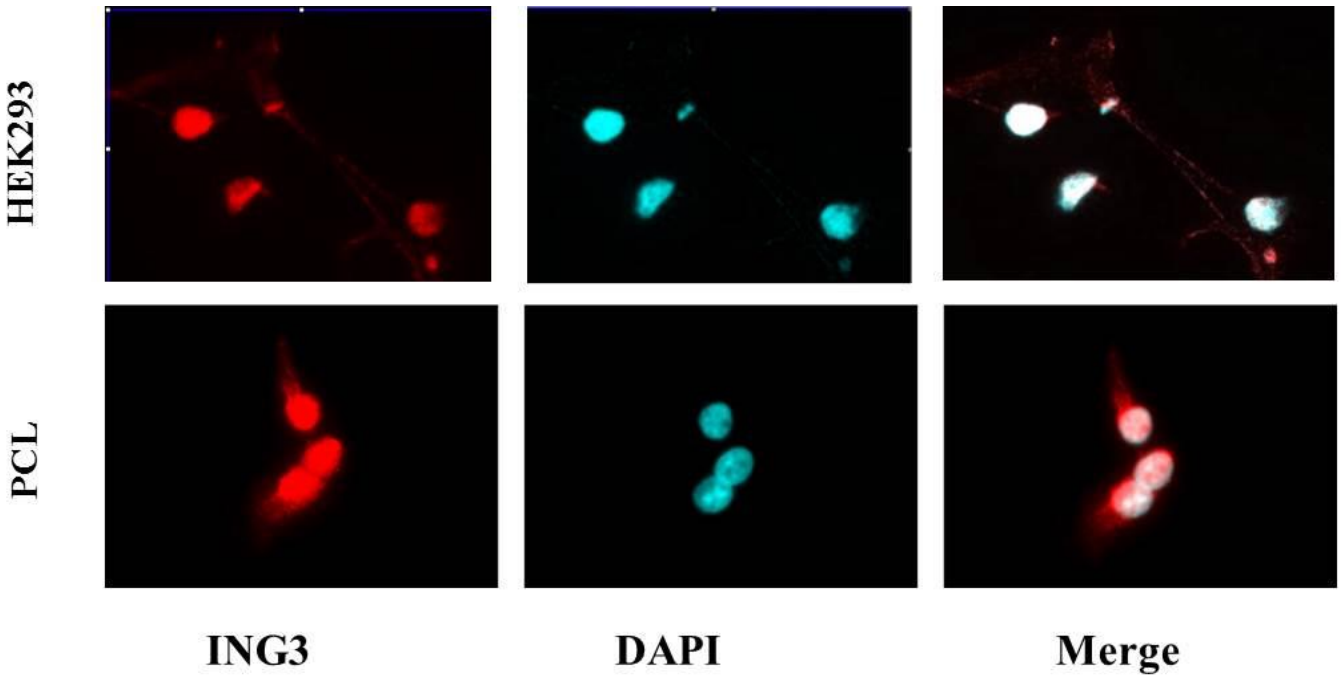
HEK293
PCL
ING3
DAPI
Merge

Figure 3.9 ING3 localization in parental prostate cancer cell lines by immunofluorescence and Western Blot.

A) Localization of ING3 in all five parental prostate cell lines (RWPE-1, LNCaP, VCaP, PC3 and DU145) by Western blot experiments. For cytoplasmic (C) and nuclear (N) fractionations, the REAP method was used. α Tubulin and Lamin A were used as cytoplasmic and nuclear controls, respectively. ING3 (2A2) was used to detect ING3 protein localization.
B) ING3 localization in the same parental prostate cell lines by immunofluorescence. ING3 (2A2) as primary antibody and Alexa 568 anti-mouse as secondary antibody were stained in red, DAPI in cyan blue for nucleus parts and pink-orange for the merge of both colors.

A

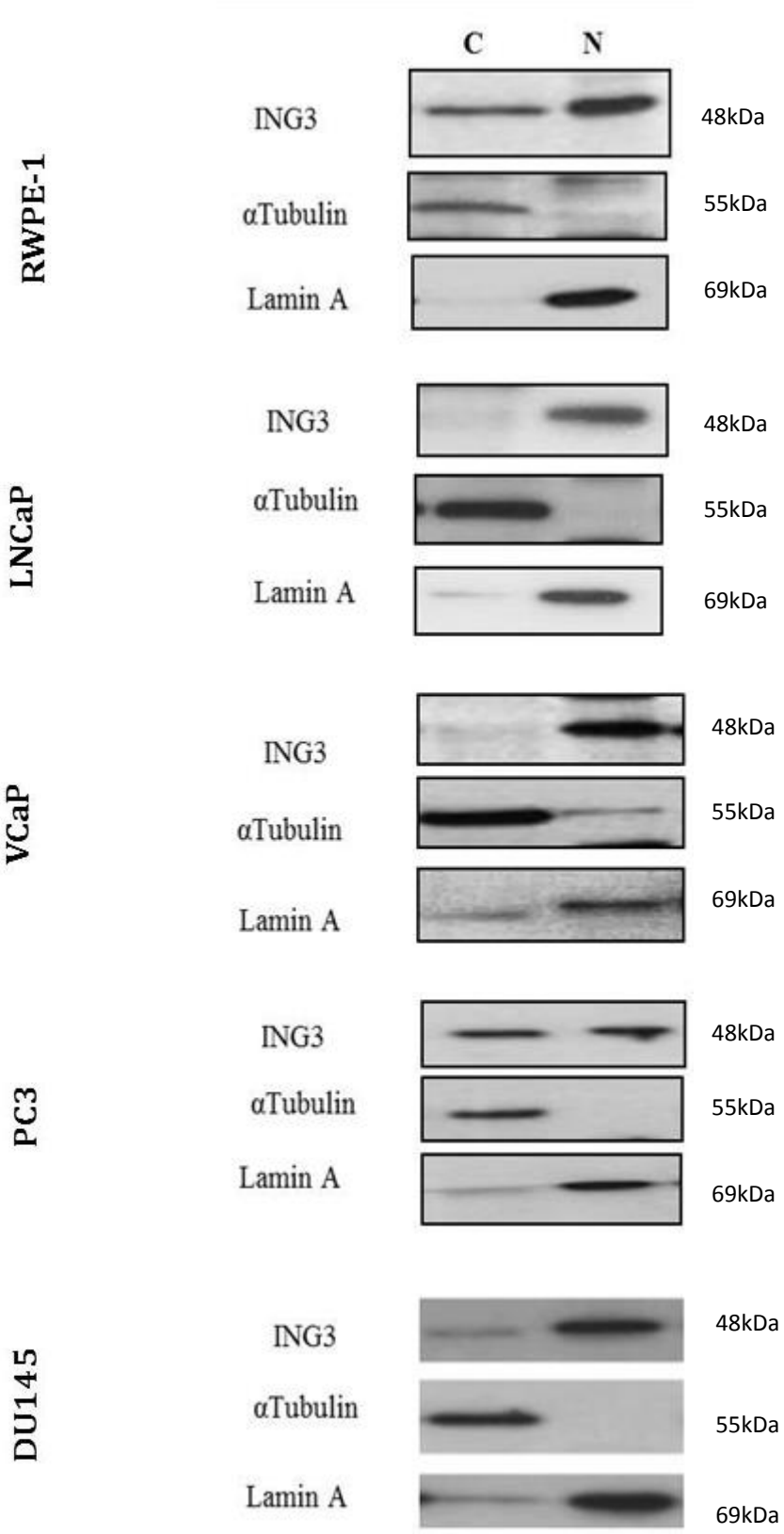
C
N
RWPE-1
ING3
αTubulin
Lamin A
48kDa
55kDa
69kDa
LNCaP
ING3
αTubulin
Lamin A
48kDa
55kDa
69kDa
VCaP
ING3
αTubulin
Lamin A
48kDa
55kDa
69kDa
PC3
ING3
αTubulin
Lamin A
48kDa
55kDa
69kDa
DU145
ING3
αTubulin
Lamin A
48kDa
55kDa
69kDa

B

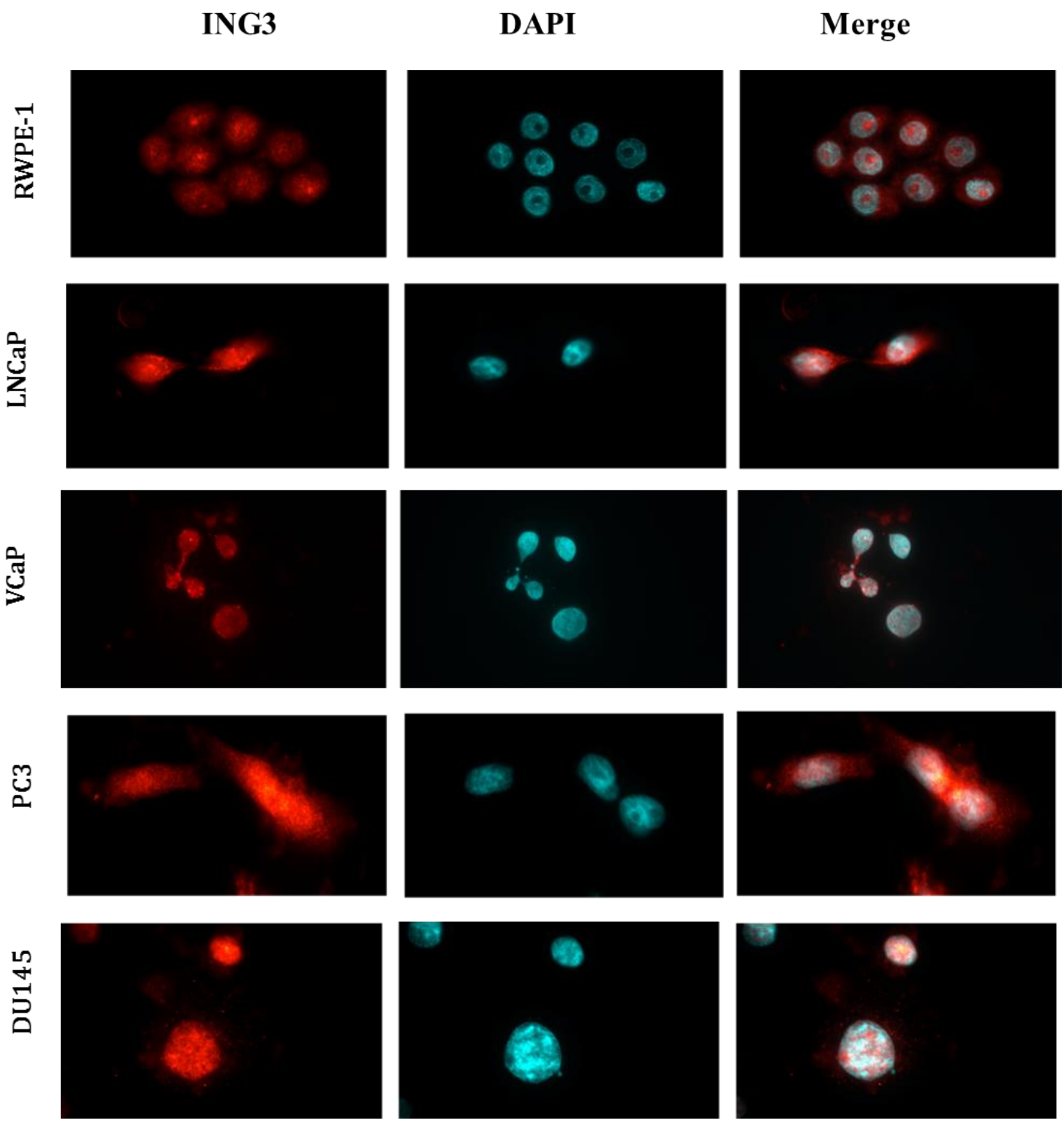

Figure 3.10 ING3 localization PCA cell lines stably over-expressing ERG by Western Blot and immunofluorescence.

Western blot analysis for ING3 localization in three overexpressing ERG cell lines: RWPE-1-ERG and its control (A), LNCaP-ERG and its control (B) and PC3-ERG and its control (C). α Tubulin and Lamin A were used as cytoplasmic and nuclear controls, respectively. PCL is HEK-293 transfected with ING3 as a positive control.

Immunofluorescence experiments to detect localization of ING3 in over expressing ERG cell lines: RWPE-1-ERG and its control (D), LNCaP-ERG and its control (E) and PC3-ERG and its control (F). ING3 (2A2) as primary antibody and Alexa 568 anti-mouse as secondary antibody were stained in hot red, DAPI in cyan blue for nucleus and orange for the merge of both colors.

A

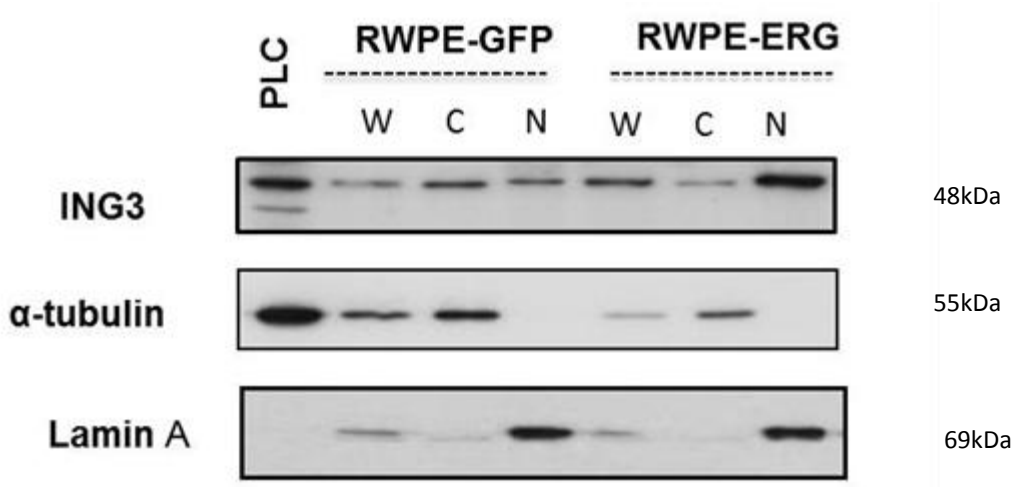
PLC
RWPE-GFP
RWPE-ERG
W C N W C N
ING3
α-tubulin
Lamin A
48kDa
55kDa
69kDa

B

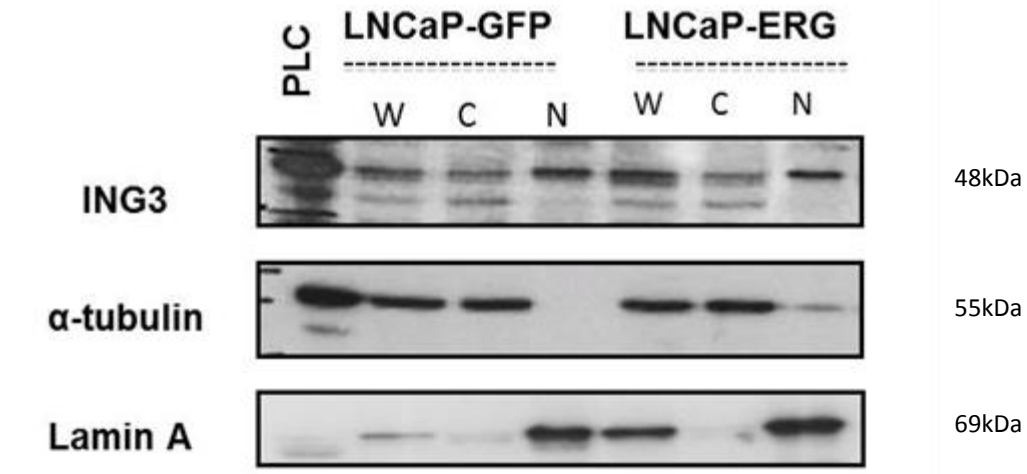
PLC
LNCaP-GFP
LNCaP-ERG
W C N W C N
ING3
α-tubulin
Lamin A
48kDa
55kDa
69kDa

C

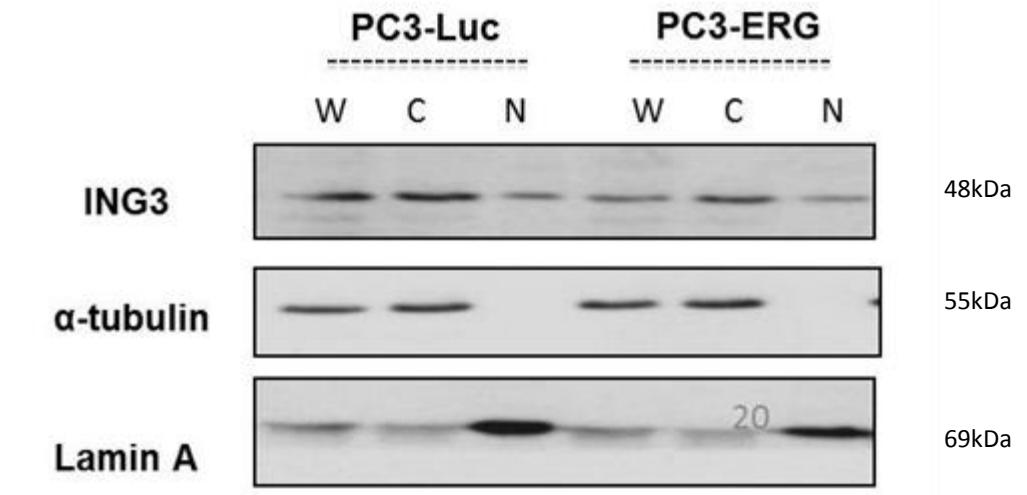
PC3-Luc
PC3-ERG
W C N W C N
ING3
α-tubulin
Lamin A
48kDa
55kDa
69kDa

D

E

F

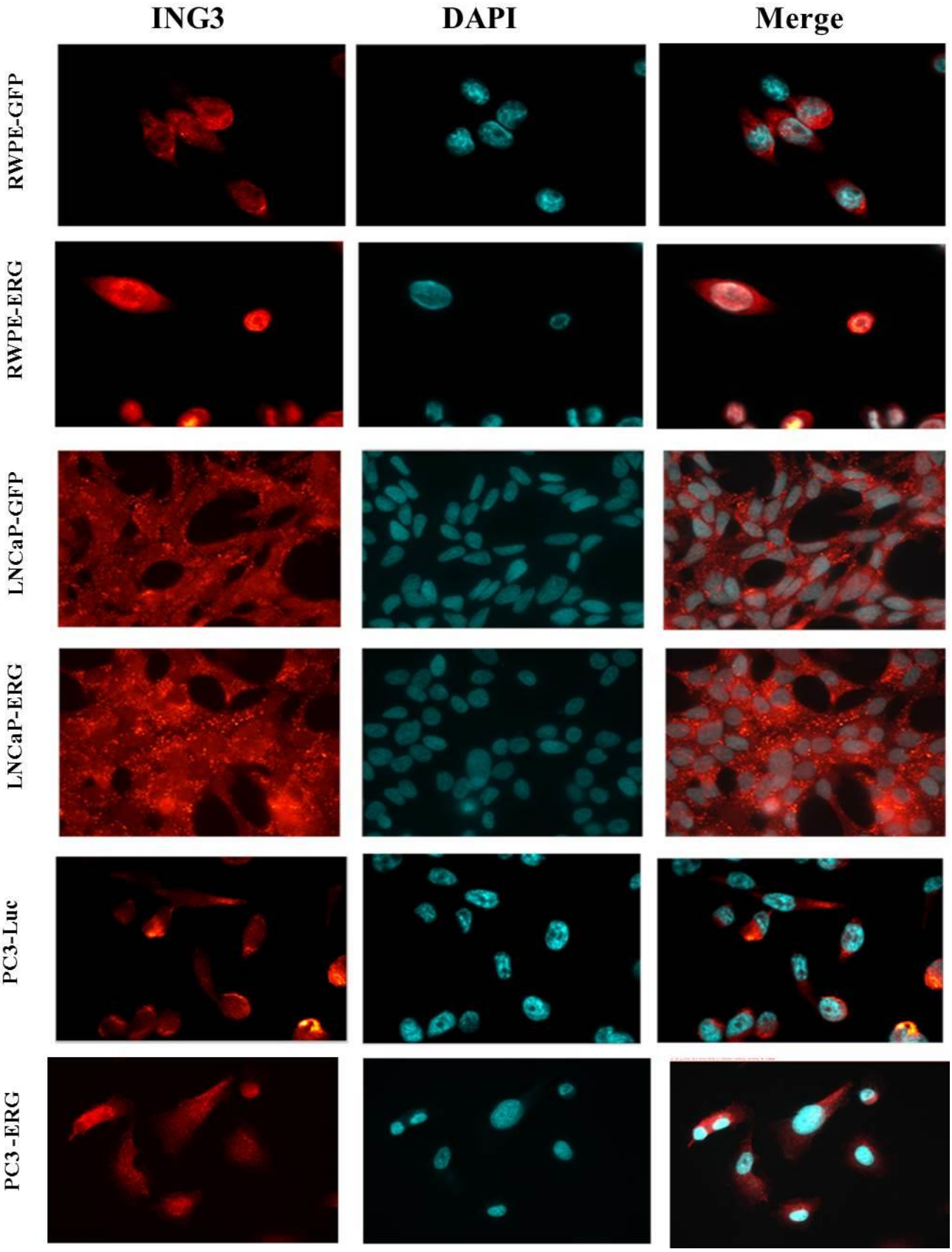
ING3
DAPI
Merge
RWPE-GFP
RWPE-ERG
LNCaP-GFP
LNCaP-ERG
PC3-Luc
PC3 -ERG

Figure 3.11 ING3 localization in normal human Kidney tissue.

Normal human kidney tissue samples were used as a control for Immunohistochemistry experiments. A) Western blot analysis for ING3 of fractionated proteins from kidney tissue, Lamin A was used as a nuclear expression control. B) Immunofluorescence for localization of ING3. Upper panel: shows tissue sections incubated with PBS to test the antibody sensitivity. Lower panel shows tissue sections incubated with ING3 (2A2) antibody as primary antibody and Alexa 568 anti-mouse as secondary antibody was stained in (hot red), DAPI in (cyan blue) for nuclei and (pink) for the merge.

A

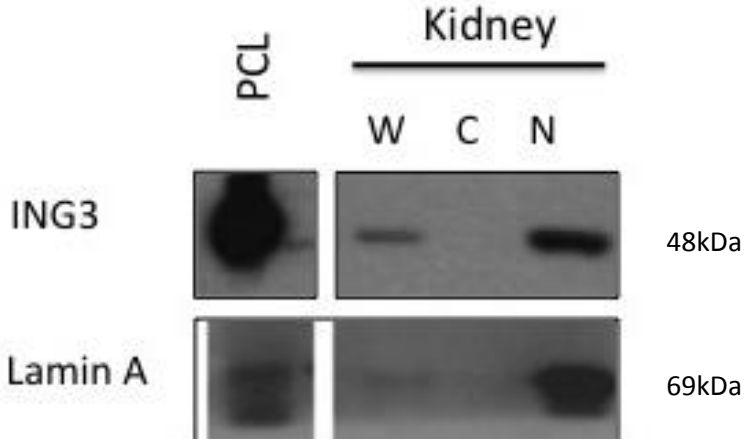
PCL
Kidney
W
C
N
ING3
48kDa
Lamin A
69kDa

B

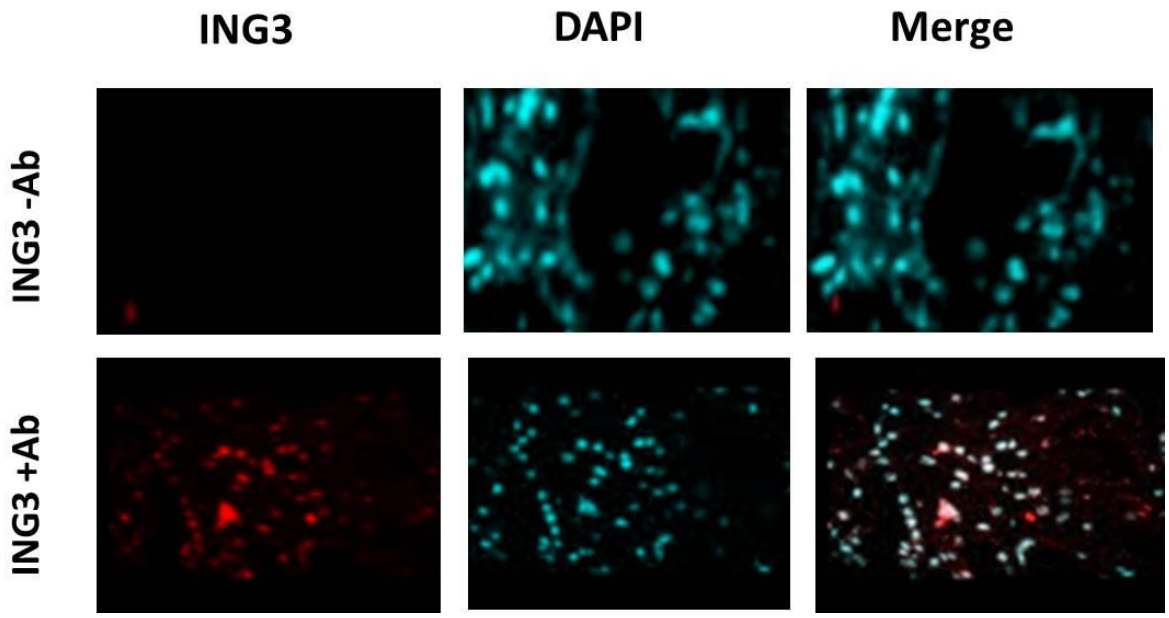
ING3
DAPI
Merge
ING3 -Ab
ING3 +Ab

3.5 ING3 increases cell invasion and migration in prostate cancer cell lines

To assess invasion and migration in prostate cancer affected by ING3 *in*-vitro, we performed the invasion and migration assays using si-RNA ING3 to knock down ING3 in DU145 cells. We chose this cell line based on the initial screening of all four prostate cancer cell lines. Along with the VCaP cell line, the DU145 cell line showed higher levels of ING3 compared to the other cell lines. qRT-PCR was performed to detect the mRNA expression of ING3 in both ING3 knockdown and control cells. The results demonstrate mRNA expression of *ING3* in a successful knockdown of *ING3* in the siRNA-*ING3* DU145 cells in comparison to cells transfected with control siRNA (Figure 3.12). The ability of invasion was assessed after 48 hours and a significant decrease was noticed in *ING3*-knocked down cells compared to the control cells (Figure 3.13A). Similarly, the migration ability was decreased in ING3 knocked down cells compared to the control. When images were taken after 24 hours, migration was significantly lower in the siING3 cells (see Figure 3.13B).

Figure 3.12 Successful knockdown of ING3 in DU-145 cells.

ING3 was knocked down in DU145 cell lines compared to DU145 cells transfected with scrambled siRNA. The mRNA levels of ING3 in DU145 cells transfected with siRNA ING3 down-regulated relative to cells transfected with control siRNA quantified by qRT-PCR. GUSB was used as an internal control. Student t-test used to calculate the p value where $p<0.05$ was considered significant. The figure represent three times independent experiments (n=3). ING3 and GUSB used primers are described in table 2.3.

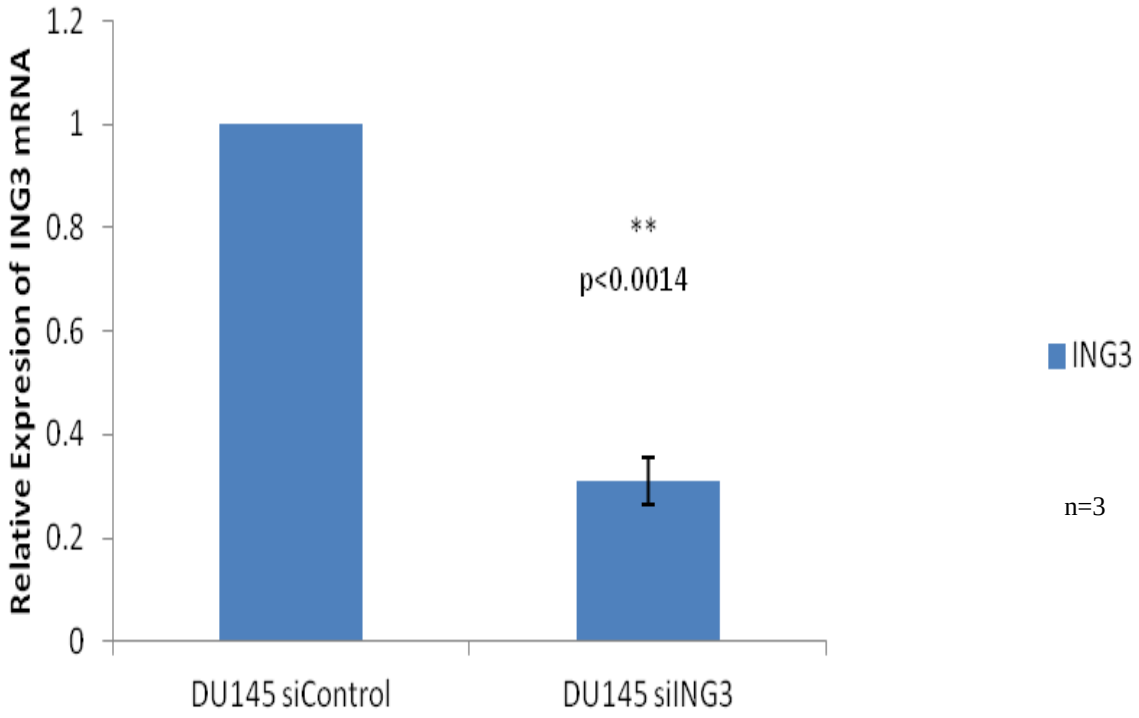
Relative Expresion of ING3 mRNA
1.2
1
0.8
0.6
0.4
0.2
0
**
p<0.0014
DU145 siControl
DU145 siING3
ING3
n=3

Figure 3.13 Effect of ING3 expression on cancer cell invasion and migration.

A. DU145 cells were transfected with siRNA, non-targeting (siControl) and si-*RNA ING3*. $5x10^4$ cells per ml were left to transfer through membrane for 24 and 48 hours in triplicate then the mean ± SD was calculated. $p<0.05$ was considered statistically significant.

B. Monolayer of DU145 cells. Upper panel: Cells transiently transfected with non-targeting siRNA: Lower panel: DU145cells transiently transfected with siRNA *ING3*. Cells were then subjected to a wound healing assay and images were taken after 0, 16 and 24 hours to assess migration.

A

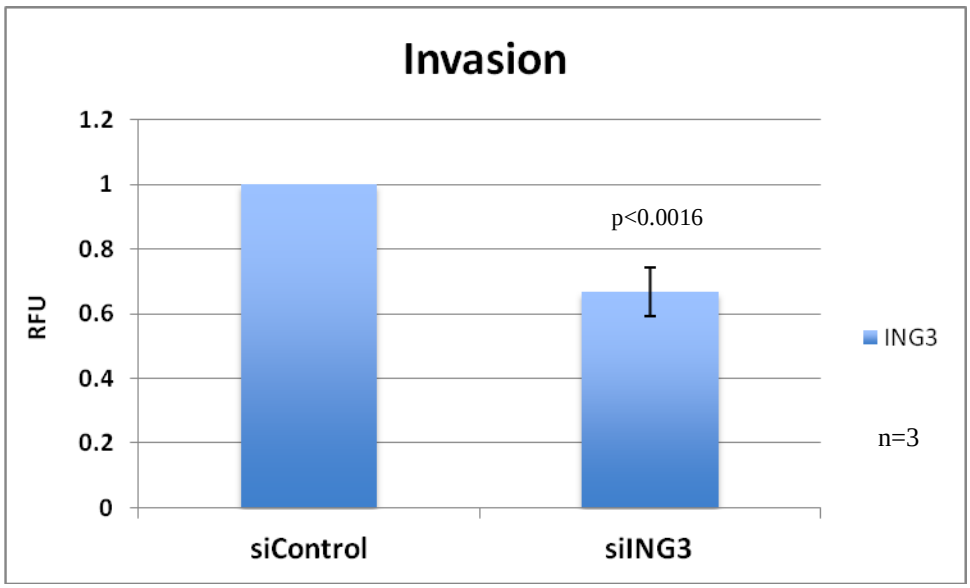
Invasion
1.2
1
0.8
0.6
0.4
0.2
0
RFU
p<0.0016
ING3
n=3
siControl
siING3

B

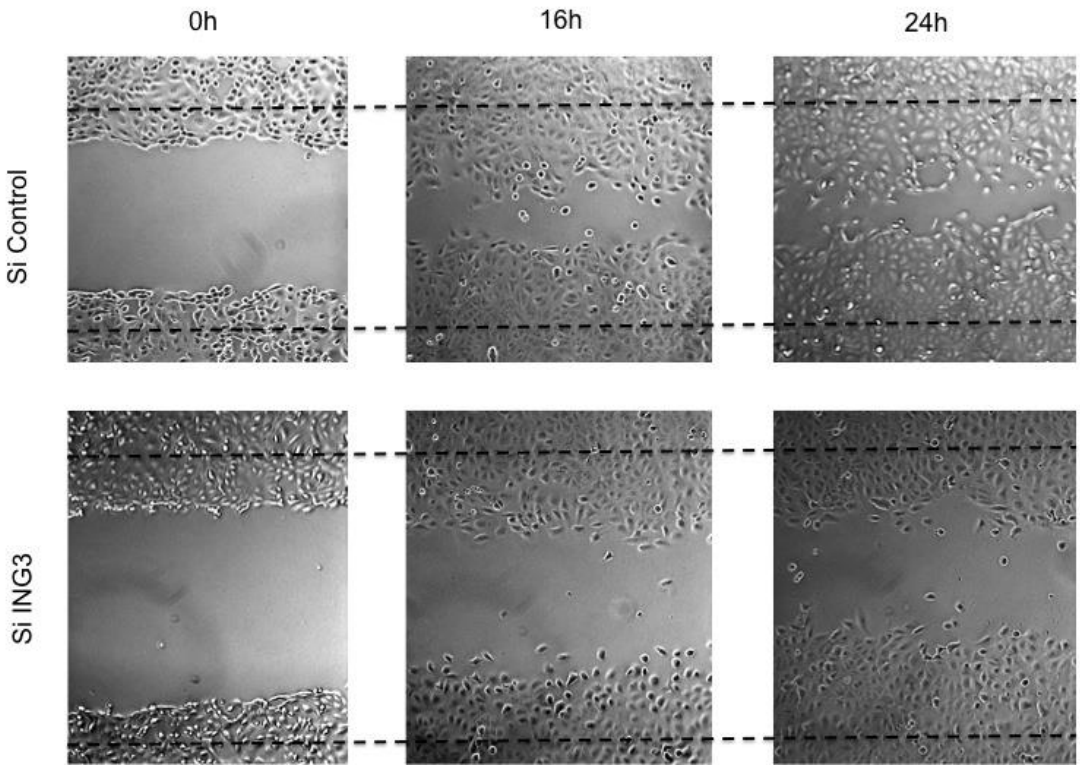
0h
16h
24h
Si Control
Si ING3

3.6 ING3 and Clinical data

3.6.1 ING3 expression in clinical prostate samples

To explore ING3 expression in prostate cancer tissues, we examined a cohort of (n= 304) patients who were diagnosed with PCA on Transurethral resection of prostate (TURP) samples. Patients were grouped into three categories:

1. Patients with unsuspected PCA (defined as patients with no previous diagnosis of PCA, who were found to have PCA at the time of histological exam with a Gleason Score (GS) ≤7.
2. Patients with advanced prostate cancer (AdvPCA); defined as patients with no prior diagnosis of PCA, but for whom the histological findings demonstrate a GS of 8-10.
3. Patients with previous diagnosis of PCA who were on hormonal therapy and progressed requiring channel TURP to relieve obstructive symptoms were referred as castration resistant prostate cancer (CRPC).

The cohort consisted of 615 cores from two TMAs which included benign prostate tissue (n=83), localized PCA cores (n=233), AdvPCA (n=173) and CRPC cores (n=126), assembled into two TMAs. ING3 protein expression was assessed by fluorescence immuno-histochemical staining using the AQUA analysis system. Using this system ING3 nuclear staining is stained red and counterstained blue with DAPI. The generated score is a percentage of the nuclear area that is positive for ING3 and nuclear staining which is stained blue by DAPI. ING3 positivity is based on threshold image levels to remove background. It reflects positivity that is within the nuclear area which is defined by DAPI. The green color represents cytokeratin which is a protein expressed in the membrane of epithelial cells. This defines the membrane of the cells since

prostate tumors are of epithelial origin (Figure 3.14). This figure was performed by Mr. Brant Pohorelic using the AQUA method.

There was no significant differences in the expression of ING3 between benign and PCA or CRPC however the expression of ING3 in CRPC was slightly increased compared to AdvPCA based on the error bar of 95% CI of mean percent of cell of that expressed ING3 in used TMAs. ING3 staining was decreased in association to disease progression. ING3 mean intensity levels were highest in benign prostate tissues (mean 3.2 ±0.54) compared to PCA (mean 2.5 ± 0.26) ($p<0.437$); AdvPCA (mean 1.5 ± 0.32) ($p<0.004$) and CRPC (mean 2.28 ± 0.32) ($p< 0.285$) (Figure 3.15).

Figure 3.14 Fluorescent immunohistochemical staining of ING3 in Prostate samples.

Representative samples of TMA cores showing fluorescent immuno-histochemicalm staining of ING3 using AQUA platform of two prostate tissue samples. A-B) Benign core and Cancer core in C-D). The score is a percentage of the nuclear area that is positive for ING3 staining. Blue; Nuclear staining with DAPI; Green; Cytokeratin staining; Red: ING3 staining. Then, all three compartments are merged. The right panel demonstrates a cancer sample and its magnified part from white small box, whereas the left panel shows the benign samples and its magnified part. (The image proved by Mr. Brant Pohorelic)

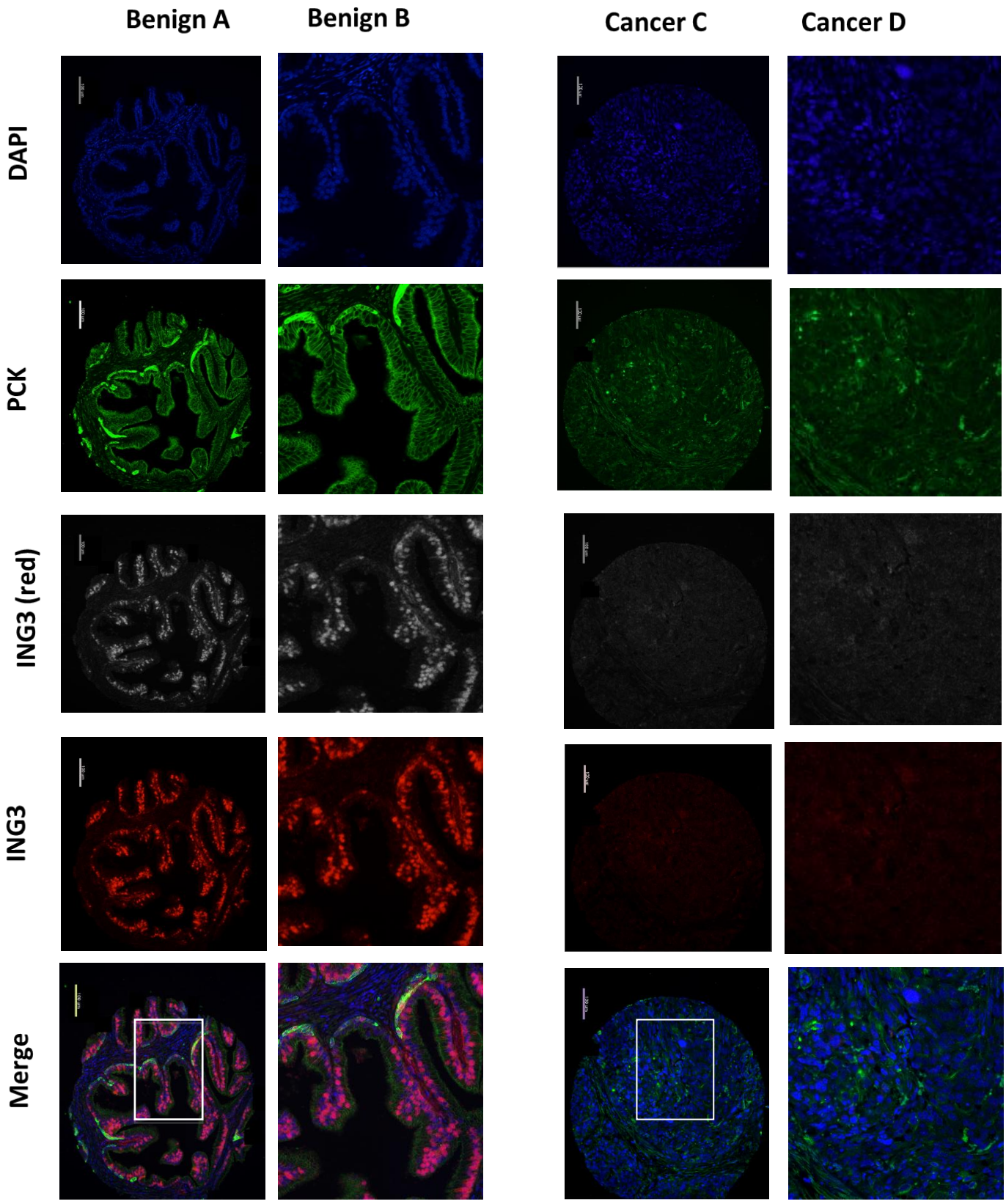
Benign A
Benign B
Cancer C
Cancer D
DAPI
PCK
ING3 (red)
ING3
Merge

Figure 3.15 ING3 expression in clinical samples.

Mean expression of the percentage of cells which expressed nuclear ING3 protein levels in correlation with disease progression between benign and prostate cancer (A) and between benign and each type of prostate cancer progression (PCA, AdvPCA and CRPC) separately (B). Error bars represent 95% CI of mean percentage of cells expressing ING3 based on AQUA analysis. (BN=benign, PCA= localized prostate cancer, AdvPCA= Advanced prostate cancer, CRPC= castration resistance prostate cancer). The primary antibody used is anti- ING3 (2A2). (PATH Dx) refers to Pathological Diagnosis.

A

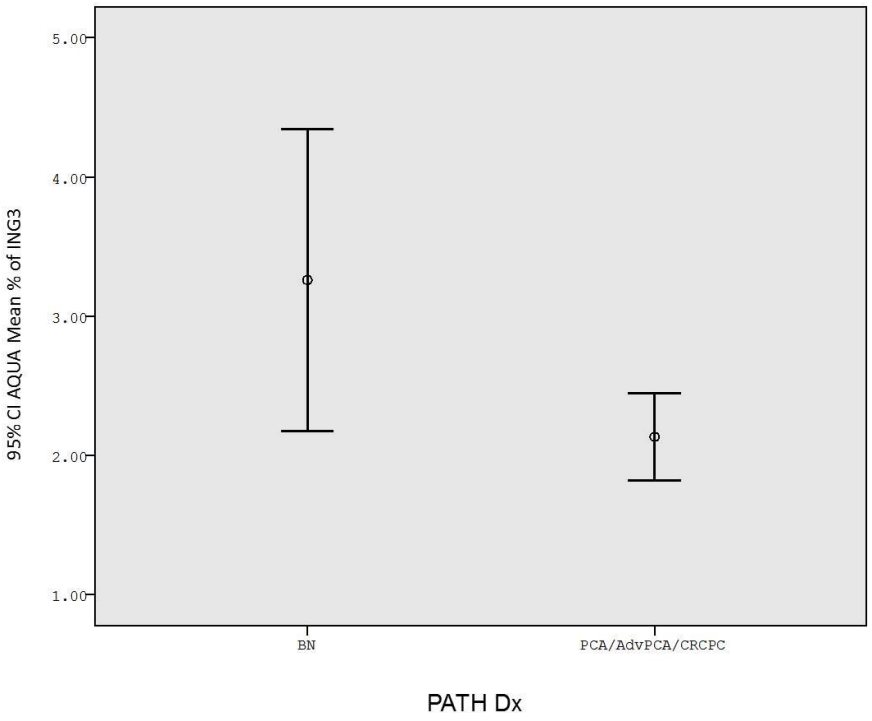
5.00
4.00
3.00
2.00
1.00
95% CI AQUA Mean % of ING3
BN
PCA/AdvPCA/CRCPC
PATH Dx

$p<0.015$

B

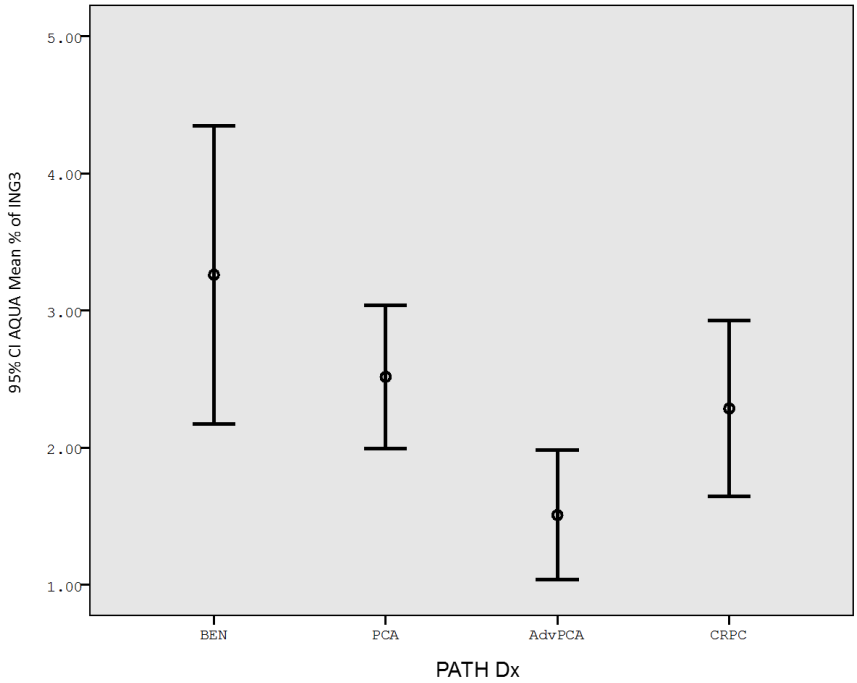
5.00
4.00
3.00
2.00
1.00
95% CI AQUA Mean % of ING3
BEN
PCA
AdvPCA
CRPC
PATH Dx

3.6.2 ING3 and ERG in Clinical samples:

To assess the correlation between ING3 expression and ERG, we investigated the levels of ING3 in ERG positive samples by separating them into two groups: ERG negative and ERG positive. In addition, samples were separated according to the percentage of cells expressing low levels of ING3, (≤ 0.15) and moderate to high levels of ING3 (≥ 0.15) based on fluorescent immuno-histochemical staining of ING3 using AQUA platform. .Chi-square statistical analysis test showed significant correlation between ERG and ING3 expression ($p=0.019$) where there is a decrease of ING3 levels in ERG positive samples (Figure 3.16 A).

We further assessed ING3 expression to AR based on intensity of AR protein levels where 0 is considered negative and 1, 2 and 3 are weak, moderate and strong protein level intensity, respectively. The samples separated into two groups based on AR expression were compared where one group has 0, 1, 2 (any expression of AR) and the second group has samples with high levels of AR (AR3). Our results show that the levels of ING3 is increased significantly in the group where AR is highly expressed ($p<0.0001$) as shown in (Figure 3.16 B).

Figure 3.16 Correlation between ING3, ERG and AR protein intensity levels.

A) Percentages distribution of ING3 in ERG negative and positive samples with AR3. The cut off of ING3 being ≤ 0.15.

B) Percentage distribution of ING3 in samples with any expression of AR (AR 0, 1, 2) versus samples with high levels of AR (AR3).

Chi-square test from SPSS software used for statistical analysis to compare between samples. $p<0.05$ was considered statistically significant.

A

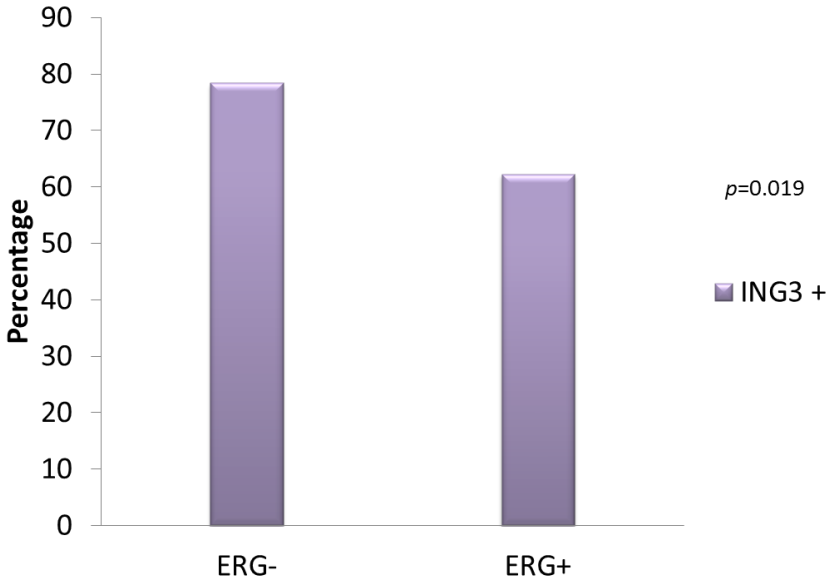
90
80
70
60
50
40
30
20
10
0
Percentage
ERG-
ERG+
p=0.019
ING3 +

B

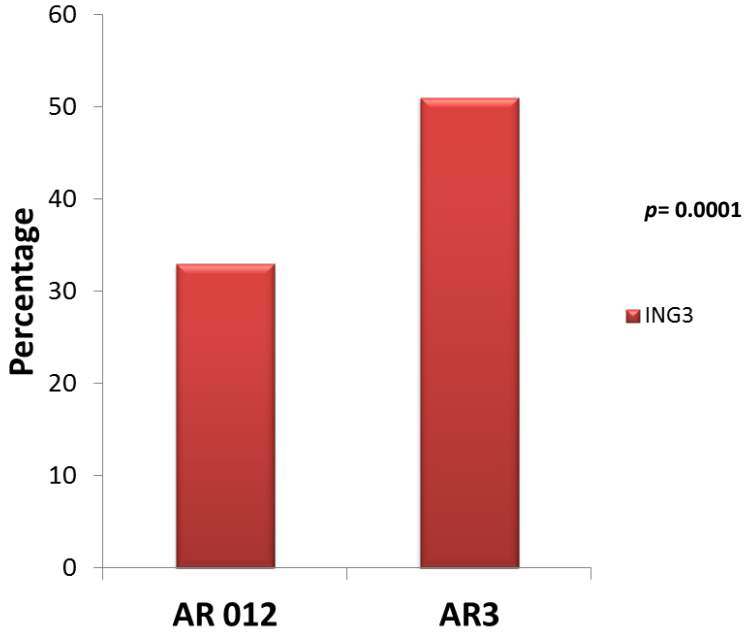
60
50
40
30
20
10
0
Percentage
AR 012
AR3
p= 0.0001
ING3

3.6.3 ING3 and Gleason Score in Clinical samples

To investigate the correlation between disease progression and ING3 expression, AQUA system was used to determine the levels of ING3 protein expression with the grading scale based on the score as a percentage of the nuclear area that is positive for ING3 staining. Samples were grouped into three categories GS <7, GS 7 and GS >7. ING3 was significantly decreased in the GS7 and GS >7 groups compared to GS<7 ($p< 0.039$). Since a Gleason's Score of 7 represents different pathological groups (GS 3+4 and GS 4+3), another investigation on correlation between ING3 and Gleason's score was carried out on these groups. The indicated bars of the mean expression of staining for ING3 in the clinical samples showed that GS4+3 to be associated with a significantly higher ING3 expression compared to GS3+4 or GS<7 ($p<0.041$) (Figure 3.17).

Figure 3.17 Correlation between ING3 percentage level and Gleason score.

The percentage of ING3 positive nuclear cells based on AQUA analysis in relation to Gleason score:

A) Representative percentage of cells with ING3 expression in tissue samples with GS <7 in green, GS =7 orange and GS >7 pink.

B) Representative percentage of cells with ING3 expression in tissue samples with more specific Gleason Scores. GS <7 green, GS7 (3+4) orange and GS7 (4+3) pink. Chi-square statistical test using SPSS software and the value of $p<0.05$ was considered statistically significant.

A

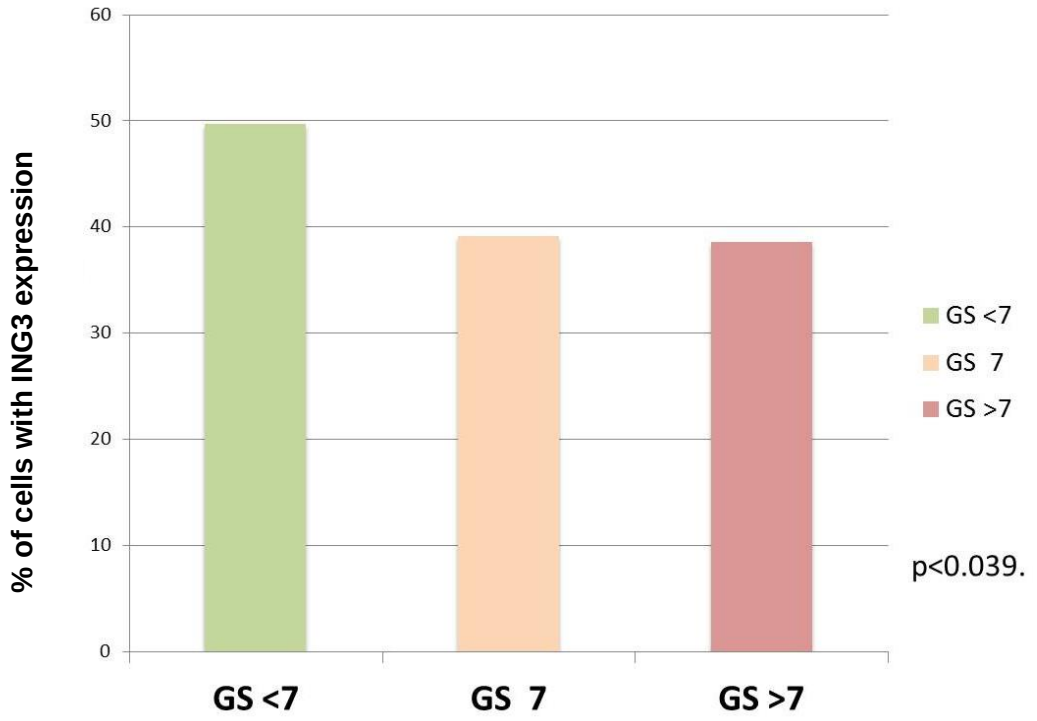
60
50
40
30
20
10
0
% of cells with ING3 expression
GS <7
GS 7
GS >7
p<0.039.
GS <7
GS 7
GS >7

B

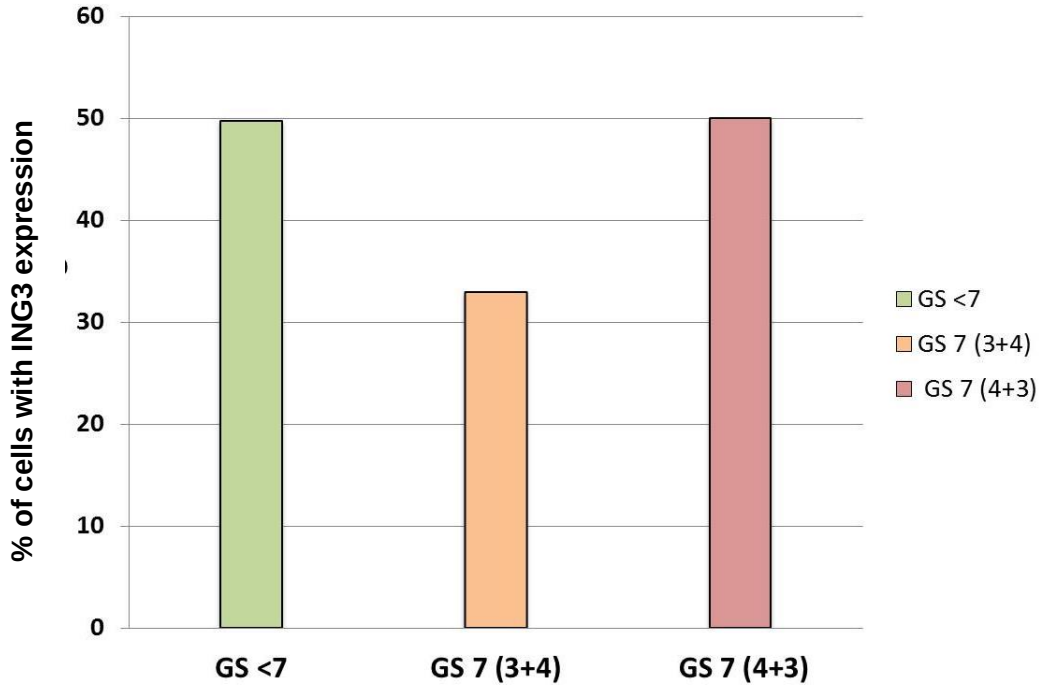
60
50
40
30
20
10
0
% of cells with ING3 expression
GS <7
GS 7 (3+4)
GS 7 (4+3)
GS <7
GS 7 (3+4)
GS 7 (4+3)

3.6.4 ING3 and lethal outcome

A cohort with 304 cases of TURP (90 cases with low ING3 and 214 with high ING3 expressions) was used to evaluate ING3 staining in correlation with lethal disease. Lower expression of ING3 was associated with a marginally significant better outcome for the patients compared with higher ING3 expression ($p < 0.052$). Patients expressing higher levels of ING3 were associated with higher rates of cancer specific mortality, compared to patients with lower levels. Overall survival of all prostate cancer patients ($n = 304$, $p = 0.052$) can be seen in (Figure 3.18 A). This significance was more pronounced in the group of patients with ERG negative tumors ($p=0.018$) (Figure 3.18 B).

Cox regression analysis including ING3 percentage expression, Gleason's score and tumor volume were utilized to assess significance to cancer-specific mortality of the full cohort (Figure 3.18 C). ING3 mean percentage expression was still significant in predicting lethal outcome when considering GS and tumor volume ($p<0.027$).

Figure 3.18 Correlation between ING3 protein percentage levels and lethal disease of prostate cancer.

The overall survival analysis of patients with tumors expressing low ING3 levels (below median, <0.15) compared to patients with high levels of ING3 in all prostate cancer samples (A) and in ERG negative samples (B). Significant differences in the over-all survival between both groups were determined by Kaplan-Meier survival analysis. C) Cox regression model adjusted for Gleason's score and tumor volume showing percentage of cells expressing ING3 to be significantly associated with lethal PCA HR is hazard ratio and student t-test p value ($p<0.05$) is considered statistically significant.

A

All PCA samples included

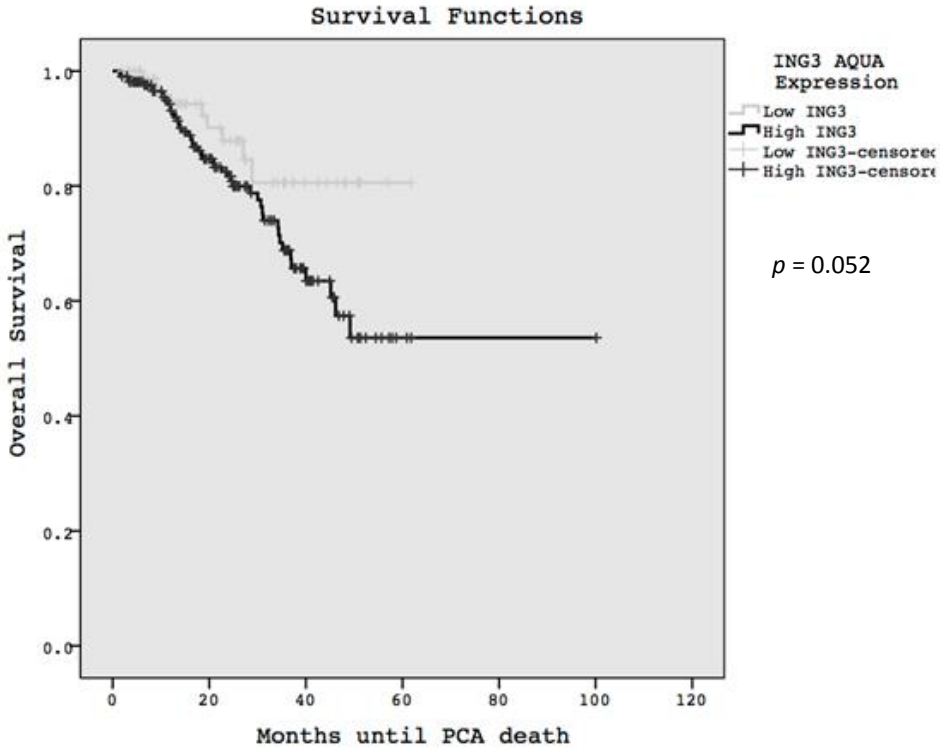

$p = 0.052$

B

All PCA with ERG negative samples included

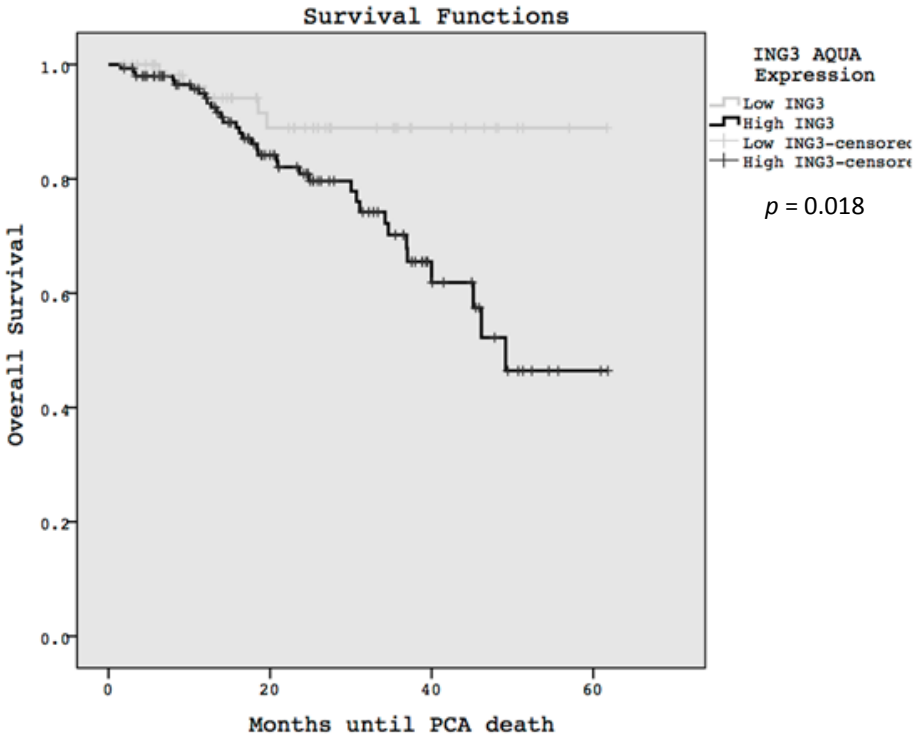

$p = 0.018$

C

Cox regression

	P value	HR
Gleason Score ≤ 7 vs.> 7	0.001	3.602
ING3 ≤ 0.155 vs. > 0.155	0.027	2.059
Volume ≤ 5% vs. >5 %	0.589	1.789

Chapter Four: Discussion

4.1 ING3 and ERG in prostate cancer

Prostate cancer is the most common malignancy in men and still a leading cause of cancer-related death in Western countries. In 2013, in Canada, there has been an estimated incidence of approximately 23,600 new cases of PCA and mortality occurred in over 3,900 cases [16].

In the prostate, androgen, through binding its receptor (AR), acts to regulate gene networks and various signalling pathways that promote cell growth and survival. Therefore, androgen deprivation therapy (ADT) is the most common treatment option for locally advanced or metastatic prostate cancer. However, most patients receiving ADT eventually progress to a castration-resistant state that leads to death [94] .

Recently, a recurrent ETS gene fusion as a consequence of gene rearrangement has been identified in most prostate cancers, which are characterized by a rearrangement between the 5' regulatory elements of an androgen-regulated gene *TMPRSS2* and the coding region of a member of the *ETS* gene family (*ERG, ETV1, ETV4 and ETV5*) [95]. These rearrangements result in androgen-driven expression of ETS transcription factors. The most frequent rearrangement is *ERG-TMPRSS2* fusion, which was identified in 50% of prostate cancers [96]. Fusion of *TMPRSS2* and *ERG* resulted in androgen mediated *ERG* overexpression in prostate cancer [97]. Additionally, *ERG-TMPRSS2* usually co-occurs with the loss of tumor repressor genes, including *PTEN* [98].

The inhibitor of growth family member 3 (*ING3*) is a member of the *ING* tumor suppressor family, which represents as novel tumor suppressor proteins and comprise of five-conserved genes. ING3 is ubiquitously expressed in normal human tissues and regulates gene transcription, cell cycle control and apoptosis [79]. Deregulated *ING3* expression has been found in human head and neck squamous cell carcinomas, melanomas and hepatocellular carcinoma [82-84]. However, no studies have examined *ING3* expression levels and function in prostate cancer or investigated its relation to *TMPRSS2-ERG* fusion.

4.1.1 Importance of studying ERG fusion in prostate cancer

The expression of *ERG* fusion in prostate cancer cell lines indicates their aggressiveness as it is present in over 60% of prostate cancer cases [57]. Deletion of the tumor suppressor *PTEN* is also common in many cancers including prostate cancer [60]. The expressions of ERG, AR and PTEN in prostate cell lines were previously reported in different studies [92, 93]. The prostate cancer cell lines used in this study were screened to confirm the protein levels of these known genes. Since VCaP cells were the only prostate cancer cell lines that have markedly higher protein levels of ERG compared to the other prostate cell lines (Figure 3.1), we were interested in using these cells to test our hypothesis about the potential involvement of ERG in regulating ING3 expression levels. Therefore, we knocked down ERG in VCaP cells and investigated *ING3* levels where the results showed a slight increase of *ING3* levels in those ERG knocked down cells (Figure 3.7).

4.1.2 ING3 is inversely related to ERG expression

ING3 is a stable subunit of the human NuA4/Tip60 histone acetyltransferase (HAT) complex and is required for acetylation of chromatin substrates [87]. Fortson et al. [88] demonstrated that *ERG* binds to HAT and inhibits its function in VCaP prostate cell lines. This suggested a role of *ERG* in protein acetylation. This was in line with the results shown in (Figure 3.7 A) which demonstrates that the knockdown of *ERG* endogenous expression mRNA, increases the levels of *ING3* mRNA. In addition, the expression of *ING3* at the protein level also showed a slight increase in *siERG* VCaP cells. Further work is needed to investigate if there is a direct interaction between ERG and ING3.. Future directions may include the investigation of the binding site of *ERG* on the *ING3* promoter by chi-sequencing assay and co-IP analysis.

In this study, *ERG* was introduced in three prostate cell lines (RWPE-1, LNCaP and PC3). The qRT-PCR results indicated a negative correlation between *ERG* and *ING3* where *ERG* overexpressing cell lines showed a significant decrease in *ING3* expression in comparison to their controls (Figure 3.6 A). This result was also in agreement with our clinical data where *ERG* positive samples showed a decrease in the percentage of cells that have nuclear expression of ING3 (Figure 3.16 A), however the level of ING3 in AR positive samples was significantly high (Figure 3.16 B). It was interesting to see that PC3-ERG cell lines have higher level of ING3 compared to RWPE1-ERG and LNCaP-ERG. This might suggest a role of AR in regulating ING3 expression. PC3 cells are AR negative while RWPE-1 and LNCaP are AR positive. Therefore, the excess amount of ERG could have acted as a negative feedback for the expression of AR where ERG inhibits its expression and activity [99]. Our clinical data indicates that samples with high levels of AR (AR3) have a positive correlation with ING3 percentage in

nuclear component of the cells ($p < 0.0001$) as shown in (Figure 3.16 B). From these results, we conclude that there is more significance association between ING3 and AR than between ING3 and ERG.

4.1.3 ING3 expression and its role as a tumor suppressor

The novel ING tumor-suppressor family proteins (*ING1-5*) have been discovered over the past decades and are recognized as the regulators of transcription, cell cycle checkpoints, DNA repair, and apoptosis. They have also been reported to promote cellular senescence and inhibit angiogenesis [68, 78]. Few studies investigated the expression of *ING3* in different types of cancers and all of them support its role as a tumor suppressor gene [80-82].

4.1.4 ING3 expression in prostate cancer

A study done by Mehmet Gunduz et al. [83] demonstrated that mRNA expression of *ING3* in the head and neck areas was reduced in 50 % of 71 patient samples, however, 60% of patients showed better survival when they had higher to normal levels of *ING3* compared with 35% of patients with low levels of *ING3*. In addition, Lu et al. [81] showed lower levels of *ING3* in cancer samples compared with normal liver tissues using both *in*-vitro and human samples of HCC. Moreover, in the same study, wound-healing assay on hepatocellular cell lines transfected with *ING3* showed a significant reduction of migration in those cell lines. These studies suggest a tumor suppressor role of *ING3* in cancer. In contrast to these studies, our results demonstrated that Kaplan Maier survival curve indicates that lower *ING3* levels in PCA is associated with a better survival rate compared to higher levels of *ING3* (Figure 3.18). In addition, our observation in wound healing and invasion assays on DU145 cell lines with *siING3* showed that there was a

reduction of invasion and migration when *ING3* was suppressed which does not support the role of *ING3* as a tumor suppressor in prostate cancer (Figure 3.13 A and B). Similar role has been observed in another member of the *ING* family (*ING2*) which was reported to be up-regulated in colon cancer [100] . This indicates that some INGs family have different roles in different types of cancers. *ING2* reported as a tumor suppressor in hepatocellular carcinoma, head and neck squamous cell carcinoma (HNSCC), and melanoma [71-73], but has an oncogenic role in colon cancer [100]. *ING3*, similar to *ING2*, showed down regulation in those three types of cancer but there is no study of ING3 on colon cancer. It would be interesting to study the expression of *ING3* in colon cancer, which would lead to evaluation of the functional roles of *ING2* and *ING3* in depth. Furthermore, retesting all three reported cancers with the specific antibody ING3 (2A2) might also lead to different findings.

4.1.5 Inhibition of ING3 in DU145 cell lines is associated with decreased invasion and migration

After observing the effect of high expression of ING3 in Kaplan Maier survival curve of prostate cancer from TURP cohort of all samples and ERG negative samples, we chose DU145 cell lines to test the cells' migration ability after the *ING3* knockdown for two reasons. First, VCaP and DU145 were the only two prostate cancer cells which showed high levels of ING3 expression. Second, since VCaP cells harbour both *ERG* and *AR*, to avoid any effect of *AR* and *ERG* in the role of *ING*3, we decided to choose DU145 cells to study the role of *ING3* in prostate metastasis. We also performed the same experiments on VCaP cells to examine the effect of inhibition of *ING3* on cell migration in the presence of both *AR* and *ERG*. However, the experiments failed due to difficulties in performing a wound gap in this cell line, which requires cells to grow in

clusters, and taking longer period of time for duplication, thus affecting the efficiency of transient transfection of *ING3*. Metastasis is one of the main hallmarks of cancer and there are different procedures to assess the metastatic potential *in*-vitro studies. One methodology, is evaluating epithelial mesenchymal transition, EMT, which changes the morphology of epithelial cells from firm organized to more spindle-like shape in order to travel to distant organs. Therefore, demonstrating levels of EMT markers such as E-cadherin, N-cadherin and vimentin in DU145 manipulated cells would support the role of ING3 as an oncogene in prostate cancer.

4.1.6 Localization of ING3 in prostate cancer

ING3 is a nuclear protein, however, the translocation of nuclear ING3 to the cytoplasm has been reported in melanoma [82]. We investigated the localisation of ING3 in prostate cancer and our observation indicates that ING3 is mainly located in the nucleus of the prostate cell lines; moreover, the clinical cohorts show a nuclear expression of ING3 (Figure 3.14) using AQUA system.

In conclusion, although numerous experiments were initially attempted with commercial ING3 antibody, using the specific antibody made a great difference when confirming the localisation of ING3 as a nuclear protein and the expression of ING3 in clinical data and in cell lines. To our knowledge, this is the first study to investigate ING3 expression in prostate cell lines and tissue samples.

4.2 Future Directions

In summary, this study is the first to report the expression of *ING3* in prostate cancer and the association of this expression to *ERG* gene fusion. We also determined the localization of ING3

in prostate cell lines and in FFPE samples. One of the main novelties of our study is that it is the first to investigate the expression levels of ING3 in relation to disease progression and clinical outcome. However, one of the limitations here is the inability to directly link *ING3* with *ERG* and *AR*. Therefore, further studies to characterize this association and the functional role of *ING3* and its therapeutic usage in prostate cancer are needed. Specifically, characterizing the connection between *ING3* and each of *ERG* and *AR* would increase our understanding of the collaborative role, if any; these genes play in PCA tumorigenesis. Demonstrating the interaction between *ING3* and *ERG* by investigating the binding sites of *ERG* on the *ING3* promoter using chip-assay would support a direct role of ERG in regulating ING3 expression. In addition, identifying the relation of *ING3* to metastasis by investigating the effect of knocking down *ING3* in prostate cell lines and then assessing the effect on EMT signalling would lead to a better understanding of the role of *ING3* in prostate cancer. This can also be done by performing some *in*-vivo studies to support findings in EMT studies.

When we tested the ING3 (2A2) antibody and the Proteintech antibody on prostate cancer cell lines and clinical samples, each antibody provided different results. Therefore, it is significant to evaluate the expression of *ING3* in previously reported cancers such as melanoma, head and neck and hepatocellular carcinoma, which could provide new results supporting a new role for ING3 in these cancers. Furthermore, it would be interesting to investigate the role of *ING3* in other types of cancers and identify the role of other *INGs* family members in prostate cancer.

References

1. Kumar, V.L. and P.K. Majumder, *Prostate gland: structure, functions and regulation.* International urology and nephrology, 1995. **27**(3): p. 231-43.
2. Lee, C.H., O. Akin-Olugbade, and A. Kirschenbaum, *Overview of prostate anatomy, histology, and pathology.* Endocrinology and metabolism clinics of North America, 2011. **40**(3): p. 565-75, viii-ix.
3. McNeal, J.E., *Normal histology of the prostate.* The American journal of surgical pathology, 1988. **12**(8): p. 619-33.
4. Albertsen, P.C., J.A. Hanley, and J. Fine, *20-year outcomes following conservative management of clinically localized prostate cancer.* JAMA : the journal of the American Medical Association, 2005. **293**(17): p. 2095-101.
5. Frick, J. and W. Aulitzky, *Physiology of the prostate.* Infection, 1991. **19 Suppl 3**: p. S115-8.
6. Kumar, V., R.S. Cotran, and S.L. Robbins, *Robbins basic pathology*. 7th ed2003, Philadelphia, Penn. ; London: Saunders. xii, 873 p.
7. Berry, S.J., et al., *The development of human benign prostatic hyperplasia with age.* The Journal of urology, 1984. **132**(3): p. 474-9.
8. Roehrborn, C.G., *Benign prostatic hyperplasia: an overview.* Reviews in urology, 2005. **7 Suppl 9**: p. S3-S14.
9. Bostwick, D.G., et al., *High-grade prostatic intraepithelial neoplasia.* Reviews in urology, 2004. **6**(4): p. 171-9.
10. Bostwick, D.G., *The pathology of early prostate cancer.* CA: a cancer journal for clinicians, 1989. **39**(6): p. 376-93.
11. Singh, A.S. and W.D. Figg, *In vivo models of prostate cancer metastasis to bone.* The Journal of urology, 2005. **174**(3): p. 820-6.
12. Datta, K., et al., *Mechanism of lymph node metastasis in prostate cancer.* Future oncology, 2010. **6**(5): p. 823-36.
13. Pouessel, D., et al., *Liver metastases in prostate carcinoma: clinical characteristics and outcome.* BJU international, 2007. **99**(4): p. 807-11.
14. Siegel, R., D. Naishadham, and A. Jemal, *Cancer statistics, 2013.* CA: a cancer journal for clinicians, 2013. **63**(1): p. 11-30.
15. Society, A.C. *Prostate cancer overview* 2013 26 Aug 2013; Available from: http://www.cancer.org/cancer/prostatecancer/overviewguide/prostate-cancer-overview-key-statistics.
16. Society, C.C. *Canadian cancer statistics 2013*. 2013; Available from: http://www.cancer.ca/~/media/cancer.ca/CW/cancer%20information/cancer%20101/Canadian%20cancer%20statistics/canadian-cancer-statistics-2013-EN.pdf.
17. UK, C.R. *Prostate cancer incidence statistics*. 2013 22 January 2013; Available from: http://www.cancerresearchuk.org/cancer-info/cancerstats/types/prostate/incidence/.
18. Siegel, R., et al., *Cancer treatment and survivorship statistics, 2012.* CA: a cancer journal for clinicians, 2012. **62**(4): p. 220-41.
19. Glass, A.S., K.C. Cary, and M.R. Cooperberg, *Risk-based prostate cancer screening: who and how?* Current urology reports, 2013. **14**(3): p. 192-8.

20. Kheirandish, P. and F. Chinegwundoh, *Ethnic differences in prostate cancer.* British journal of cancer, 2011. **105**(4): p. 481-5.
21. Jemal, A., et al., *Global cancer statistics.* CA: a cancer journal for clinicians, 2011. **61**(2): p. 69-90.
22. Marks, S., *Prostate & cancer : a family guide to diagnosis, treatment, & survival* 4th ed 2009: Da Capo Lifelong. 359.
23. Hsing, A.W., L.C. Sakoda, and S.C. Chua, *Obesity, metabolic syndrome, and prostate cancer.* The American journal of clinical nutrition, 2007. **86**(3): p. 843S-857S.
24. McCormack, M., *Diagnosis and Management of Prostatic Disease* 2006: Rogers Media Pub. 156.
25. Gleason, D.F., *Classification of prostatic carcinomas.* Cancer chemotherapy reports. Part 1, 1966. **50**(3): p. 125-8.
26. Gleason, D.F. and G.T. Mellinger, *Prediction of prognosis for prostatic adenocarcinoma by combined histological grading and clinical staging. 1974.* The Journal of urology, 2002. **167**(2 Pt 2): p. 953-8; discussion 959.
27. Gleason, D.F., *Histologic grading of prostate cancer: a perspective.* Hum Pathol, 1992. **23**(3): p. 273-9.
28. Publications, H.H. *Understanding your prostate pathology report*. 2007 April 27, 2011 [cited 2013; Available from: http://www.harvardprostateknowledge.org/understanding-your-prostate-pathology-report.
29. Malcom, M., *Prostate cancer* 2003, Now York: Oxford University Press Inc. 96.
30. Hospital, M. *Comperhensive Prostate Program* 2013 [cited 2013; Available from: http://middlesexhospital.org/our-services/hospital-services/cancer-center/cancer-programs-and-services/comprehensive-prostate-program/stage-and-grade.
31. Institute, N.C. *Prostate Cancer Treatment (PDQ)*. 2013 [cited 2013; Available from: http://www.cancer.gov/cancertopics/pdq/treatment/prostate/Patient/page4.
32. Horwich, A., *Systemic Treatment of Prostate Cancer* 2010, New York: Oxford University Press Inc. p89.
33. Sharifi, N., J.L. Gulley, and W.L. Dahut, *An update on androgen deprivation therapy for prostate cancer.* Endocrine-related cancer, 2010. **17**(4): p. R305-15.
34. Bartel, D.P., *MicroRNAs: genomics, biogenesis, mechanism, and function.* Cell, 2004. **116**(2): p. 281-97.
35. Cortez, M.A., et al., *MicroRNAs in body fluids--the mix of hormones and biomarkers.* Nature reviews. Clinical oncology, 2011. **8**(8): p. 467-77.
36. Lovat, F., N. Valeri, and C.M. Croce, *MicroRNAs in the pathogenesis of cancer.* Seminars in oncology, 2011. **38**(6): p. 724-33.
37. Zhang, L., et al., *microRNAs exhibit high frequency genomic alterations in human cancer.* Proceedings of the National Academy of Sciences of the United States of America, 2006. **103**(24): p. 9136-41.
38. Walter, B.A., et al., *Comprehensive microRNA Profiling of Prostate Cancer.* Journal of Cancer, 2013. **4**(5): p. 350-7.
39. Pang, Y., C.Y. Young, and H. Yuan, *MicroRNAs and prostate cancer.* Acta biochimica et biophysica Sinica, 2010. **42**(6): p. 363-9.

40. Mitchell, P.S., et al., *Circulating microRNAs as stable blood-based markers for cancer detection.* Proceedings of the National Academy of Sciences of the United States of America, 2008. **105**(30): p. 10513-8.
41. Bryant, R.J., et al., *Changes in circulating microRNA levels associated with prostate cancer.* British journal of cancer, 2012. **106**(4): p. 768-74.
42. Loeb, S. and H.B. Carter, *Limitations and use of PSA derivatives in the screening and risk stratification of prostate cancer.* Urologic oncology, 2009. **27**(6): p. 583-4.
43. Adhyam, M. and A.K. Gupta, *A Review on the Clinical Utility of PSA in Cancer Prostate.* Indian journal of surgical oncology, 2012. **3**(2): p. 120-9.
44. Liong, M.L., et al., *Blood-based biomarkers of aggressive prostate cancer.* PloS one, 2012. **7**(9): p. e45802.
45. Ferdinandusse, S., et al., *Subcellular localization and physiological role of α-methylacyl-CoA racemase.* Journal of lipid research, 2000. **41**(11): p. 1890-1896.
46. Jiang, Z., et al., *Expression of α-methylacyl-coa racemase (p504s) in various malignant neoplasms and normal tissues: a study of 761 cases.* Human pathology, 2003. **34**(8): p. 792-796.
47. Luo, J., et al., *Alpha-methylacyl-CoA racemase: a new molecular marker for prostate cancer.* Cancer research, 2002. **62**(8): p. 2220-6.
48. Zhou, M., et al., *Alpha-Methylacyl-CoA racemase: a novel tumor marker over-expressed in several human cancers and their precursor lesions.* Am J Surg Pathol, 2002. **26**(7): p. 926-31.
49. Rubin, M.A., et al., *Decreased α-methylacyl CoA racemase expression in localized prostate cancer is associated with an increased rate of biochemical recurrence and cancer-specific death.* Cancer Epidemiology Biomarkers & Prevention, 2005. **14**(6): p. 1424-1432.
50. Yin, Y. and W.H. Shen, *PTEN: a new guardian of the genome.* Oncogene, 2008. **27**(41): p. 5443-53.
51. Hollander, M.C., G.M. Blumenthal, and P.A. Dennis, *PTEN loss in the continuum of common cancers, rare syndromes and mouse models.* Nature reviews. Cancer, 2011. **11**(4): p. 289-301.
52. Mulholland, D.J., et al., *Pten loss and RAS/MAPK activation cooperate to promote EMT and metastasis initiated from prostate cancer stem/progenitor cells.* Cancer research, 2012. **72**(7): p. 1878-89.
53. Laudet, V., et al., *Molecular phylogeny of the ETS gene family.* Oncogene, 1999. **18**(6): p. 1351-9.
54. Birdsey, G.M., et al., *Transcription factor Erg regulates angiogenesis and endothelial apoptosis through VE-cadherin.* Blood, 2008. **111**(7): p. 3498-506.
55. Ichikawa, H., et al., *An RNA-binding protein gene, TLS/FUS, is fused to ERG in human myeloid leukemia with t(16;21) chromosomal translocation.* Cancer research, 1994. **54**(11): p. 2865-8.
56. Clark, J.P. and C.S. Cooper, *ETS gene fusions in prostate cancer.* Nature reviews. Urology, 2009. **6**(8): p. 429-39.
57. St John, J., et al., *TMPRSS2-ERG Fusion Gene Expression in Prostate Tumor Cells and Its Clinical and Biological Significance in Prostate Cancer Progression.* Journal of cancer science & therapy, 2012. **4**(4): p. 94-101.

58. Green, W.M., et al., *Immunohistochemical evaluation of TMPRSS2-ERG gene fusion in adenosis of the prostate.* Human pathology, 2013. **44**(9): p. 1895-901.
59. Tomlins, S.A., et al., *Recurrent fusion of TMPRSS2 and ETS transcription factor genes in prostate cancer.* Science, 2005. **310**(5748): p. 644-8.
60. Yoshimoto, M., et al., *Absence of TMPRSS2:ERG fusions and PTEN losses in prostate cancer is associated with a favorable outcome.* Modern pathology : an official journal of the United States and Canadian Academy of Pathology, Inc, 2008. **21**(12): p. 1451-60.
61. Sreenath, T.L., et al., *Oncogenic activation of ERG: A predominant mechanism in prostate cancer.* Journal of carcinogenesis, 2011. **10**: p. 37.
62. Bismar, T.A., et al., *ERG protein expression reflects hormonal treatment response and is associated with Gleason score and prostate cancer specific mortality.* Eur J Cancer, 2012. **48**(4): p. 538-46.
63. Teng, L.H., et al., *ERG Protein Expression Is of Limited Prognostic Value in Men with Localized Prostate Cancer.* ISRN urology, 2013. **2013**.
64. Demichelis, F., et al., *TMPRSS2:ERG gene fusion associated with lethal prostate cancer in a watchful waiting cohort.* Oncogene, 2007. **26**(31): p. 4596-9.
65. He, G.H., et al., *Phylogenetic analysis of the ING family of PHD finger proteins.* Molecular biology and evolution, 2005. **22**(1): p. 104-16.
66. Gong, W., et al., *Function of the ING family of PHD proteins in cancer*. The international journal of biochemistry & cell biology, 2005. **37**(5): p. 1054-65.
67. Russell, M., et al., *Grow-ING, Age-ING and Die-ING: ING proteins link cancer, senescence and apoptosis.* Experimental cell research, 2006. **312**(7): p. 951-61.
68. Soliman, M.A. and K. Riabowol, *After a decade of study-ING, a PHD for a versatile family of proteins.* Trends Biochem Sci, 2007. **32**(11): p. 509-19.
69. Garkavtsev, I., et al., *Suppression of the novel growth inhibitor p33ING1 promotes neoplastic transformation.* Nature genetics, 1996. **14**(4): p. 415-20.
70. Li, X., K. Kikuchi, and Y. Takano, *ING Genes Work as Tumor Suppressor Genes in the Carcinogenesis of Head and Neck Squamous Cell Carcinoma.* Journal of oncology, 2011. **2011**: p. 963614.
71. Luo, Z.G., et al., *Genetic alterations of tumor suppressor ING1 in human non-small cell lung cancer.* Oncology reports, 2011. **25**(4): p. 1073-81.
72. Guo, X.B., et al., *Down-regulation of miR-622 in gastric cancer promotes cellular invasion and tumor metastasis by targeting ING1 gene.* World J Gastroenterol, 2011. **17**(14): p. 1895-902.
73. Zhang, H.K., et al., *Decreased expression of ING2 gene and its clinicopathological significance in hepatocellular carcinoma.* Cancer letters, 2008. **261**(2): p. 183-92.
74. Borkosky, S.S., et al., *Frequent deletion of ING2 locus at 4q35.1 associates with advanced tumor stage in head and neck squamous cell carcinoma.* Journal of cancer research and clinical oncology, 2009. **135**(5): p. 703-13.
75. Lu, F., et al., *Nuclear ING2 expression is reduced in human cutaneous melanomas.* British journal of cancer, 2006. **95**(1): p. 80-6.
76. Byron, S.A., et al., *Negative regulation of NF-kappaB by the ING4 tumor suppressor in breast cancer.* PloS one, 2012. **7**(10): p. e46823.

77. Zheng, H.C., et al., *The nuclear to cytoplasmic shift of ING5 protein during colorectal carcinogenesis with their distinct links to pathologic behaviors of carcinomas.* Human pathology, 2011. **42**(3): p. 424-33.
78. Nagashima, M., et al., *A novel PHD-finger motif protein, p47ING3, modulates p53-mediated transcription, cell cycle control, and apoptosis.* Oncogene, 2003. **22**(3): p. 343-50.
79. Shah, S., et al., *ING function in apoptosis in diverse model systems.* Biochemistry and cell biology = Biochimie et biologie cellulaire, 2009. **87**(1): p. 117-25.
80. Gunduz, M., et al., *Allelic loss and reduced expression of the ING3, a candidate tumor suppressor gene at 7q31, in human head and neck cancers.* Oncogene, 2002. **21**(28): p. 4462-70.
81. Lu, M., et al., *Downregulation of inhibitor of growth 3 is correlated with tumorigenesis and progression of hepatocellular carcinoma.* Oncology letters, 2012. **4**(1): p. 47-52.
82. Wang, Y., et al., *Prognostic significance of nuclear ING3 expression in human cutaneous melanoma.* Clinical cancer research : an official journal of the American Association for Cancer Research, 2007. **13**(14): p. 4111-6.
83. Gunduz, M., et al., *Downregulation of ING3 mRNA expression predicts poor prognosis in head and neck cancer.* Cancer science, 2008. **99**(3): p. 531-8.
84. Yang, H.Y., et al., *Expression and prognostic value of ING3 in human primary hepatocellular carcinoma.* Experimental biology and medicine, 2012. **237**(4): p. 352-61.
85. Fukuda, H., et al., *Simple histone acetylation plays a complex role in the regulation of gene expression.* Briefings in functional genomics & proteomics, 2006. **5**(3): p. 190-208.
86. Isharwal, S., et al., *p300 (histone acetyltransferase) biomarker predicts prostate cancer biochemical recurrence and correlates with changes in epithelia nuclear size and shape.* The Prostate, 2008. **68**(10): p. 1097-104.
87. Doyon, Y., et al., *Structural and functional conservation of the NuA4 histone acetyltransferase complex from yeast to humans.* Molecular and cellular biology, 2004. **24**(5): p. 1884-96.
88. Fortson, W.S., et al., *Histone deacetylase inhibitors, valproic acid and trichostatin-A induce apoptosis and affect acetylation status of p53 in ERG-positive prostate cancer cells.* International journal of oncology, 2011. **39**(1): p. 111-9.
89. Namiki, K., et al., *Persistent Exposure to Mycoplasma Induces Malignant Transformation of Human Prostate Cells.* PloS one, 2009. **4**(9): p. e6872.
90. Boland, D., et al., *A panel of CAb antibodies recognize endogenous and ectopically expressed ING1 protein.* Hybridoma, 2000. **19**(2): p. 161-5.
91. Suzuki, K., et al., *REAP: A two minute cell fractionation method.* BMC research notes, 2010. **3**(1): p. 294.
92. Minner, S., et al., *ERG status is unrelated to PSA recurrence in radically operated prostate cancer in the absence of antihormonal therapy.* Clinical cancer research : an official journal of the American Association for Cancer Research, 2011. **17**(18): p. 5878-88.
93. Whang, Y.E., et al., *Inactivation of the tumor suppressor PTEN/MMAC1 in advanced human prostate cancer through loss of expression.* Proceedings of the National Academy of Sciences of the United States of America, 1998. **95**(9): p. 5246-50.

94. Taplin, M.E., *Androgen receptor: role and novel therapeutic prospects in prostate cancer.* Expert Rev Anticancer Ther, 2008. **8**(9): p. 1495-508.
95. Kumar-Sinha, C., S.A. Tomlins, and A.M. Chinnaiyan, *Recurrent gene fusions in prostate cancer.* Nat Rev Cancer, 2008. **8**(7): p. 497-511.
96. Nam, R.K., et al., *Expression of the TMPRSS2:ERG fusion gene predicts cancer recurrence after surgery for localised prostate cancer.* Br J Cancer, 2007. **97**(12): p. 1690-5.
97. Narod, S.A., A. Seth, and R. Nam, *Fusion in the ETS gene family and prostate cancer.* British journal of cancer, 2008. **99**(6): p. 847-51.
98. Leinonen, K.A., et al., *Loss of PTEN is associated with aggressive behavior in ERG positive prostate cancer.* Cancer epidemiology, biomarkers & prevention : a publication of the American Association for Cancer Research, cosponsored by the American Society of Preventive Oncology, 2013.
99. Yu, J., et al., *An integrated network of androgen receptor, polycomb, and TMPRSS2-ERG gene fusions in prostate cancer progression.* Cancer Cell, 2010. **17**(5): p. 443-54.
100. Kumamoto, K., et al., *ING2 is upregulated in colon cancer and increases invasion by enhanced MMP13 expression.* International journal of cancer. Journal international du cancer, 2009. **125**(6): p. 1306-15.